

**DEVELOPMENT OF AN INDUSTRIAL IMAGE ACQUISITION SYSTEM FOR  
THE MEASUREMENT AND DIMENSIONAL CONTROL OF WOOD  
FURNITURE COMPONENTS**

**by**

**BRIAN JUNG**

**B.Sc., The University of British Columbia, 2001**

**A THESIS SUBMITTED IN PARTIAL FULFILLMENT OF THE  
REQUIREMENTS FOR THE DEGREE OF**

**MASTER OF SCIENCE**

**in**

**THE FACULTY OF GRADUATE STUDIES**

**(Forestry)**

**THE UNIVERSITY OF BRITISH COLUMBIA**

**SEPTEMBER 2006**

**©Brian Jung, 2006**

## **Abstract**

The Canadian secondary wood products industry has seen substantial growth since the early 1990's; however, the industry continues to face fierce global competition from European and Asian competitors. These competitors have maintained competitiveness by reducing production costs through the utilization of either advanced manufacturing technologies and/or low labour costs. Due to global pressures, Canadian companies have now started to focus on different areas to reduce production costs. Quality is one area that Canadian companies are focusing on because quality problems can contribute to a 2 to 5% revenue loss. To assist the Canadian industry in cost reductions, a proof-of-concept of a real-time automated quality control system was developed. The system took existing machine vision technologies from other industries and adapted them to a system designed specifically for the value-added industry. Basic optical metrology techniques were used to map the surface profile of the parts leaving a machine centre. Three different basic profiles (tongue, groove and chamfer) were used to test the prototype system. The accuracy of the system was verified against several other measurement systems; digital calipers, digital micrometer and laser profilometer. To meet the industry requirements, the system's target accuracy was set to  $\pm 0.1\text{mm}$ . The prototype system, however, was not able to deliver consistent results due to a lack of camera resolution and a lack of precision in the mounting hardware. Fortunately, these problems can be remedied with modifications to the hardware and software.

## Table of Contents

ABSTRACT.....	II
TABLE OF CONTENTS .....	III
LIST OF TABLES .....	VI
LIST OF FIGURES .....	VII
1 INTRODUCTION.....	1
2 OBJECTIVES .....	3
3 BACKGROUND .....	4
3.1 Importance of Secondary Wood Products to Canada .....	4
3.2 Current Quality Control Technologies in the Secondary Wood Industry.....	8
3.2.1 Levels of SPC being used .....	9
3.2.2 Industry's Attitude towards Quality Control (WPQC Interview).....	11
3.3 Quality Control .....	12
3.3.1 Statistical Process Control: Monitoring Variability.....	13
3.3.2 Statistical Process Control: Monitoring Attributes .....	17
3.4 Machine Vision Systems.....	18
3.4.1 Machine Vision: Image Acquisition Device.....	18
3.4.2 Machine Vision: Illumination .....	19
3.4.3 Machine Vision: Technique.....	19
3.4.4 Problems with Machine Vision Systems .....	21
3.5 Machine Vision Systems in Other Industries.....	24
3.5.1 Machine Vision in the Primary Lumber Industry .....	24
3.5.2 Machine Vision in the Automotive Industry .....	25
3.5.3 Machine Vision used to measure surface roughness .....	26

3.5.4	Machine Vision in the Plastics and Metals Industry.....	27
3.6	Problem Areas in Wood Machining .....	29
3.6.1	Tongue and Groove Joints .....	29
3.6.2	Chamfers .....	32
<b>4</b>	<b>METHODS .....</b>	<b>34</b>
4.1	Preliminary Trials .....	34
4.1.1	Double-End-Tenoner .....	35
4.1.2	Preliminary Industrial Trial.....	36
4.2	Laboratory Scanning System Hardware .....	38
4.2.1	Lens Aberration Testing .....	40
4.2.2	Perspective Distortion.....	42
4.3	Software .....	48
4.3.1	Image acquisition Software.....	48
4.3.2	Image Analysis – Lens Calibration.....	49
4.3.2.1	Magnification Distortion Calibration.....	52
4.3.2.2	Depth Distortion Calibration.....	57
4.3.3	Image Analysis.....	59
4.3.3.1	Tongue and Groove Image Analysis.....	60
4.3.3.2	Chamfer Image Analysis.....	61
4.3.4	Control charts.....	66
4.3.5	Laboratory Testing.....	67
<b>5</b>	<b>RESULTS AND DISCUSSION .....</b>	<b>72</b>
5.1	Laboratory test results.....	72
5.2	System Improvements.....	78



5.2.1	Camera resolution .....	78
5.2.2	Depth of Field .....	78
5.2.3	Calibration Equipment .....	79
5.2.4	Mounting base.....	79
5.2.5	Laser-line shadowing.....	80
5.2.6	Laser-line intensity.....	81
5.2.7	Software improvements .....	82
5.3	Wood Machining Tolerances .....	82
5.4	System Applications .....	82
<b>6</b>	<b>CONCLUSION .....</b>	<b>84</b>
	<b>REFERENCE.....</b>	<b>87</b>
	<b>APPENDIX A: HARDWARE SPECIFICATIONS .....</b>	<b>92</b>
	<b>APPENDIX B: LENS ABERRATION TEST DATA.....</b>	<b>93</b>
	<b>APPENDIX C: 3-POINT CIRCLE FIT .....</b>	<b>96</b>
	<b>APPENDIX D: CONTROL CHARTS FROM COLLECTED DATA .....</b>	<b>98</b>
	<b>APPENDIX E: PART DRAWINGS.....</b>	<b>110</b>
	<b>APPENDIX F: ANOVA TEST DATA.....</b>	<b>111</b>
	<b>APPENDIX G: BONFERRONI TEST .....</b>	<b>112</b>
	<b>APPENDIX H: NORMAL PROBABILITY PLOT .....</b>	<b>113</b>

## List of Tables

Table 1. Example of calibration ratio. ....	54
Table 2. Varying degrees of polynomial tested. ....	56
Table 3. Example data used in 1 <sup>st</sup> order simple linear polynomial fit. ....	58
Table 4. ANOVA test results. ....	77
Table 5. Bonferroni test results. ....	77

## List of Figures

Figure 1. Furniture exports growth trends (excluding patio furniture) (Statistics Canada, 2003). 6	6
Figure 2. Furniture Sales Revenues/Housing Starts relationship. The increase in furniture sales is proportionate to housing starts (Statistics Canada, 2003). .... 7	7
Figure 3. Users of statistical process control are generally larger plants (Anderson & Patterson, 1996, p. 37). .... 10	10
Figure 4. Quality control programs within British Columbia value-added wood sector by revenue. Most companies use informal/in-house quality programs (Kozak & Maness, 2001, p. 52). .... 11	11
Figure 5. Hypothetical control chart monitoring plywood thickness that is in control. .... 14	14
Figure 6. Hypothetical plywood boards showing different amounts of within board variation. . 15	15
Figure 7. Hypothetical Range chart: Board A is acceptable and Board B is not acceptable. .... 16	16
Figure 8. Hypothetical control chart monitoring plywood thickness heading towards an out of control situation. .... 17	17
Figure 9. Pattern Projection technique; laser-line illuminates object for camera. Changes in elevation across the component cause the laser-line to appear stepped (Cielo, 1988, pp.301). .... 20	20
Figure 10. Basic triangulation used in pattern projection. From the camera's perspective, the laser-line will appear stepped between the two elevations ( $h_1$ and $h_2$ ). The distances ( $w_1$ and $w_2$ ) between the stepped laser-line is used to calculate the elevations of step $h_1$ and $h_2$ . .... 21	21
Figure 11. Edge distortion caused by varying magnification across the lens (Nikon, 2004). .... 22	22

Figure 12. Coma caused by light rays not passing through a single focal point (Kidger, 2002, pp. 72). .....	22
Figure 13. Image containing coma (bright spots) (Nikon, 2004). .....	23
Figure 14. Curvature of field caused by curved focal plane. ....	23
Figure 15. Log scanner (left) and Cant scanner (right) (LMI 3D Machine Vision, 2004). ....	24
Figure 16. Wineman Technology's wheel scanner is another example of a machine vision system used in the automotive industry (Masi, 2003, pp. 24,25). ....	25
Figure 17. Machine vision based surface roughness measurement system (Sandak and Tanaka, 2005, p. 271). ....	26
Figure 18. ODAC <sup>®</sup> (left) and SIMAC <sup>®</sup> (right) are systems used for measuring plastic extrusions, wires and pipes (Zumbach Electronics AG, 2004). ....	27
Figure 19. Profilemaster CCD/Laser arrangement (left) and measured profiles (right) (Zumbach Electronics AG, 2004). ....	28
Figure 20. Tongue and Groove (T&G) Joint. ....	30
Figure 21. Rebate joint (left) and Mortise and Tenon joint (right) (diyidata.com, 2004). ....	31
Figure 22. Chamfer. ....	32
Figure 23. Non-conforming chamfers (Canwood Furniture Inc. 2002). ....	33
Figure 24. DET out-feed. Cutter and sanding heads are located in each of the machine stations. Both ends of the component are profiled through one pass. ....	35
Figure 25. DET main machining components. ....	36
Figure 26. Preliminary scanning hardware setup and scans of tongue components taken at Canwood Furniture Inc. ....	37
Figure 27. Test apparatus - parts. ....	39
Figure 28. Calibration/Test Grid used to test for Aberrations. ....	41

Figure 29. Perspective causes the boy on the near sidewalk to appear taller than the boy on the opposite sidewalk (Microsoft, 2005). .....	43
Figure 30. Cross-sectional view of the AQCS prototype system showing hardware location. ...	44
Figure 31. Perspective distorted tongue scanned image (left scanned data / right cross section of part / bottom comparison of captured image and real world). .....	44
Figure 32 Effects of depth perspective distortion compared to real world position. ....	46
Figure 33. Components and the operation of a telecentric lens (Wilson, 2004, p. 37). ....	47
Figure 34. Image acquisition user interface. ....	48
Figure 35. Example of image acquisition software acquired text file. ....	49
Figure 36. Stepped Calibration Block. ....	50
Figure 37. Laser-line alignment setup. ....	50
Figure 38. Sequence of flat calibration block calibration images. ....	51
Figure 39. Sequence of overlaid calibration block images showing magnification distortion. ...	51
Figure 40. Stepped calibration block image. ....	52
Figure 41. Image of flat calibration block with bounding box applied. ....	52
Figure 42. Example of image converted into line segments and end points. ....	53
Figure 43. 1 <sup>st</sup> order simple linear regression fit. ....	54
Figure 44. Groove image converted into defining points and calibrated (1. original image, 2. un-calibrated end points, 3. calibrated end points overlaying un-calibrated end points). 56	
Figure 45. Based on the centroid; $Y_1$ is distance between the first step and the second step. $Y_i$ 's are found for every object in the image. ....	57
Figure 46. Depth distortion calibration polynomial fit. ....	58
Figure 47. Distortion calibration routing repositioning groove to correct position. ....	59

Figure 48. Calibrated critical dimensions on the tongue (A. Left shoulder depth, B. Left shoulder width, C. Tongue width, D. Right shoulder width, C. Right shoulder depth. .....	60
Figure 49. Transition point used to separate board surface and chamfer face.....	61
Figure 50. Chamfer laser-line is filtered to generate a single line. ....	62
Figure 51. Hypothetical chamfer with minimum and maximum data point highlighted.....	63
Figure 52. Three-point circle fit equation fitting a circle between the minimum, maximum points and a test point. ....	64
Figure 53. Multiple test-points chosen to verify three-point circle fit equation. ....	64
Figure 54. Radius calculated for each test-point. The smallest radius, (16,1) is the break point. .....	65
Figure 55. Board surface length, chamfer face length and chamfer angle are used in control charts. ....	65
Figure 56. Steps required in preparing data for control charts. ....	67
Figure 57. Subalpine fir test parts. ....	68
Figure 58. Solarius Development LaserScan profilometer. ....	69
Figure 59. Defective components TM3 and GM5. ....	70
Figure 60. Defective components T1 and G9. ....	70
Figure 61. Distance “A” is beyond the profilometer’s scanning range. ....	71
Figure 62. Subalpine fir parts affected by drying stresses. ....	73
Figure 63. Average measurements of both shoulders of part TM3 from the three measurement methods. ....	74
Figure 64. Average measurements of both shoulders of part GM5 from the three measurement methods. ....	74

Figure 65. Average measurements of both tongue depth of T1 and G9 from the three measurement methods.....	75
Figure 66. Measurement variation results from each measurement method. ....	76
Figure 67. Calibration block focusing problem. ....	79
Figure 68. Shadowing due to offset laser-line. ....	80
Figure 69. Overlapping laser-lines to eliminate shadowing. ....	81
Figure 70. Laser A illuminates Laser B's shadowed areas and vice versa. ....	81

# 1 Introduction

The Canadian secondary wood products industry is a highly competitive sector that faces stiff competition both from wood and non-wood producers such as plastics, glass and steel. Although the industry is rapidly growing and a major contributor to the national economy, it lacks the same levels of cost efficiency found in its European and Asian counterparts. To reduce operating costs, European companies have utilized highly efficient manufacturing technologies, while Asian companies have relied on low labour costs. To improve competitiveness, Canadian companies need to reduce operating costs without compromising product quality.

Statistically based quality control is one potential cost saving technology that is currently highly underutilized in Canadian secondary wood products companies. An effective statistical quality control program can increase cost efficiency by both increasing throughput and decreasing waste. By monitoring the manufacturing process with a quality program, potential tolerance and conformance problems are caught before rejected components are produced. Quality programs can also help pinpoint and diagnose processes with chronic quality problems. This reduces time and materials wasted to rework or replace rejected components. Traditional quality control programs are inefficient because they require staff to pull components off the production line for inspection. To eliminate this inefficiency, some industries have adopted sophisticated automated real-time quality control systems that automatically collect and analyze quality data without disrupting the manufacturing process.

Canadian secondary wood products companies have expressed several concerns with automated quality control programs. Firstly, many Canadian companies are



relatively small compared to their global competitors so they lack the necessary capital to implement and maintain sophisticated quality systems. Secondly, they feel that quality systems may not have the flexibility for their small and customized production runs; Canadian companies often require flexibility because most machine centers will produce a variety of different components in a single production day. The proposed system will address these two concerns since there are currently no affordable automated quality control systems that are dedicated to the secondary wood products industry in Canada. This research explores the possibility of developing an affordable real-time quality control system tailored specifically to the Canadian secondary wood industry.

## 2 Objectives

This research attempts to improve the competitiveness of the Canadian secondary wood products industry by developing a proof of concept for a low cost and highly flexible automated real-time quality control system (AQCS). The system will utilize proven technologies that are being utilized in other industries and adapt them to a system that fulfills the requirements of Canadian companies. The proof of concept system was developed as a case study at Canwood Furniture Inc. The objective of this project were as follows:

- Measure to an accuracy of 0.1 mm;
- Accommodate all angular parts leaving any machine center;
- Simple and quick setup procedure;
- Track machine performance by producing X-bar and S Charts; and
- Inexpensive to implement and maintain.

### **3 Background**

#### ***3.1 Importance of Secondary Wood Products to Canada***

Through exports and employment, the primary lumber industry has long been a major contributor to the Canadian economy. In 1999, the Canadian lumber industry shipped \$19.6 billion worth of product (Industry Canada, 2003). The United States is Canada's largest market with approximately \$10 billion worth of annual softwood lumber shipments (Industry Canada, 2003). However, increasing foreign competition has hampered the industry (Industry Canada Manufacturing Branch, n.d.). For example, between the years 1997 to 2002, 27 sawmills were shut down and 13,000 forest-based jobs were lost in British Columbia (British Columbia Ministry of Forests, 2003). The decline in the lumber industry has brought on industry-wide restructuring. Companies have had to diversify to meet their customers' changing needs or face closure. The secondary wood products sector has also faced similar events.

The sector experienced positive growth throughout the 1980s, reaching its peak in 1988. However, growth was suddenly adversely affected with the introduction of the Free Trade Agreement (FTA) in 1989 and a recession between 1990 and 1991 (Industry Canada, 1999). For many years, the sector operated under the protection of high tariffs, but the FTA eliminated these tariffs, forcing an industry-wide restructuring. Many companies were forced to consolidate into larger organizations to improve production efficiencies and lower operating costs.

For example, in British Columbia, the restructuring led to the rebirth of a smaller, yet improved industry, where production and exports grew rapidly. For the first time, in 1995, exports exceeded imports. The industry, at this point in time, consisted of an

amalgamation of furniture, cabinets, architectural millwork, engineered wood products, remanufactured products, pallets, and novelty/crafts/artwork producers, mostly made up of small single plant family run operations and large plants. The main products being manufactured include (Kozak & Maness, 2003, p.96):

- Remanufactured wood products
- Shakes and shingles
- Pallets and boxes
- Fences
- Miscellaneous other products
- Engineered wood products
- Mouldings, millwork and flooring
- Doors and windows
- Cabinetry
- Furniture
- Home systems

With growing environmental concerns from the general public, the industry and government have both placed a greater emphasis on the growth of value-added wood products (Industry Canada, 2003). Canada is the 4<sup>th</sup> largest exporter of furniture in the world in 2004, with China being the largest exporter (U.E.A, 2005). The United States is Canada's largest export market (Industry Canada, 2003). The majority of the industry is located in Central Canada, where 82% of the firms reside in Quebec and Ontario and the remainder are split between Western Canada (13%) and Atlantic Canada (5%) (Industry Canada, 2003).

In 2001, furniture and related wood products firms employed 103,609 people across Canada and earned \$13.1 billion (\$7.5 billion from export sales) (Industry Canada, 2003). Statistical data show a yearly increase of approximately 17.3% per year in exports of household furniture for all of Canada (Figure 1).

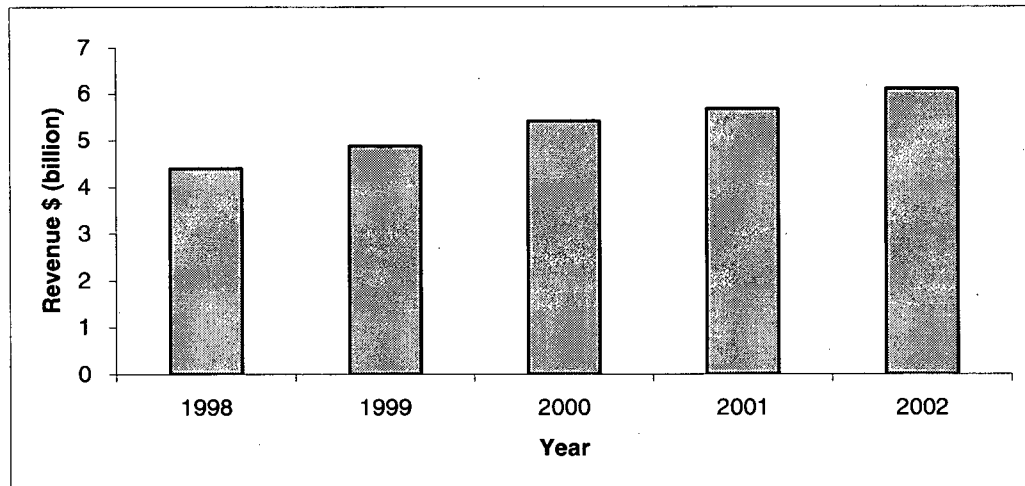


**Figure 1. Furniture exports growth trends (excluding patio furniture) (Statistics Canada, 2003).**

The increasing demand for secondary products is the result of a variety of different factors. Although it initially hindered growth, the Free Trade Agreement has allowed Canada to more easily export its secondary wood products to the United States, making it the largest consumer of Canadian secondary wood products. In the short-run, demand for furniture and other secondary wood products will fluctuate with the rise and fall of the economy as consumers are willing to spend their disposable incomes more freely during prosperous times (Industry Canada, 2003). In the long run, housing starts and population growth will dictate the demand for secondary products (Industry Canada, 2003). Figure 2 shows the increasing parallel trends of sales revenue in Canada for housing starts and furniture.

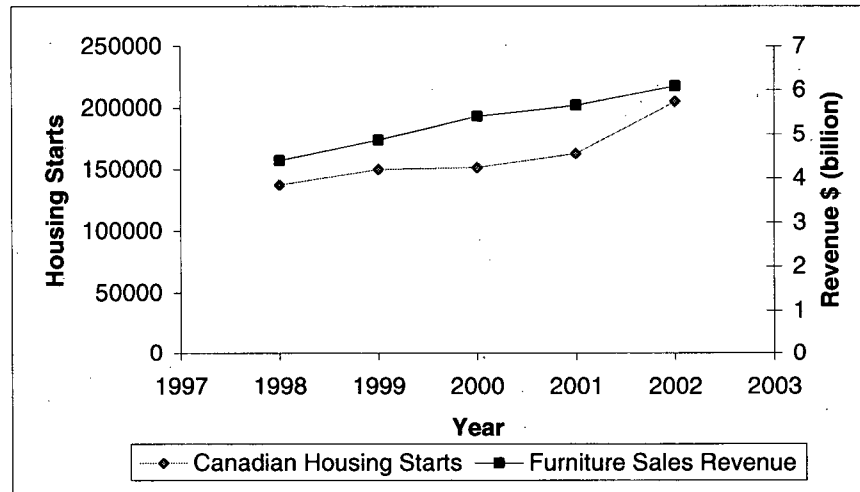


**Figure 2. Furniture Sales Revenues/Housing Starts relationship. The increase in furniture sales is proportionate to housing starts (Statistics Canada, 2003).**

The restructuring of the secondary wood industry has led to substantial improvements, but the industry must be prepared to deal with new challenges (Saint-Pierre, 1999). For example, globalization is one growing challenge that the industry faces. Globalization can help create new foreign markets for Canadian products, but it can also increase competition within these new markets (Statistics Canada, 2003). This will also increase competition within the Canadian domestic market since foreign companies will have freer access. Currently, the greatest competitive threats come from Europe and Asia.

Due to high operating costs in Europe, its secondary wood products industry has been forced to optimize and automate. Optimization and automation have allowed European companies to produce high-end goods more efficiently and less costly than their Canadian counterparts (Europa, 2004). While being less technologically sophisticated, Asian and Mexican companies can generally offer better prices because of lower labour costs.

To maintain competitive pricing, Canadian companies need to minimize operating costs. Currently, Canadian companies are losing up to 5% of their revenues due to defective parts (Chiu, personal communication, 2003). This problem is mainly attributed to the lack of proper quality standards and systems (Chiu, personal communication, 2003). Organizations such as the Wood Products Quality Council (WPQC) have been developed to aid in the development and implementation of quality control standards within the Canadian secondary wood products sector. However, it is possible to reduce costs even further with the addition of automated quality control systems (AQCS) capable of monitoring production in real-time.

### ***3.2 Current Quality Control Technologies in the Secondary Wood Industry***

The secondary wood products industry is composed of several large-scale operations that generate hundreds of million dollars a year in sales revenues. However, as a whole, the industry is mainly composed of small design-oriented shops, with limited access to capital, a history of low paying jobs and a poorly educated workforce. For these reasons, the industry lacks the advanced quality control technologies found in other manufacturing industries (Kozak & Maness, 2001). In most Canadian shops, measuring tapes and digital calipers are the only quality control tools being used; however, the user and the inspection process limits the effectiveness of these tools. The user's judgment and fatigue can affect the accuracy of the measurements. These tools are also not conducive in a real-time quality control system because the workers must stop production and pull parts off the production line for inspection. This is a time consuming process where only a small sample of parts are inspected.

Moreover, most high volume factories that produce more than one particular product at a time will use batch processing, a production method where each machine centre is configured to repeatedly perform one dedicated operation per setup (Edgar, 2004). Processing identical parts in a batch improves throughput because dedicated machines can process parts more quickly and the number of setups are reduced (Lucero & de Queiroz, 2004). However, efficiency is lost whenever production is slowed down or stopped. This makes measuring tapes and digital calipers inefficient quality control tools because workers must slow or stop the machines to remove parts and perform quality checks.

### **3.2.1 Levels of SPC being used**

Unlike other manufacturing industries where SPC programs are used extensively, the secondary wood industry has not yet widely adopted these techniques. This was shown in a survey of 125 furniture and 75 cabinet manufacturers across the United States that determined the levels of statistical methods used for quality control in manufacturing operations (Anderson & Patterson, 1996). Although the survey was conducted in the United States, the results may reflect Canadian companies because they operate within similar cultures. The survey shows that larger companies are more likely to have a QC system than smaller companies (Figure 3) (Anderson & Patterson, 1996).



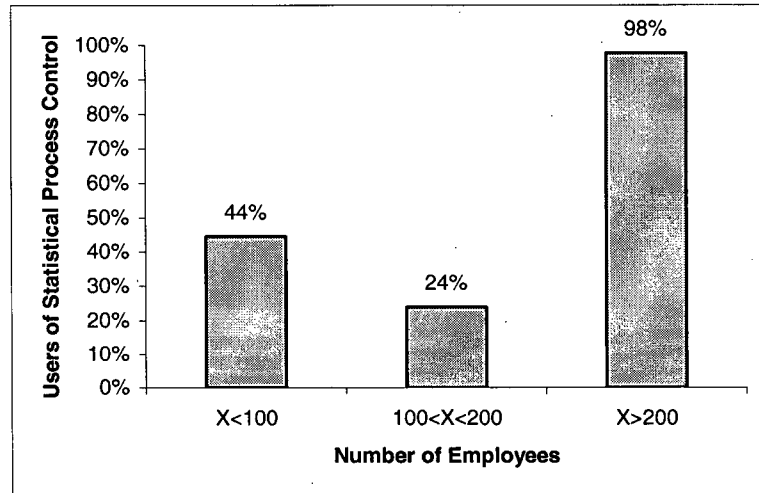


**Figure 3. Users of statistical process control are generally larger plants (Anderson & Patterson, 1996, p. 37).**

Generally, larger companies have larger operating budgets and produce larger volumes, making it possible to fund and use statistical process control (SPC) based quality control systems. A survey conducted in British Columbia (Kozak & Maness, 2001) has also shown that companies with lower sales revenues are less likely to have quality control programs in place (Figure 4).

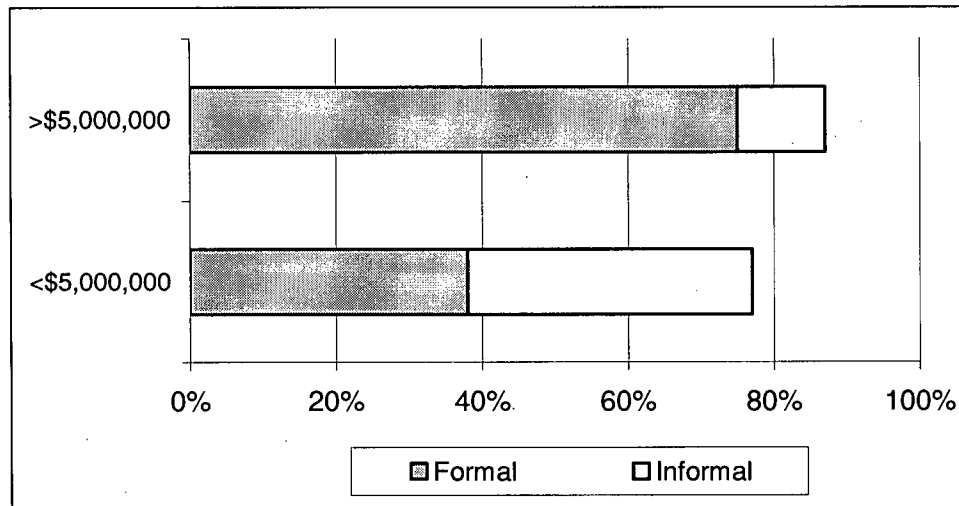


**Figure 4. Quality control programs within British Columbia value-added wood sector by revenue. Most companies use informal/in-house quality programs (Kozak & Maness, 2001, p. 52).**

Unfortunately, the industry in British Columbia and many parts of Canada is mostly composed of small shops, implying that a large percentage of the industry does not use SPC.

### **3.2.2 Industry's Attitude towards Quality Control (WPQC Interview)**

To gain a better understanding of the industry's position on quality control (QC), an interview was conducted with the Wood Products Quality Council (WPQC) based in Vancouver, Canada, which works to educate and implement the WOODMARK Quality System in Canadian secondary wood products companies (Chiu, personal communication, 2003). According to the WPQC, most companies expressed difficulties in justifying the implementation of a QC system when first visited by the WPQC. Company owners believe that QC is a waste of money and will slow production, while workers fear that QC programs will cut jobs.

This belief may stem from a lack of understanding and formal training. Product consistency is lost without a system or standards since quality is at the mercy of each employee's personal judgment and motivation to enforce. Judgment from the same employee will also differ throughout the day because of human error. In some companies, this lack of knowledge has also led to improper implementation of in-house developed QC systems. Problems with improperly maintained QC equipment has also lead to quality problems.

Based on WPQC records, the lack of a proper QC system can cost a company between 2% to 5% of its revenues (Chiu, personal communication, 2003). Companies using WPQC quality programs have found substantial savings and have quickly repaid their initial startup costs. Even though many of the value-added wood producers stated that the process of quality certification was difficult to implement, approximately 90% said that they would definitely go through the process again and that it was definitely "worth it." More than 60% of the companies interviewed felt that the quality assurance program that they had implemented had been effective in increasing profitability. Based on the opinions expressed by industry and the WPQC, cost is one the major barriers hindering the further use of SPC systems.

### ***3.3 Quality Control***

Traditionally, quality was defined as the product's fitness for use, which was broken down into quality of design and quality of conformance (Montgomery, 1997, p.4). Quality of design relates to how well the product was designed based on engineering, materials, reliability and specifications, while quality of conformance relates to how well the product meets design specifications (Montgomery, 1997, p.4). In 1978, the American

National Standards Institute offered a standardized definition of quality as, “the totality of features and characteristics of a product or service that bears on its ability to satisfy given needs” (American Society for Quality Control, 1978). However, this definition does not address a major cause of quality issues, that being variability. It is inherent and normal that small amounts of variability exist in all manufactured goods and it is at the discretion of the manufacturer to set limits on acceptable levels of variation. Variability becomes a quality problem when these limits are exceeded. Therefore, the modern definition states that quality is inversely proportional to variability, where minimizing variability is highly desired (Montgomery, 1997, p.5).

### **3.3.1 Statistical Process Control: Monitoring Variability**

Statistical process control (SPC) refers to the seven tools used to monitor variability (Montgomery, 1997, pp.12-14). They are as follows:

- Histogram or stem-leaf display
- Check sheet
- Pareto chart
- Cause and effect diagram
- Defect concentration diagram
- Scatter diagram
- Control charts

Of the seven tools, controls charts were found to be the most suitable tool for the AQCS. Control charts can monitor critical dimensions of a product and graphically display any variation problems (Young & Winistorfer, 1999, p. 13).

The  $\bar{x}$  ( $\bar{x}$  bar) chart (also called the mean chart) and the R chart (also called the range chart) are the two most commonly used control charts for measuring variation. The  $\bar{x}$  chart can be used to monitor a specific dimension on a part. For example, Figure 5 shows a hypothetical  $\bar{x}$  chart monitoring plywood thickness.

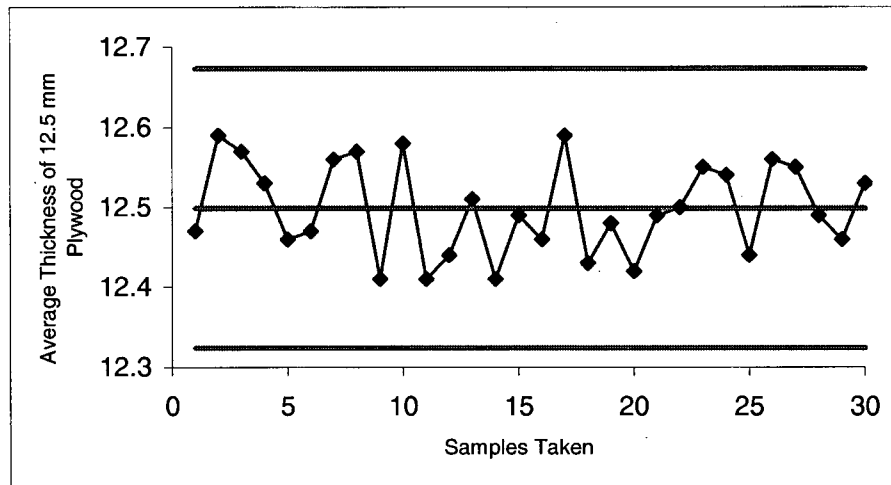


**Figure 5. Hypothetical control chart monitoring plywood thickness that is in control.**

The centerline in the control chart is the grand sample mean ( $\bar{\bar{X}}_{GM}$ ) and, for this example, the centerline represents the average plywood thickness or target thickness (Bluman, 1997, p.664). The two remaining horizontal lines are the upper control limit (UCL) and lower control limit (LCL), each calculated based on acceptable natural amounts of variation found in the system (Bluman, 1997, p.664). During production, samples are measured and plotted on the chart and the dimension being inspected must fall within the UCL and LCL.

Under certain circumstances, the averaging of the values used to calculate the sample means could inadvertently hide out-of-control measurements and create a  $\bar{x}$  chart that appears to be in control (Montgomery, 1997, p.211). For demonstration purposes,

Figure 6 shows two plywood boards that contain highly exaggerated within board variation.

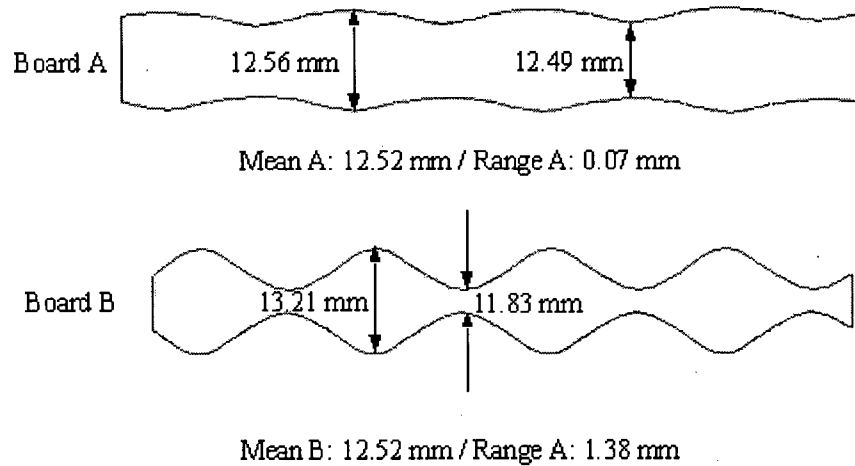


**Figure 6. Hypothetical plywood boards showing different amounts of within board variation.**

It is clearly evident that board B contains more within board variation compared to board A. However, the calculated sample means are identical at 12.52 mm. Even though board B is obviously nonconforming and should be rejected, this will not be apparent in the  $\bar{x}$  chart.

The R chart is used as a means of verifying the validity of the results obtained the  $\bar{x}$  chart. The R chart monitors the range between the maximum and minimum dimension of each sample and uses ranges to obtain the within sample standard deviation (Montgomery, 1997, p.180). An S chart can be used to monitor standard deviation directly, but the R chart is preferable because it only requires a small sample size ( $n < 10$  or 12) (Montgomery, 1997, p.185). Figure 7 shows an R chart for the sample boards

from Figure 5. Based on the control limits shown in Figure 5 and Figure 7, board A falls within the acceptable range, while board B falls outside of the acceptable range.

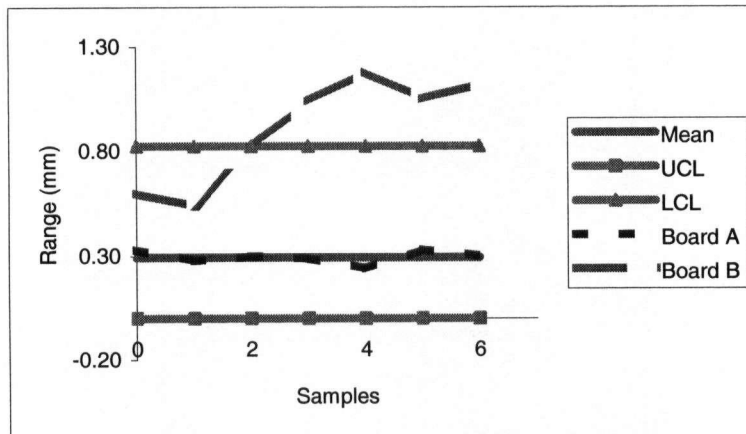


**Figure 7. Hypothetical Range chart: Board A is acceptable and Board B is not acceptable.**

Control charts can help prevent defects by warning machine operators of an impending out of control situation as shown in Figure 8, where the plot is shifting upwards towards the upper control limit (Montgomery, 1997, p.133). This shift warns the operator and allows the operator to make the necessary corrections before nonconformance (rejects) parts are produced.

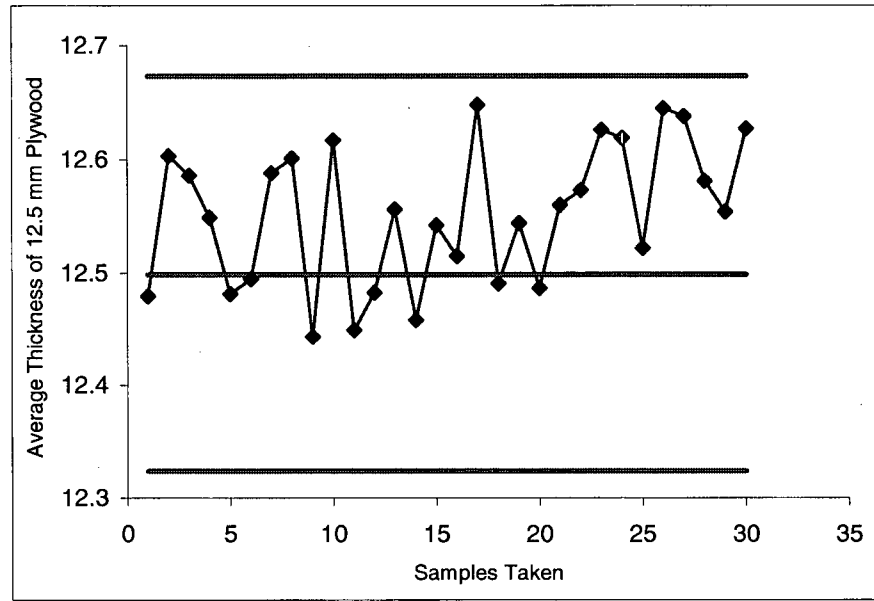


**Figure 8. Hypothetical control chart monitoring plywood thickness heading towards an out of control situation.**

Control charts can also act as process diagnostic tools (Bluman, 1997, p.665). Operators can correlate machine problems with changes in the control charts. Once the pattern of the problem has been recognized, operators can quickly link the patterns on the control chart to the mechanical problem and they know exactly what to fix with minimal downtime.

### **3.3.2 Statistical Process Control: Monitoring Attributes**

In addition to measuring variation, it is also possible to monitor specific quality characteristics/attributes to deem a part conforming or nonconforming. In most manufacturing processes, several quality characteristics are measured per part and if the item does not conform to standard on one or more of these characteristics, the item is classified as nonconforming (Montgomery, 19997). The control chart for fraction nonconforming or P-chart is one type of control chart used to monitor quality attributes.



### **3.4 Machine Vision Systems**

Modern day durable goods manufacturers have begun to embrace the concepts of machine vision as a means of improving productivity and quality (Harding, n.d.). Machine vision is a non-contact system where an image acquisition device, such as a camera, is used to collect an image of an illuminated object, which is then sent to a computer for analysis. Computers can monitor and track parts, alert operators when problems arise, or in real-time, make decisions and changes (Lawrence & Mauch, 1987, p.3). Machine vision systems are also non-contact; therefore, parts can remain on conveyors moving at full production speeds. These qualities suit the requirements of the AQCS. Machine vision systems are generally composed of a image acquisition device, illumination source and image analysis software. The following sections will describe the components, the machine vision technique used in the AQCS and some difficulties of machine vision.

#### **3.4.1 Machine Vision: Image Acquisition Device**

Optics based machine vision systems consist of an image sensor such as a digital camera, a light source and image processing software. Closed coupled discharge (CCD) and complimentary metal oxide semiconductor (CMOS) are the two digital camera technologies typically used in machine vision systems (Gurevich & Nice, 2004). Traditionally, CCD cameras are favoured because they deliver a high-quality, low-noise image, while CMOS cameras are relatively new and less favourable because they are susceptible to noise interference. However, CMOS cameras are cheaper and, with further development, may rival CCD cameras in the future (Gurevich & Nice, 2004). A CCD digital camera was used in the development of the AQCS.

### **3.4.2 Machine Vision: Illumination**

Different illumination sources are used in machine vision systems. The most common illumination sources include incandescent light bulbs, fluorescent tubes, light emitting diodes and lasers. The machine vision technique chosen for the AQCS required laser-based illumination. Lasers are commonly used in machine vision systems because laser light is highly consistent (Burke, 1996, p.245). Laser light can travel over great distances with minimal distortion. Laser light contains a specific wavelength; therefore, optical components, such as a camera, can be tuned specifically to a laser beam's wavelength, making the camera very sensitive to the laser beam but insensitive to external light sources, thus reducing noise and the possibilities of error (Cielo, 1988, p.112). Lasers can project a narrow beam of light either as a single point, single line or an array of lines or points. A single line laser was used in the development of the AQCS in this study.

### **3.4.3 Machine Vision: Technique**

Several optical metrology techniques are suitable for different inspection applications, but the pattern projection technique was found to be the most applicable technique for the system discussed in this report. By using a CCD camera and a diode laser-line, the pattern projection technique can be designed to measure three-dimensional objects such as the wooden profiles produced by value-added wood manufacturers. The laser-line is used to project a line across a three-dimensional surface. The CCD camera captures a monochromatic image of the laser lit object and a computer analyzes the image. The laser or the camera is tilted on an angle, while the remaining device is placed perpendicular to the object being scanned. This tilt causes a perspective change between

the laser-line and the camera. The perspective change causes the laser-line to shift laterally relative to the changing height of the object (Figure 9).

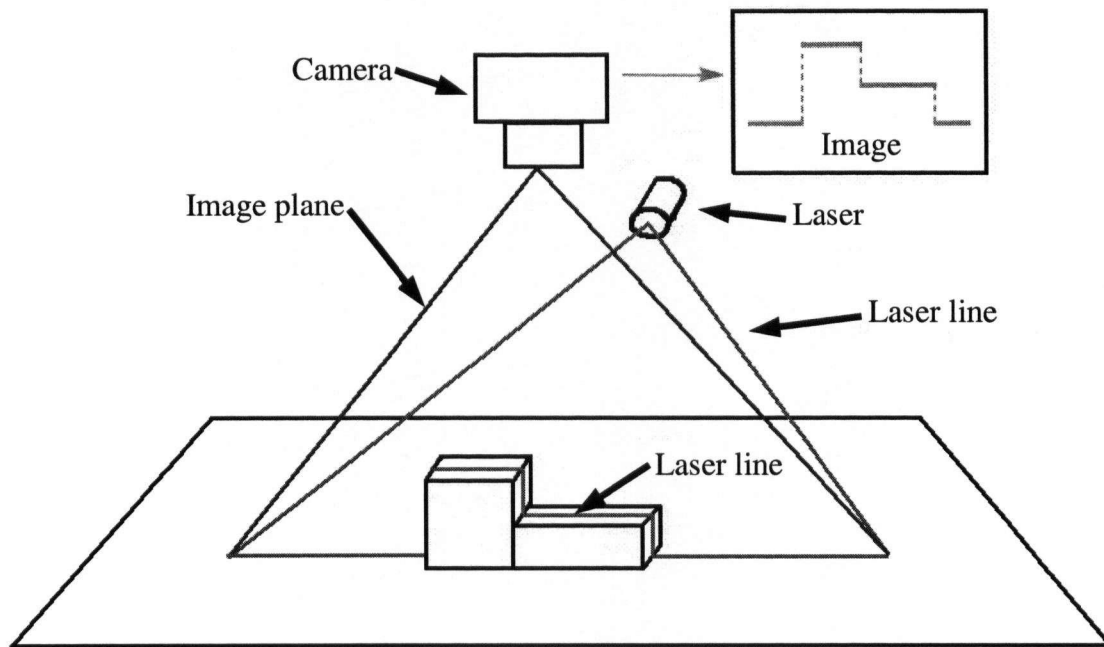


**Figure 9. Pattern Projection technique; laser-line illuminates object for camera. Changes in elevation across the component cause the laser-line to appear stepped (Cielo, 1988, pp.301).**

The width and height of the object can be measured based on the captured image in Figure 9. The width is the length of the horizontal lines in the image, while the height is determined through a triangulation technique based on the angle,  $\alpha$ , between the camera and laser-line (Figure 10). With the angle,  $\alpha$ , and the distances between the horizontal lines, basic geometry can be used to calculate the height change between each horizontal surface.

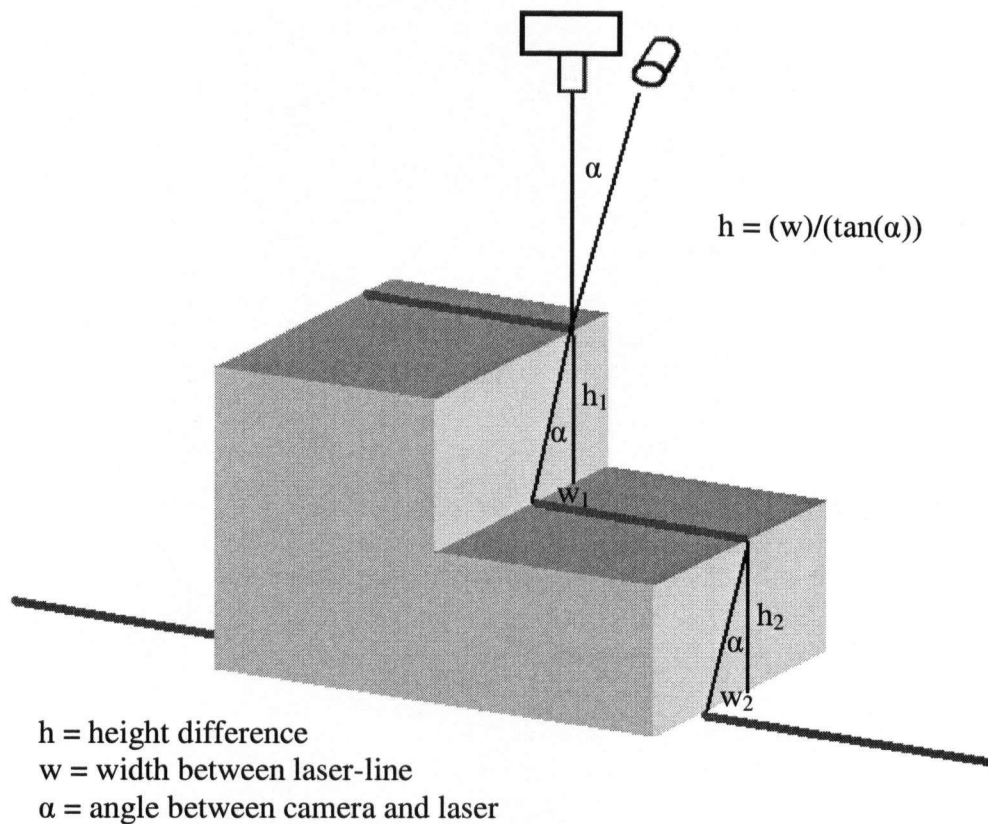


**Figure 10. Basic triangulation used in pattern projection. From the camera's perspective, the laser-line will appear stepped between the two elevations ( $h_1$  and  $h_2$ ). The distances ( $w_1$  and  $w_2$ ) between the stepped laser-line is used to calculate the elevations of step  $h_1$  and  $h_2$ .**

### **3.4.4 Problems with Machine Vision Systems**

Optical systems are, however, prone to problems such as lens aberrations (Kidger, 2002, p. 63). These are problems where the captured image is distorted, skewed and altered, making the image an inaccurate representation. Image distortion is a significant problem for machine vision systems because the accuracy of the system is dependant on the accuracy of the image. Typical forms of aberrations are pincushion, barrel, coma,

astigmatism and curvature of field. Varying magnification across the lens causes pincushion and barrel aberration (Nikon, 2004). This causes the edges of the image to become distorted (Figure 11).

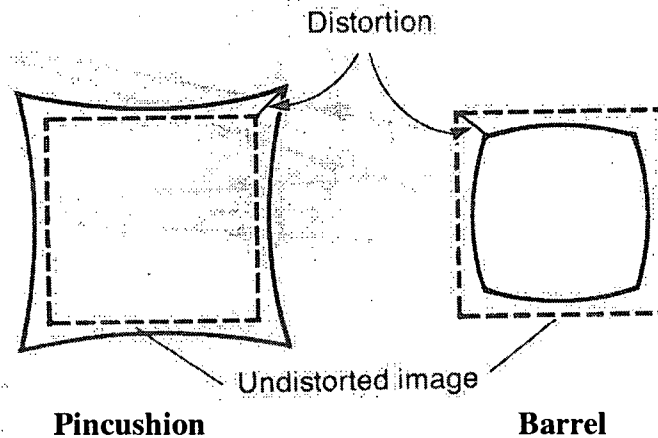


**Figure 11. Edge distortion caused by varying magnification across the lens (Nikon, 2004).**

In a perfect lens, light rays converge at one focal point, but in practice, light rays will not necessarily converge at the focal point, which causes coma aberration (Kidger, 2002, p. 72). The light rays that are projected onto the paraxial focus plane create bright spots (Figure 12 and Figure 13). Light rays entering near the edge of the lens are more prone to coma.

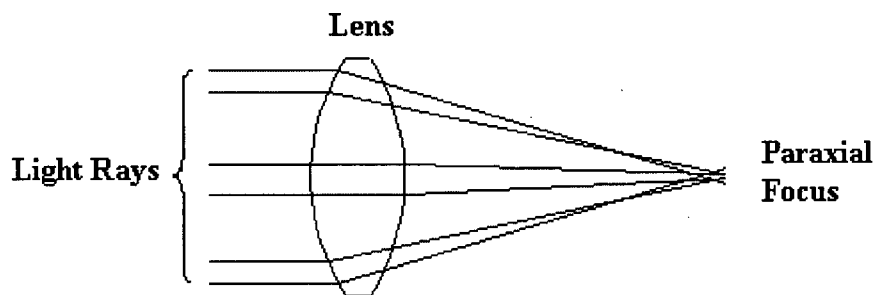


**Figure 12. Coma caused by light rays not passing through a single focal point (Kidger, 2002, pp. 72).**

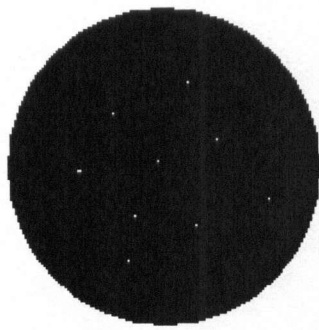
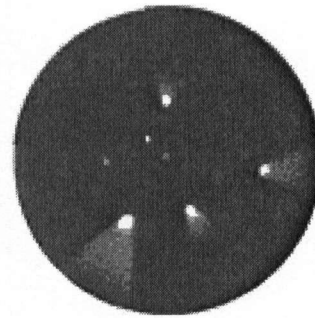


Image containing coma (1:1 scale)



Magnified image containing coma

**Figure 13. Image containing coma (bright spots) (Nikon, 2004).**

Curvature of field aberration occurs when the focal surface (CCD or CMOS chip) is not completely flat (Figure 14). This causes the center of the image to be in focus, while the periphery is out of focus; therefore, the edges of the image will appear blurry and not sharp.

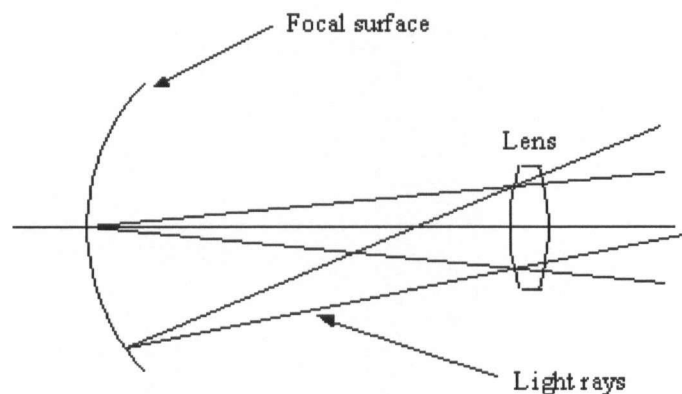


**Figure 14. Curvature of field caused by curved focal plane.**

Astigmatism aberration occurs when optical properties of the lens are not uniform. For example, the lens causes the image to only focus along one of its axes (horizontal or vertical). This type of aberration will cause the image to appear blurry.

### **3.5 Machine Vision Systems in Other Industries**

Machine vision systems are currently being used by a variety of other industries and the following are some examples that were used to guide in the development of the proof-of-concept AQCS. These systems may not necessarily use the same components as the AQCS, but they follow similar machine vision principles.

#### **3.5.1 Machine Vision in the Primary Lumber Industry**

Modern sawmills use machine vision systems in both primary and secondary breakdown processes to maximize yield. In primary breakdown, log optimizers use a laser and camera/sensor system to scan and model logs in 3-dimensions (Figure 15).

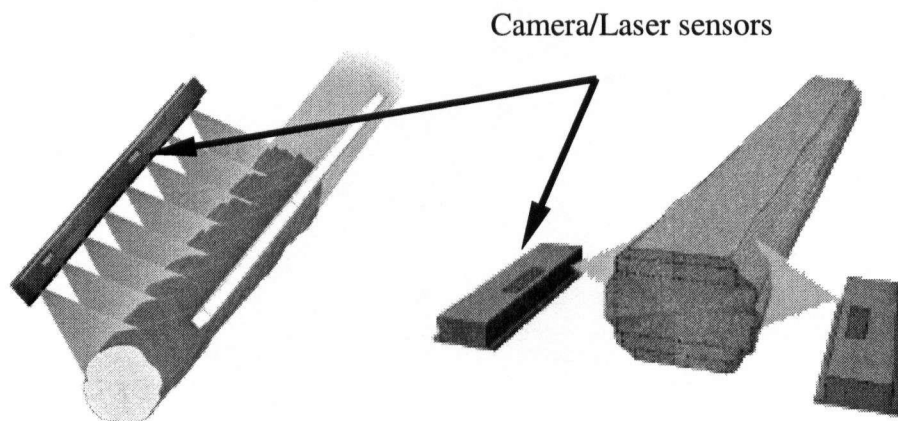


**Figure 15. Log scanner (left) and Cant scanner (right) (LMI 3D Machine Vision, 2004).**

Software processes the data and determines the optimum cutting pattern in real-time. The optimizing software can cut either for maximum lumber yield or, when markets demand a specific product, to produce a required product mix and maximize monetary returns. In secondary breakdown, cant optimizers operate on the same principal as log optimizers. Trimmer and edger optimizers are used to determine the optimum length and width of the

boards, and to detect wane<sup>1</sup> or damaged sections on the boards. Systems are also being developed to perform real-time quality control/size control in sawmills.

### 3.5.2 Machine Vision in the Automotive Industry

The automobile industry is another industry that uses machine vision to assemble and inspect engines, bodies, chassis and a variety of components. For example, Wineman Technology (Saginaw, MI, USA) has developed a machine vision system to inspect for damage and to sort a variety of cast-aluminum automobile wheel rims for 12 finishing lines (Figure 16) (Masi, 2003). Fluorescent lights and red LED backlights are used to illuminate the wheel and two CCD cameras capture an image of the wheel.

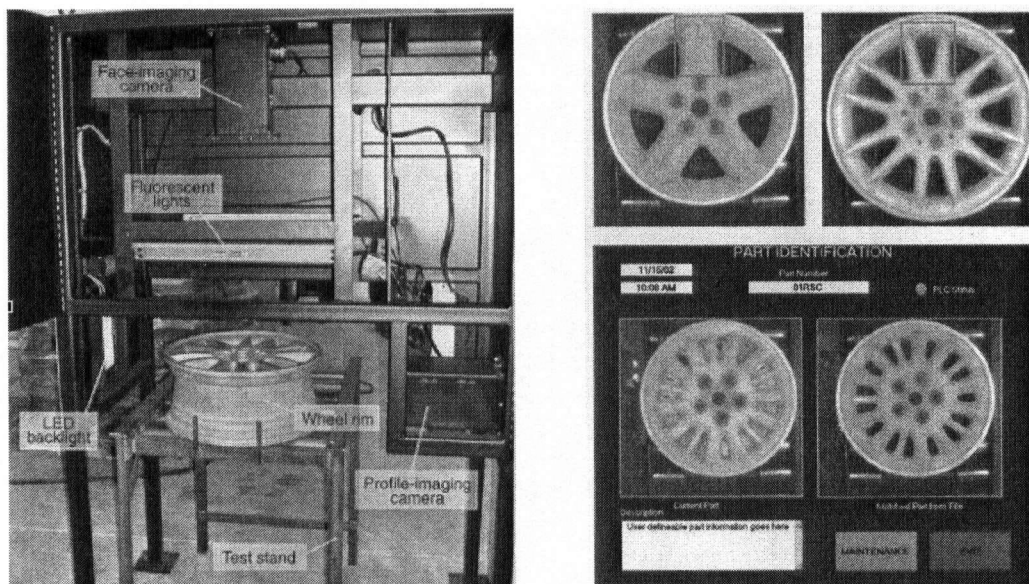


**Figure 16. Wineman Technology's wheel scanner is another example of a machine vision system used in the automotive industry (Masi, 2003, pp. 24,25).**

---

<sup>1</sup> Bark or lack of wood from any cause on edge or corner of a piece except for eased edges. (Forest Products Laboratory, 1999)



The system is able to identify part numbers, defects, different wheel widths and diameters, numbers of spokes and profiles of each wheel. According to Wineman Technology, their system is 99-percent accurate and much more efficient compared to manual sorting.

### 3.5.3 Machine Vision used to measure surface roughness

Jakub Sandak and Chiaki Tanaka have developed a machine vision based surface roughness measurement system. The system was developed to detect sawing defects by measuring the surface roughness of sawn boards. The system uses a digital video camera that is perpendicular to the surface and a tilted monochromatic light source (Figure 17). The light casts shadows across the surface, which is captured by the digital camera and analyzed.

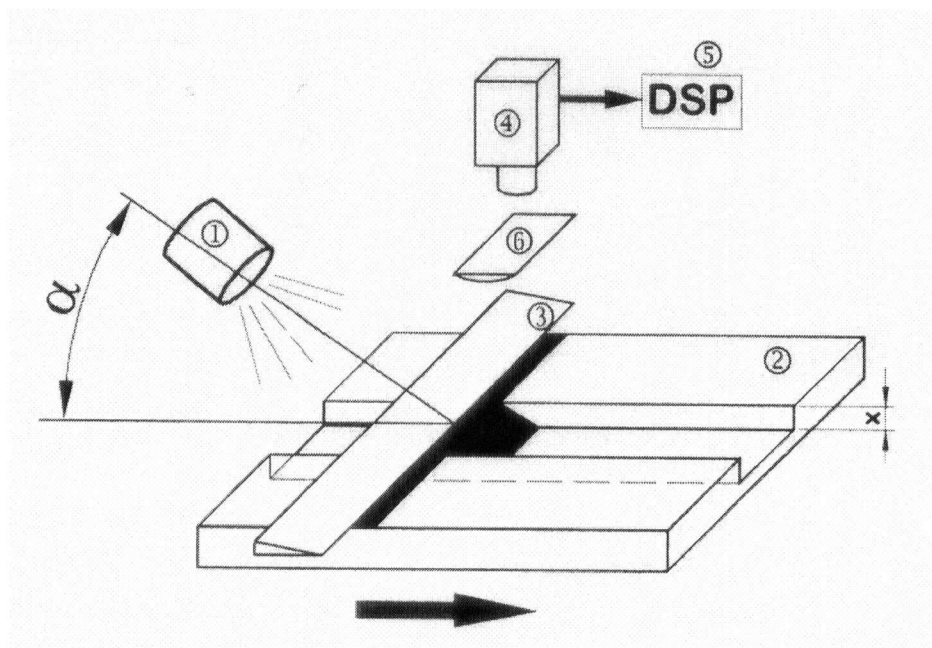


**Figure 17. Machine vision based surface roughness measurement system (Sandak and Tanaka, 2005, p. 271).**

### 3.5.4 Machine Vision in the Plastics and Metals Industry

Zumbach Electronics AG produces a variety of inline automated measurement and inspection systems for the plastics and metals industry, but does not offer any systems for the wood industry. ODAC<sup>®</sup> is a laser/CCD camera based machine vision system to measure wire, rod and pipe diameters (Figure 18).

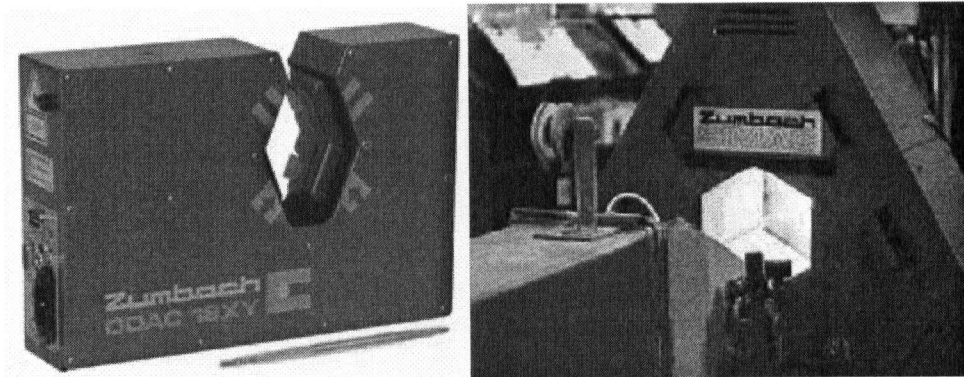


**Figure 18. ODAC<sup>®</sup> (left) and SIMAC<sup>®</sup> (right) are systems used for measuring plastic extrusions, wires and pipes (Zumbach Electronics AG, 2004).**

SIMAC<sup>®</sup> is a surface quality inspection system that uses a fluorescent light source and CCD cameras to collect images of metal and plastic pipes' surfaces (Figure 18). Profilemaster is used to inspect the profile of plastic and metal extrusions (Figure 19). This system projects onto the surface of the passing part and a CCD camera collects an image of the changing laser line.

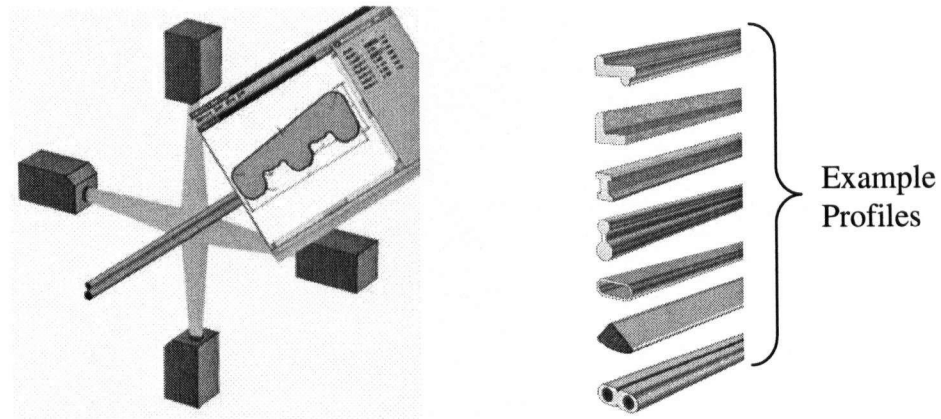


**Figure 19. Profilemaster CCD/Laser arrangement (left) and measured profiles (right) (Zumbach Electronics AG, 2004).**

However, unlike the prototype system, Profilemaster is designed to inspect materials with homogeneous surfaces, unlike wood which contains different grain patterns, different colours, knots and other acceptable but variable characteristics. The Profilemaster is also not suitable in the value-added wood industry because it can only accommodate an object that is no larger than 25x25 mm. This would limit inspection to very small parts and not the larger boards and panel products used in wood processing (Zumbach Electronics AG, 2004). The prototype system developed from this analysis will be designed specifically to suit the needs of the value-added wood industry.

### **3.6 Problem Areas in Wood Machining**

In mass production, individual parts are brought together during final assembly to form a single product. It is important that parts are produced consistently for quick and easy assembly. Consistency is achieved when variation within and between parts fall within the manufacturer's acceptable limits (Montgomery, 1997, p. 5). Inconsistencies will lead to problems in assembly where parts may fit poorly or not fit at all. In either case, the parts will need to be reworked or rejected completely and scrapped. Inconsistencies can stem from improper machine setup, tool wear, worn machine parts and inconsistent raw materials. Anecdotal evidence suggests that, in the woodworking industry, joinery problems are one of the leading causes of rework and rejects, and that this is a cause for major concern. With this in mind, the proposed system was developed to look at the commonly used tongue and groove joints and chamfer profiles.

#### **3.6.1 Tongue and Groove Joints**

Tongue and groove (T&G) joints are found in flooring, cabinetry, windows, doors, fencing and solid and composite wood furniture. The tongue and groove joint consists of a protrusion "tongue" that slides into a "groove" to create a strong and secure joint (Figure 20).

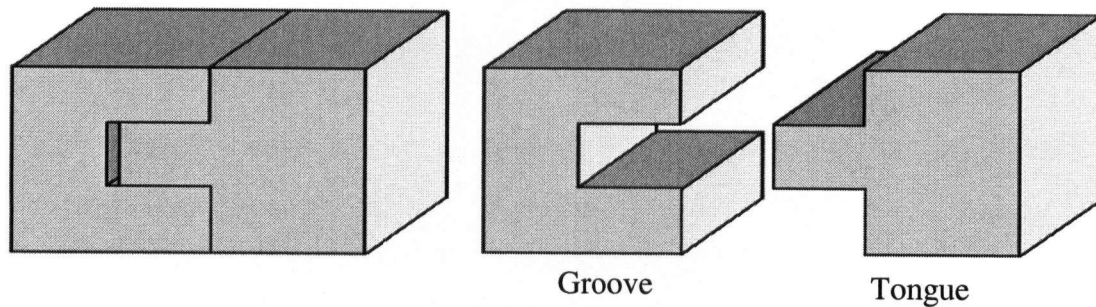


**Figure 20. Tongue and Groove (T&G) Joint.**

T&G joints can be produced with a variety of different machines and its design makes it well suited for mass production. The tongue and groove also helps to align parts during assembly, strengthens the product and weatherproofs joints (Cielo, 1988, pp.185). As for machine centers, small, low volume operations can use a table saw or table router to create the joint. Both machines have limited capacity and require multiple steps to produce one part. Because of the smaller volumes, machine operators can easily manually perform quality checks. Larger operations use automated machines such as power fed shapers, single or double-end tenoners or through-feed moulders. Shapers and single-end tenoners can only profile one edge per pass, while double-end tenoners and through-feed moulders can profile two or more parallel surfaces simultaneously. In most factories, these machines are equipped with dedicated tongue and groove tooling for quicker setup times, better-cut quality and quicker processing times. Unlike manually fed machines, mechanically fed tenoners and moulders run between 200 to 300 feet per minute, making it beneficial to use automated real-time quality control systems (Wong, personal communication, 2003).

The dimensions of the tongue and the groove are critical to the integrity of the joint. The joint must have a tight fit, but not so tight that glue used to secure the joint is squeezed out, thus, weakening the joint. An overly tight joint will also cause problems in exterior products because the moisture content will vary with the weather conditions and cause the wood to shrink or expand. If no room is allowed for expansion, the parts will crack under the pressure or cause the product to malfunction (e.g., a stuck window). Loose joints are problems because the excessive movement between the tongue and groove will weaken and misalign the joint. A misalignment of the tools used to profile the tongue and groove is another problem. Misaligned tongue and groove joints will either affect the appearance or the assembly of the parts. For example, in hardwood flooring, a misaligned tongue and groove will create a step in the floor. It should be noted that the tongue and groove joint was also chosen for this study because the shape can be easily applied to a variety of other wood joints such as the rebate and the tenon in a mortise and tenon joints (see Figure 21).

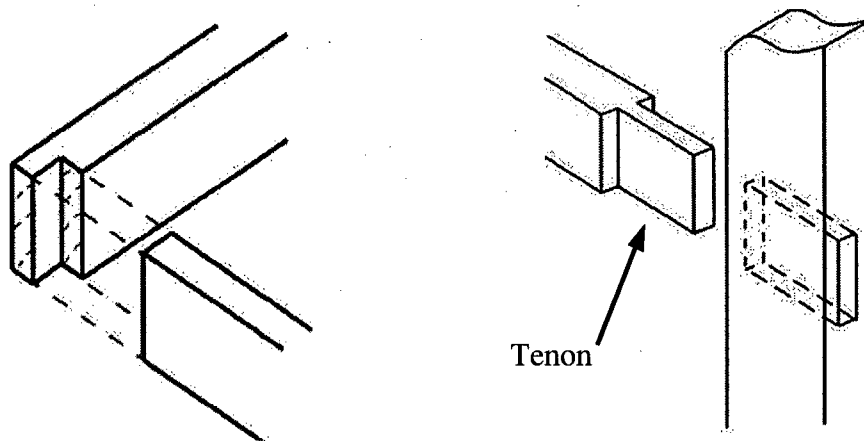


**Figure 21. Rebate joint (left) and Mortise and Tenon joint (right) (diyidata.com, 2004).**

### 3.6.2 Chamfers

A chamfer is a beveled cut, which is commonly 45-degrees, along the edge of a piece of wood that serves both aesthetic and functional purposes (Figure 22).

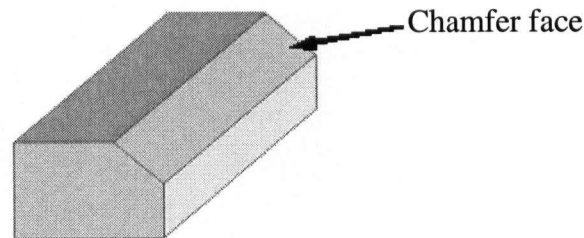


**Figure 22. Chamfer.**

Sawn and planed boards have sharp corners along their edges that are displeasing to the touch and are prone to chipping. The chamfer removes this sharpness. In some applications, chamfers are combined with tongues or grooves to create joints. The basic shape of the chamfer can also be found in a variety of different moulding applications. Like the tongue and groove joint, the chamfer can be made using a basic hand plane or with the same machines used to make the tongue and groove. The two critical dimensions in a chamfer are the width of the chamfered face and the angle of the chamfer. Nonconforming chamfers mar the aesthetics of appearance products, and in some cases, affect the fit and assembly of a product. The parts in Figure 23 are examples of nonconforming chamfers because each chamfered face is out of tolerance.

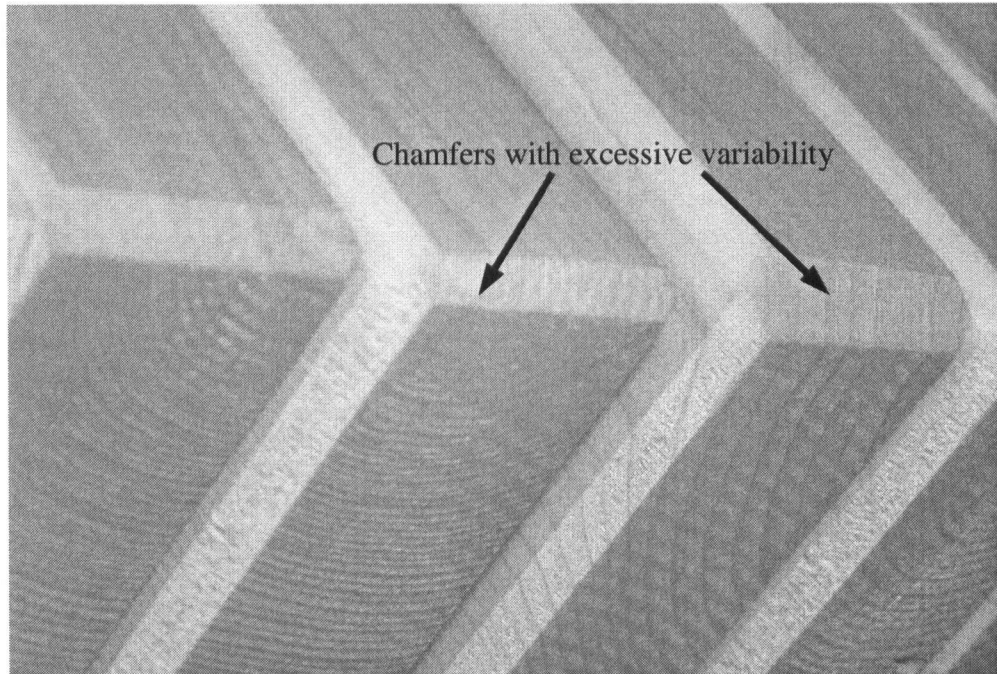


**Figure 23. Non-conforming chamfers (Canwood Furniture Inc. 2002)**



## **4 Methods**

With the assistance of an industrial partner and Forintek Canada Corp., a proof-of-concept AQCS was developed and tested. The laboratory system was designed to monitor parts leaving a double-end-tenoner (DET) because it was prone to tolerance problems, such as misaligned joints and profiles. Misalignment of joints and profiles affect the aesthetics and assembly of finished products. Therefore, the system was specifically designed to monitor the commonly used tongue and groove joints and chamfer profiles.

### ***4.1 Preliminary Trials***

To assist in the development of a prototype quality control system, a visit was made to Canwood Furniture Inc. to gain a better understanding of their production and products. Canwood Furniture Inc. is a medium size furniture manufacturer located in Penticton, British Columbia, Canada, with a 120,000 sq. ft. facility and 130 employees. Canwood Furniture Inc. produces solid pine dining, bedroom and living room furniture. Canwood's machine centres were evaluated to determine which one was most prone to tolerance problems and would benefit from the installation of the AQCS. Based on the machine evaluations and a recommendation from management, the double-end-tenoner (DET) was chosen. This machine is prone to tolerance problems due to setup errors and mechanical problems. The machine operators also stated that the machine required long and difficult setup periods and a real-time dimension verification system would improve the setup process.

### 4.1.1 Double-End-Tenoner

The double-end-tenoner (DET) is a high production machine used to edge profile and size solid wood and composite panel products. The DET is automated through-feed machine with two banks of machine stations, where one side is fixed and the other movable (Figure 24). Parts are fed through the machine on a pair of chain or belt conveyors.

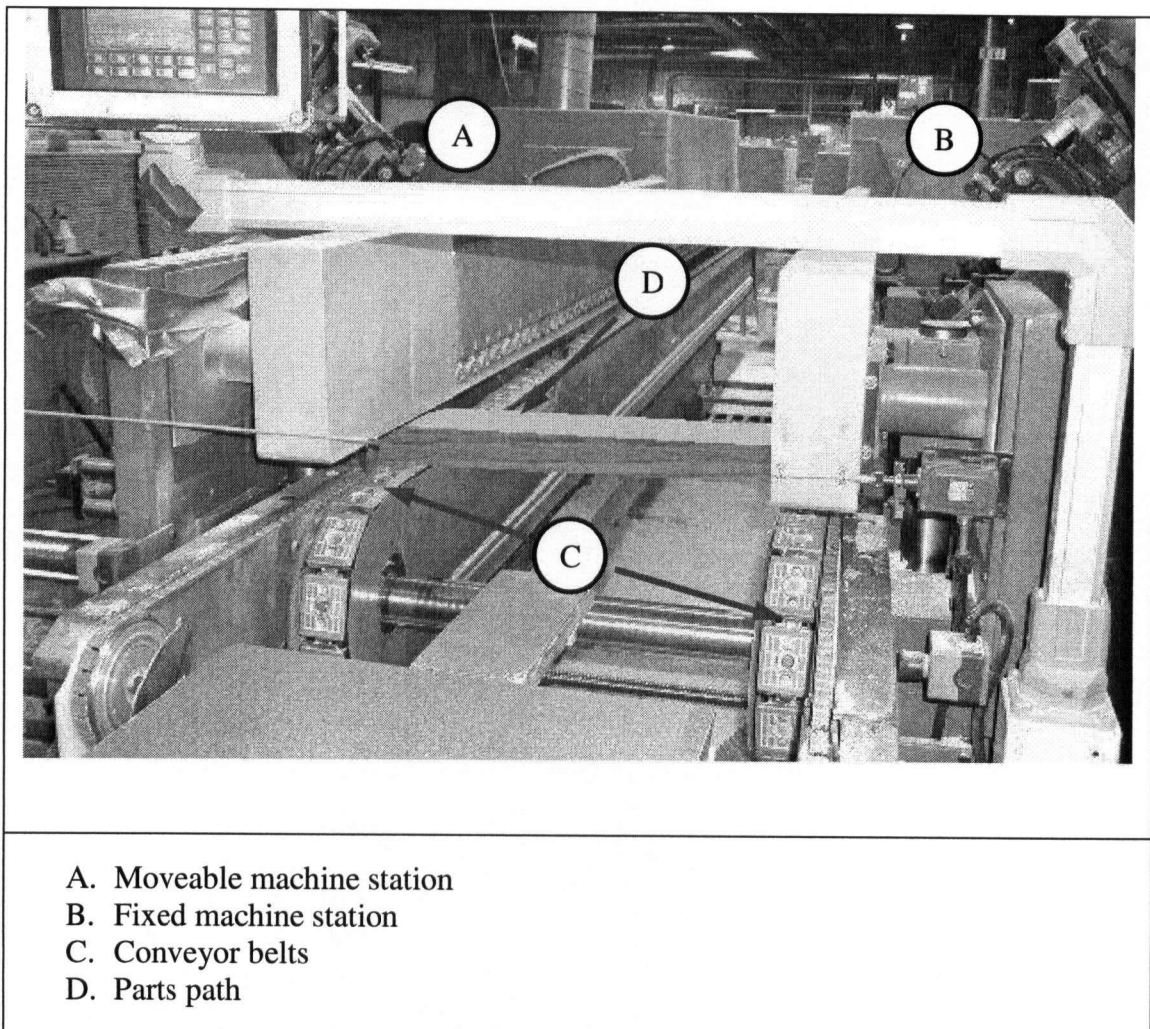


**Figure 24. DET out-feed.** Cutter and sanding heads are located in each of the machine stations. Both ends of the component are profiled through one pass.

The DET is modular, and a large number of different tools may be mounted on the machine. The first tools mounted on both sides are generally trim/scoring saw sets, which permit panels to be cut with exactly parallel surfaces (Figure 25). The distance between the two sides of the machine determines the length of the cut stock, and it can be adjusted with great accuracy. For solid wood processing, the initial sawing units may be followed by shaping, grooving dado-type cutter heads mounted at any desired angle to the work piece (Figure 25). Pneumatically controlled corner rounding units are also available to perform any work required to complete panel edge machining. The last tools in a DET for panel processing are generally profile sanding or chamfering units (Figure 25) (Industry Canada, 2003).

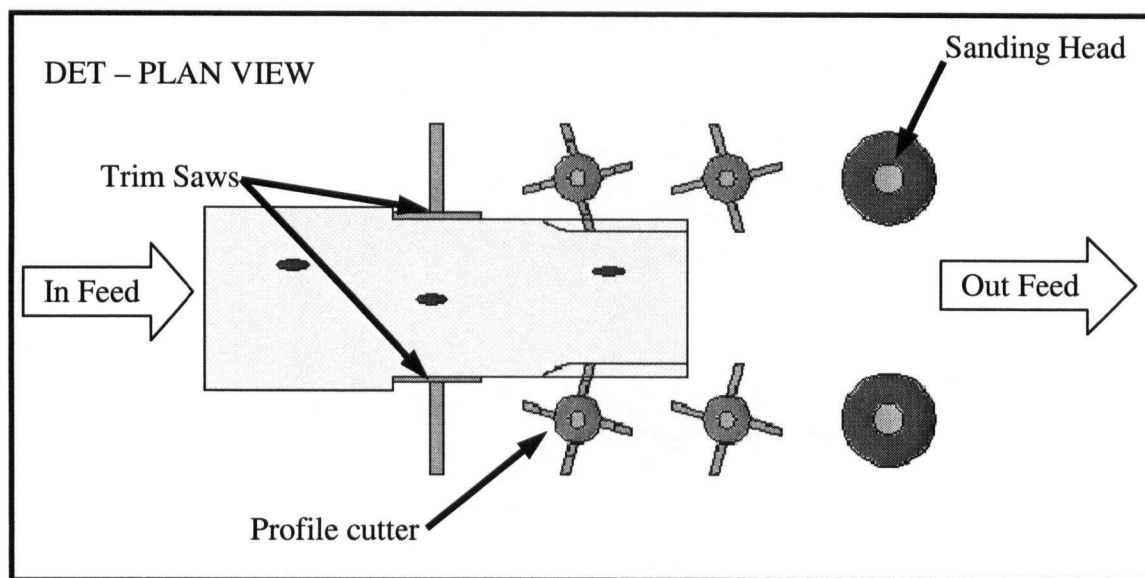


**Figure 25. DET main machining components.**

#### **4.1.2 Preliminary Industrial Trial**

During the visit to Canwood Furniture Inc., a temporary scanning system was attached to the fixed side of the DET and scans were taken of machined parts leaving the DET (Figure 26).

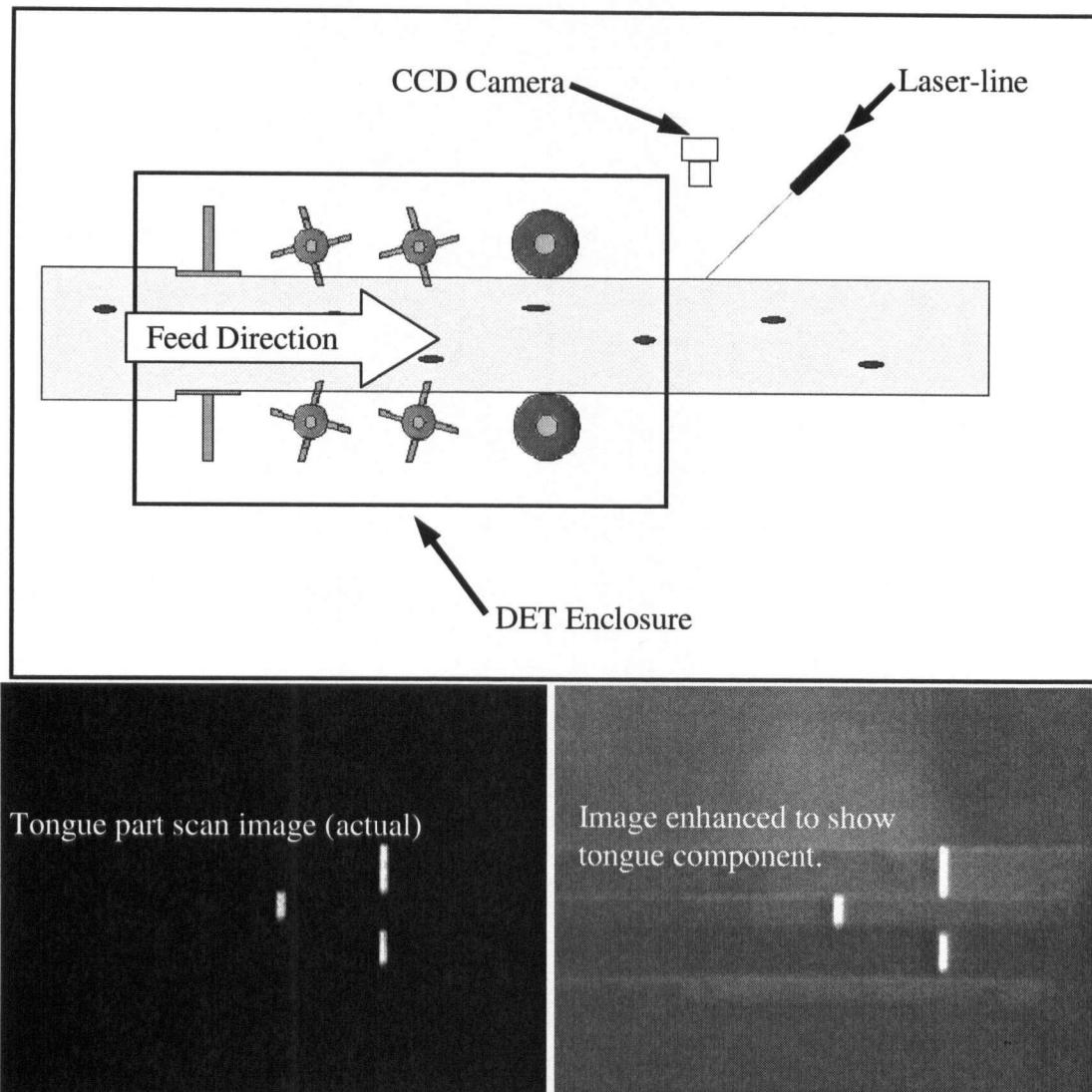


**Figure 26. Preliminary scanning hardware setup and scans of tongue components taken at Canwood Furniture Inc.**

These preliminary scans helped to establish the requirements and limitations of the AQCS. The required scan density, which is the distance between scans, was approximately one-inch. With an average recorded feed speed of 18-meters/minute, the required scan frequency is approximately 12-Hz or 0.083-seconds/scan. As stated previously, some machines operate at 91.44-meter/minute (300-feet/minute) and require a scan frequency of 720-Hz (Wong, personal communication, 2003). Dust and movement were factors that affected the scanned images. To avoid contact from airborne dust

particles, the camera and laser-line were placed outside of the enclosure and as far away as possible from the last sanding head. Dust, however, stuck to the freshly machined part and created artificial surfaces on the part, requiring that the surfaces had to be cleaned prior to scanning to avoid false readings. Long parts were prone to the most movement because the operator would pull the part off the conveyor or the part would fall off the conveyor and onto an outfeed table before the entire part was scanned. Unwanted movement caused the parts to shift in the scanned images and, in some instances, the part left the camera's field of view. Mounting the camera and laser-line closer or inside the enclosure - with proper shielding - could solve this problem since the parts are fully supported and the operators cannot reach them.

## ***4.2 Laboratory Scanning System Hardware***

As previously mentioned, the laboratory scanning system was built based on systems found in other industries. The system was developed with the assistance of Forintek Canada Corp. Western Laboratory in Vancouver, British Columbia. The system uses a Basler Vision Technology A301f camera with a Tamron lens, Lacey-Harmer laser-line, Matrox Meteor-II/1394 digital video capture card and a standard desktop computer (APPENDIX A: Hardware Specifications contains camera and laser specifications). The total parts cost was approximately \$6500 including a personal computer to run the analysis software.

During initial tests, the camera and laser-line were suspended above the scanning surface with a tubular steel frame. The laser was mounted on a 45-degree angle and the camera was mounted perpendicularly to the part being scanned below. A digital level was used to align the camera and laser. This design was chosen to test the feasibility and

the limitations of the system. After initial testing, the laser-line and camera concept proved feasible. However, vibration and movement of the apparatus would change the relationship between the camera and laser-line, therefore, altering the image. To improve consistency and repeatability, a second more sturdy and ridged test apparatus was built (Figure 27).

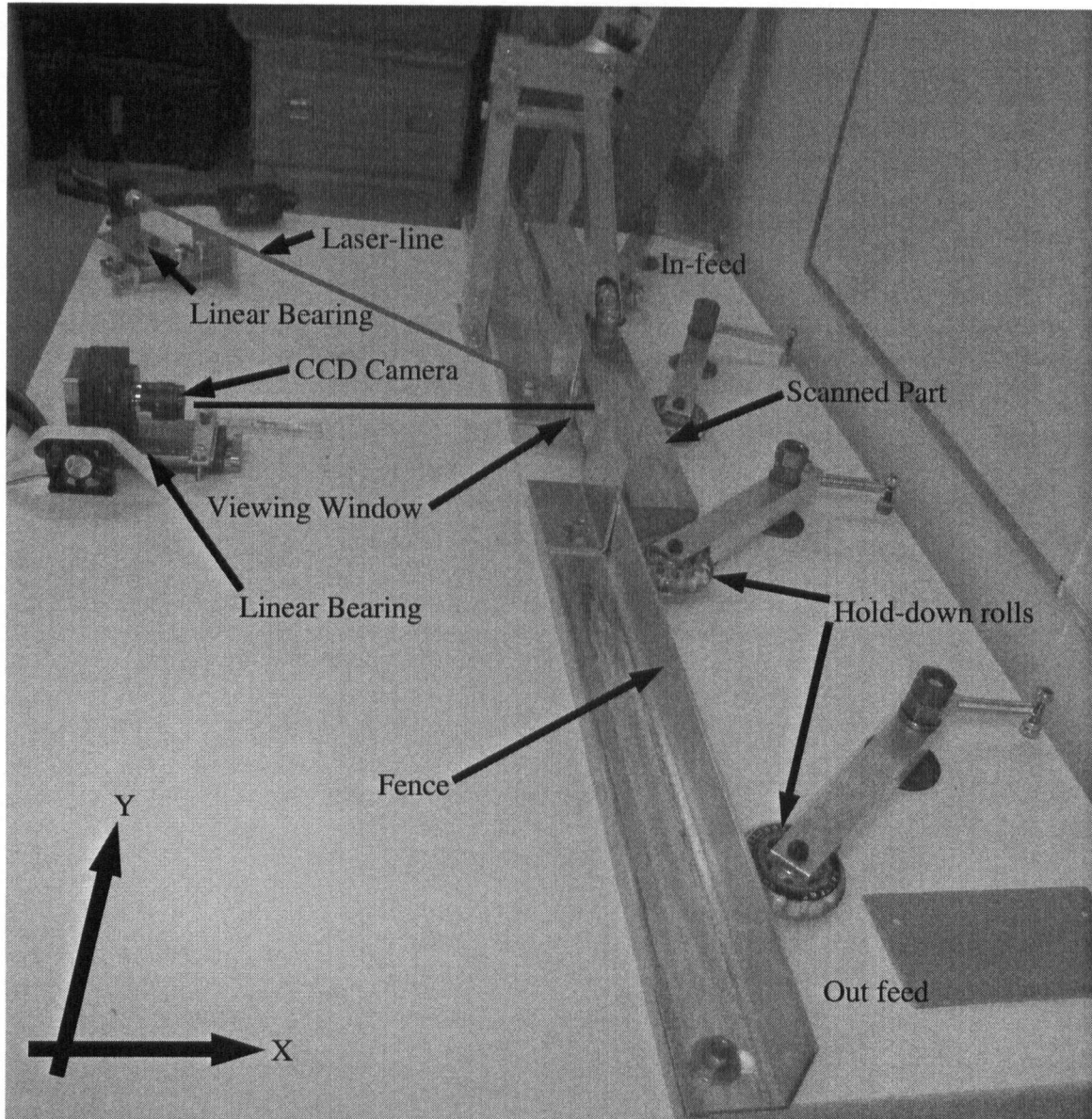


**Figure 27. Test apparatus - parts.**

The camera and laser-line were firmly mounted to a stiff/ridged table. The camera was positioned perpendicularly to the scan surface, while the laser-line was angled approximately 45-degrees relative to the camera. The camera and laser-line were mounted on top of linear-slide bearings for fine adjustments. The camera required back-and-forth movement to change the field of view, while the laser-line required side-to-side movement to position the laser-line on the part. The platform was also used to convey the parts across the camera. To compensate for the height of the linear-slide bearings underneath the camera and laser-line, the conveying surface was elevated by 19-mm. An adjustable aluminum L-angle fence was used to position the part at a fixed distance away from the camera and laser-line. Hold-down rolls were used hold the part against the fence and the conveying surface. To maintain simplicity, the parts were manually pushed across the conveying surface.

#### **4.2.1 Lens Aberration Testing**

The lens and camera were tested for aberration problems using a calibration/test grid with 5mm x 5mm squares (Figure 28).



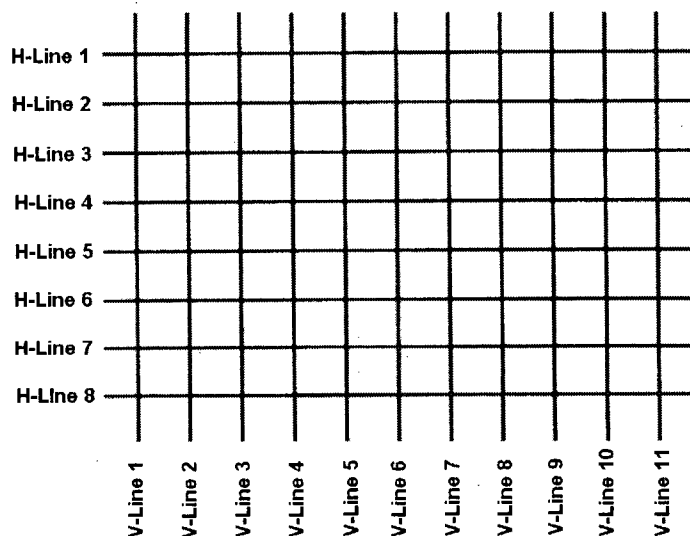


**Figure 28. Calibration/Test Grid used to test for Aberrations.**

An image of the test grid was captured and analyzed using commercially available image processing software, Matrox Inspector 4.0. Based upon a visual inspection, spherical aberration, astigmatism and coma were determined not to be present in the captured image. An edge detection tool was used to check for curvature of field, barrel and pincushion distortions.

The edge detection tool analyzes each line and returns data relating to the position, angle and width of each line (APPENDIX B). From the width and angle data, the means and standard deviations were calculated and used to determine whether the lines were straight and parallel to each other and whether the horizontal lines were perpendicular to the vertical lines. The imaging software measures the width of each line by determining the distance between the two furthest pixels across the width of the line. An undistorted line measured along the camera's central axis is approximately two pixels wide and the widths of vertical and horizontal lines in the grid are less than three pixels. Due to the curvature, pincushion or barrel distortion, the lines can appear to be thicker.



The ideal angle for the horizontal and the vertical lines are  $0^\circ$  and  $90^\circ$ , respectively. The measured angles for the horizontal and vertical line were out by  $0.25^\circ$  from their ideal orientation, which points to a misalignment between the camera and grid. To compensate for the misalignment,  $0.25^\circ$  was subtracted from both measured angles resulting in a compensated angle equal to the ideal angle; as a result, the horizontal lines were perpendicular to the vertical lines. From these test results, the aberration from this camera and lens combination is imperceptible, having negligible affects on the accuracy of the AQCS.

#### **4.2.2 Perspective Distortion**

Another form of distortion, perspective distortion, was uncovered during testing. Perspective distortion is an optical phenomenon that occurs when a three-dimensional object is converted into a two-dimensional image through a conventional lens. Perspective distortion contains two distortion types, which are magnification distortion and depth perspective distortion. Conventional lenses and our eyes cannot accurately portray objects that are at different distances from the lens (Cielo, 1988). Distance along the lens's optical axis distorts the image such that objects that are farther away from the lens will appear smaller which is referred to as magnification distortion. For example, the two boys in Figure 29 are the same height; however, from the camera's perspective the nearer boy appears taller than the boy on the opposite sidewalk.

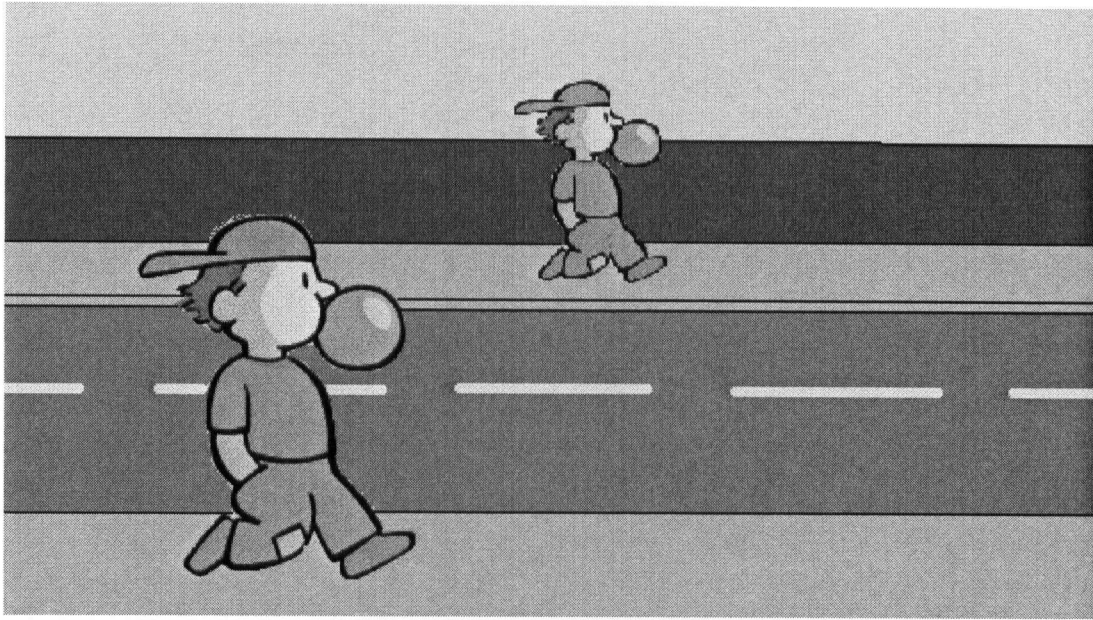


**Figure 29. Perspective causes the boy on the near sidewalk to appear taller than the boy on the opposite sidewalk (Microsoft, 2005).**

The image of the boys is analogous to the tongue part shown in Figure 30 where the shoulders are further away from the camera. Figure 31 is the scanned image used by the AQCS analysis software. The near boy represents the tongue labeled “B” and the far boy represents both shoulders labeled “A” and “C” in Figure 31. From the camera’s perspective, the tongue will appear wider than the shoulders even though the shoulders are actually wider than the tongue.

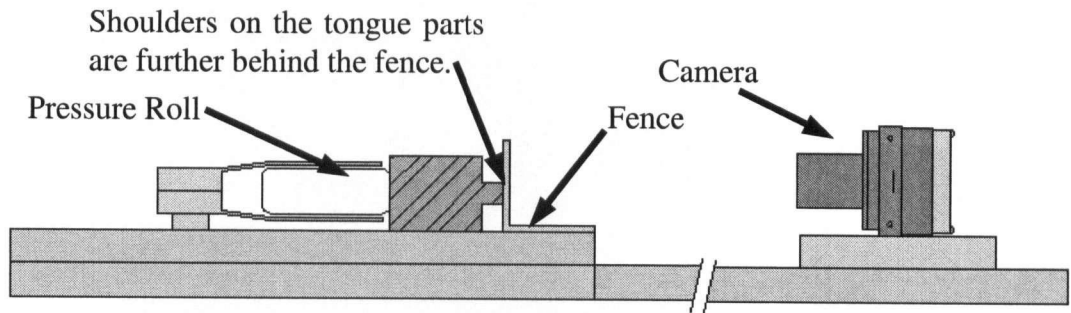


**Figure 30. Cross-sectional view of the AQCS prototype system showing hardware location.**

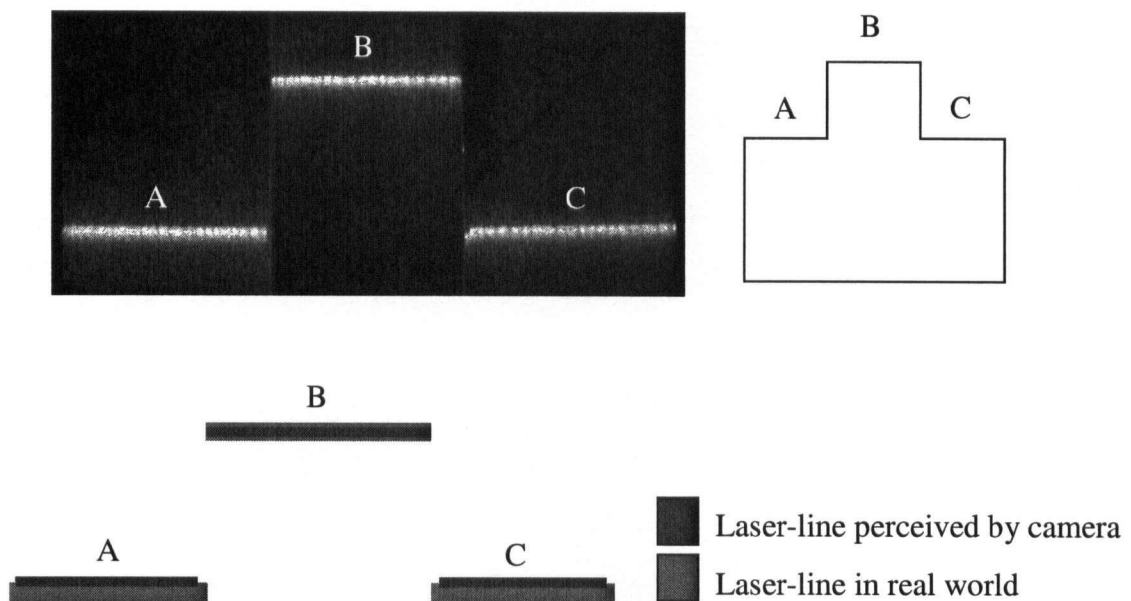


**Figure 31. Perspective distorted tongue scanned image (left scanned data / right cross section of part / bottom comparison of captured image and real world).**

The real world width for A and C is 15-mm, B is 13-mm, and the scanned pixel width for A and C is 158 pixels, and B is 143 pixels. Because of their varying dimensions, it was

necessary to normalize their widths before analyzing the dimensions. The data was converted into pixel densities (A and C is 10.5 pixels/mm and B is 11 pixels/mm).

Based on the pixel density of A and C, 105 pixels would occupy a 10-mm length while 110 pixels would occupy the same length for B. Since the pixel dimensions are fixed, the length of B will appear longer than A and C which is not true.

As the object moves laterally away from the centerline of the lens, the distance moved appears to decrease as the object moves further away from the centerline of the lens, which is referred to as depth distortion. Figure 32 is an example of depth perspective distortion.

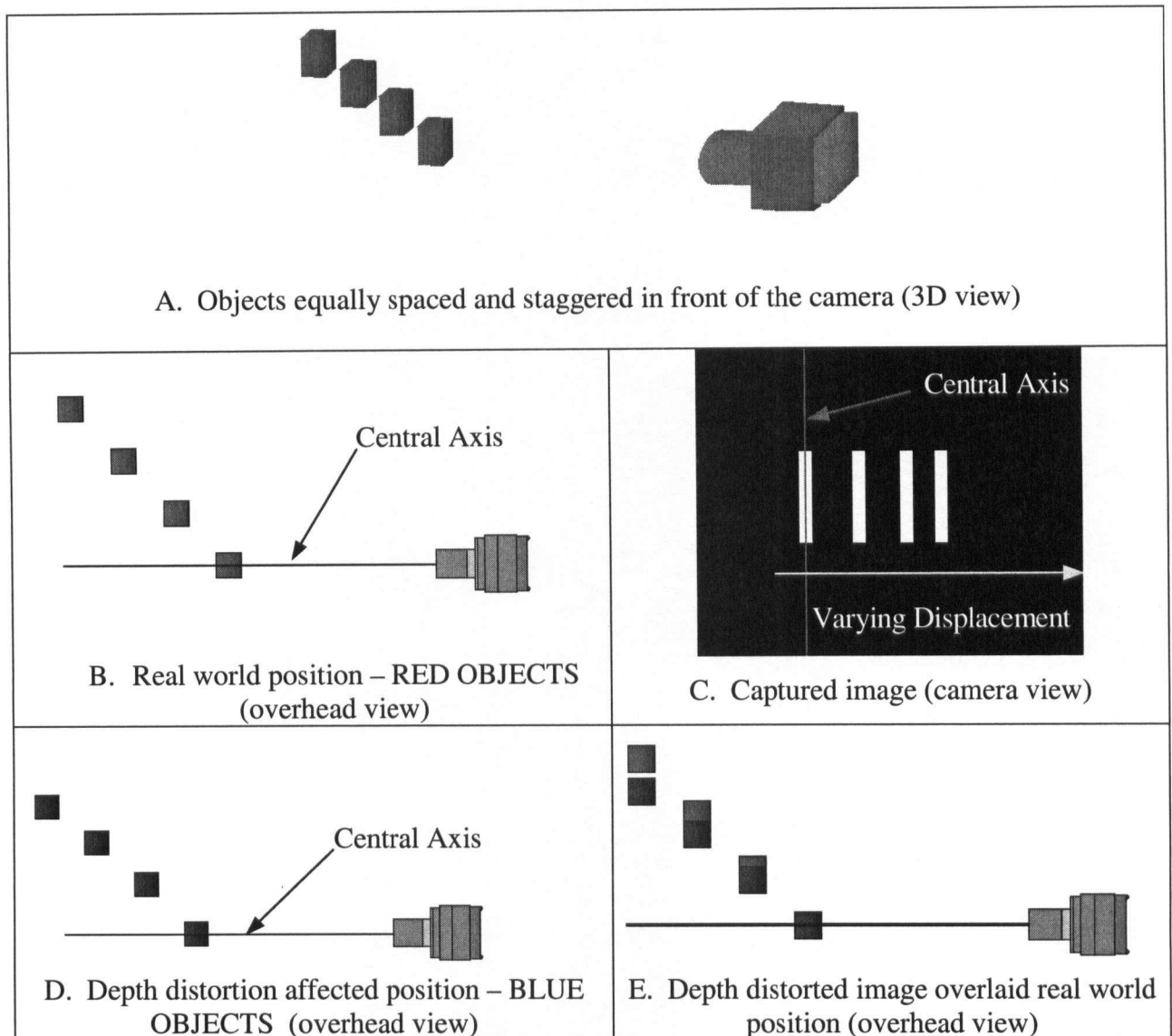


**Figure 32 Effects of depth perspective distortion compared to real world position.**

Figure 32 shows four identical objects placed in front of the camera. The red objects in Figure 32-B are spaced equally apart. The four objects in the captured image appear to shift laterally from the camera's central axis as shown in Figure 32-C. The blue objects in Figure 32-D is an overhead theoretical view of the distorted objects. This phenomenon is most visible when the real world objects are overlaid on top of the captured image (Figure 32-E).

Telecentric lenses or special software calibration routines are currently being used by the machine vision industry to prevent or correct for perspective distortion. Telecentric, or constant magnification, lenses are designed to ensure the object size does not vary as it moves along the camera's optical axis (Burke, 1996, p. 509). Telecentric lenses only allow light rays that are parallel to the optical axis to enter and exit the lens system, thereby making the magnification of the lens invariant to the object's position along the optical axis and laterally (Burke, 1996, p. 509) (Figure 33).

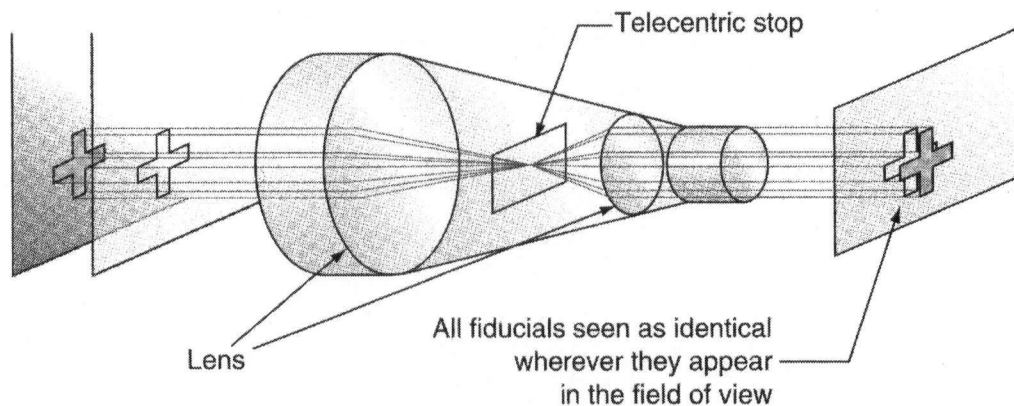


**Figure 33. Components and the operation of a telecentric lens (Wilson, 2004, p. 37).**

A limitation of telecentric lenses is a limited field of view where the object being analyzed cannot be bigger than the width of the lens. Telecentric lenses also require extra illumination or an extra sensitive camera and some resolution is lost causing the edges of the object to blur; however, thresholding software can be used to minimize edge blurring (Wilson, 2004). Unfortunately, the extra cost for a telecentric lens exceeded the budget of the proposed system, therefore, prohibiting its use in the development of this AQCS; therefore, a software calibration routine was used to correct for perspective distortion. The explanation of the software calibration routine can be found in Section 4.3.

### 4.3 Software

Two pieces of software were developed for the AQCS. The first was an image acquisition frame grabber<sup>2</sup>. The second was an image analysis program that deciphers the captured image data, calibrates the data for perspective distortion, measures the scanned objects and creates control charts<sup>3</sup>.

#### 4.3.1 Image acquisition Software

The image acquisition software interfaces the Basler CCD digital camera with the Matrox Meteor-II/1394 digital video capture card and the computer. The user interface also allows the user to adjust image capture settings, as shown in Figure 34, along side a live captured video image of a part.

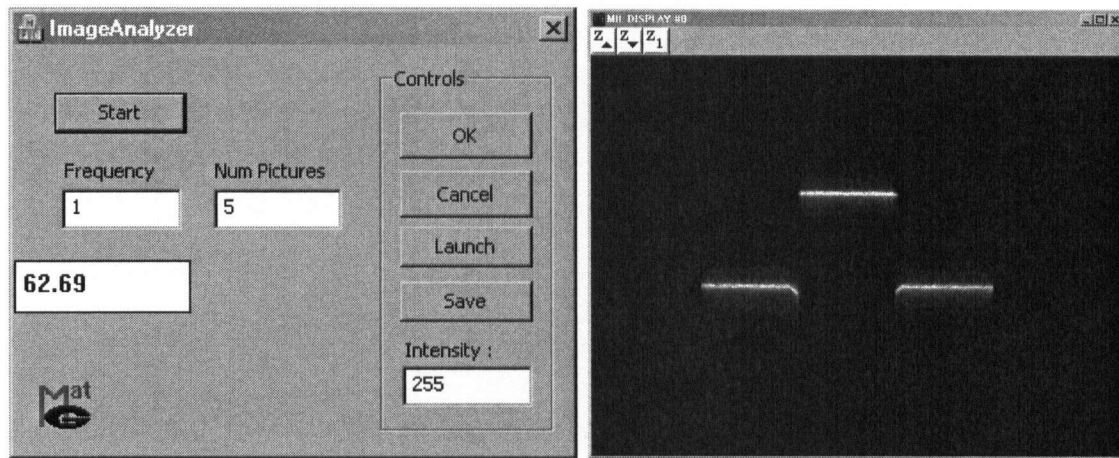


**Figure 34. Image acquisition user interface.**

The image acquisition software collects images based on the user defined capture frequency rate and the number of required images. To maximize processing speed, the

---

<sup>2</sup> Image acquisition software development assisted by Maciej Gara

<sup>3</sup> Image analysis software development assisted by Rowan Eberle

software filters the incoming image based on a user defined pixel intensity level set between 0 and 255 bits, where 0-bits is black and 255-bits is pure white. Only pixels with intensity (brightness) levels equal or greater than the user-defined threshold are recorded as a pixel map. A conservative intensity level of 128-bits was chosen for the AQCS. Based on preliminary scans, 128-bit intensity level was adequate to capture enough detail for the image analysis software to recognize the objects in the image. Increasing intensity levels beyond 128-bits reduced accuracy, while decreasing intensity introduced excessive noise and false readings. The captured images were recorded as a text file (Figure 35) containing a sequential image identification number used by the image analysis software to separate each image and the x and y position of each recorded pixel.

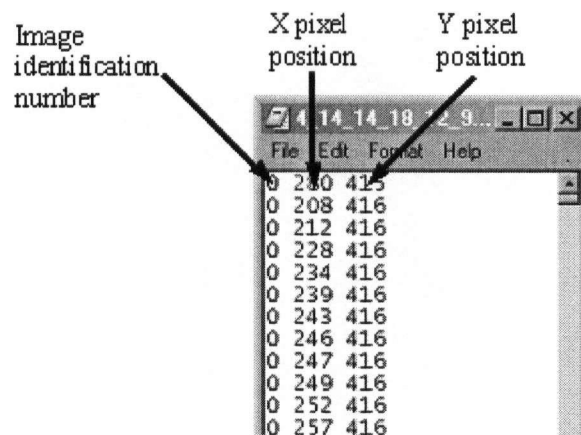


Image identification number	X pixel position	Y pixel position
0	230	416
0	208	416
0	212	416
0	228	416
0	234	416
0	239	416
0	243	416
0	246	416
0	247	416
0	249	416
0	252	416
0	257	416

**Figure 35. Example of image acquisition software acquired text file.**

#### **4.3.2 Image Analysis – Lens Calibration**

The image analysis software contains a calibration routine that corrects perspective distortion. The calibration routine captures an image of two calibration objects. The first is a block precision ground to a flat surface while the second is a stepped (2.5 mm x 2.5 mm steps) calibration block (Figure 36).



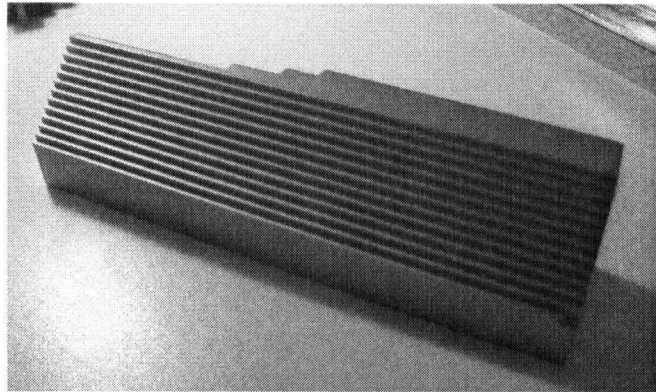


**Figure 36. Stepped Calibration Block.**

From these images, the calibration routine derives calibration coefficients to correct perspective distortion. The image is adjusted using the equations.

Before performing the calibration routine, the laser-line must be positioned in the center of the image. The center of the image references the surface that touches the fence. The laser must be placed exactly in the center of the image because shifting it to either side of the centerline indicates a surface that is further away from the fence (Figure 37). The alignment process starts by placing a flat calibration block in the viewing window against the fence and, with the help of a live image from Matrox Inspector 4.0, the laser-line was positioned in the center of the image (Figure 37).

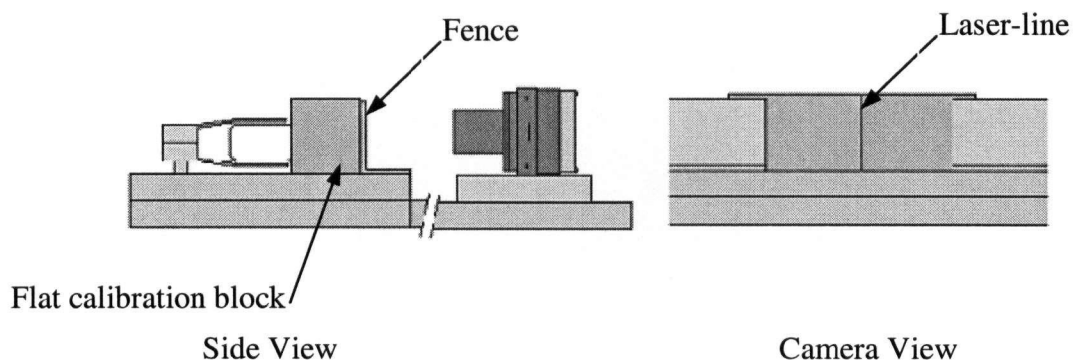


**Figure 37. Laser-line alignment setup.**

After aligning the laser-line, the image acquisition software captured 6 to 8 images of the flat calibration block. The flat calibration block was moved approximately 2 to 3 mm away from the fence between each image (Figure 38). shows a sequence of overlaid calibration block laser line images where the line at Y-coordinate 240 pixels is against the location of the fence and each proceeding line is a shift away from the fence. The red lines connect the ends of each calibration block laser line image and are both angled 4.25 degrees from vertical. This is another example of how magnification distortion causes each proceeding line to become shorter.

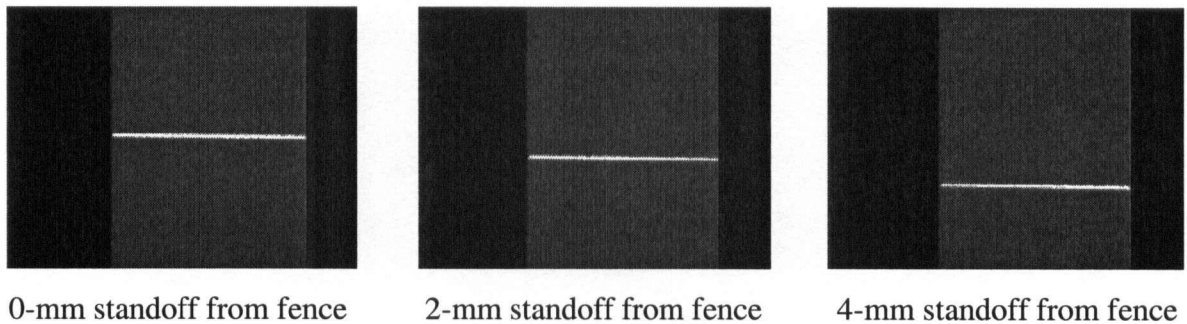


**Figure 38. Sequence of flat calibration block calibration images.**

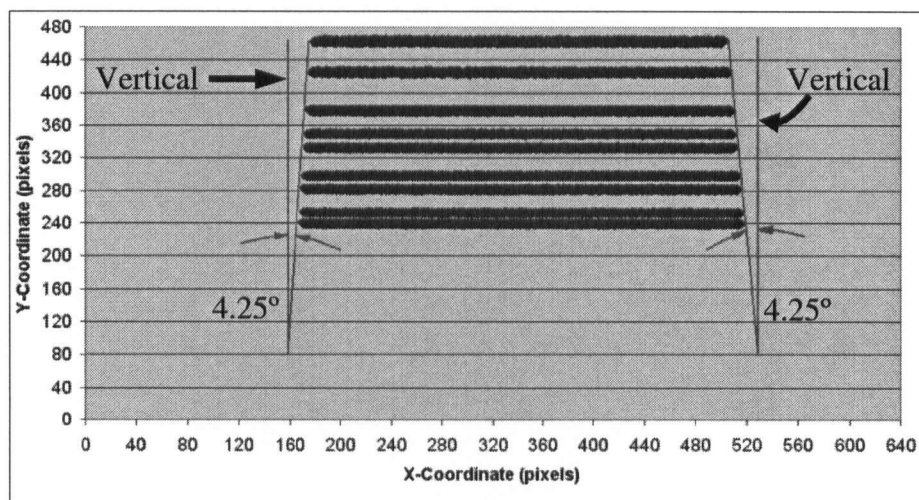


**Figure 39. Sequence of overlaid calibration block images showing magnification distortion.**

The stepped calibration block is then placed in the viewing window and a single image is captured (Figure 40). This information was used by the depth distortion calibration routine.

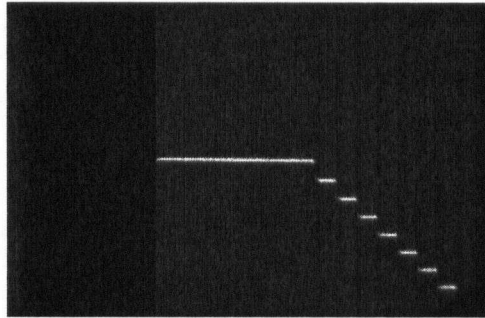


**Figure 40. Stepped calibration block image.**

#### **4.3.2.1 Magnification Distortion Calibration**

The magnification distortion calibration coefficients was generated from the flat calibration block images. The bounding box function in Matlab identified the laser-line within the captured image (Figure 41).

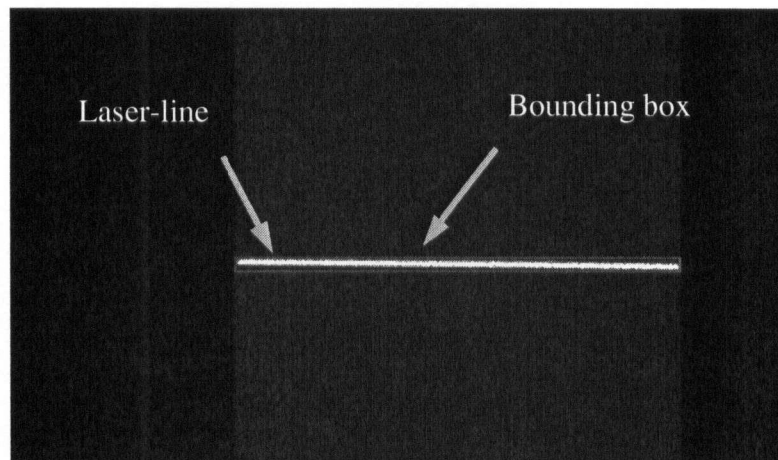


**Figure 41. Image of flat calibration block with bounding box applied.**

The bounding box can identify the length, end-points, thickness and centroid of the laser-line. Since the bounding box identifies the end-points, they were used to convert the

laser-line into a line segment where all the data points between the end-points were eliminated (Figure 42).

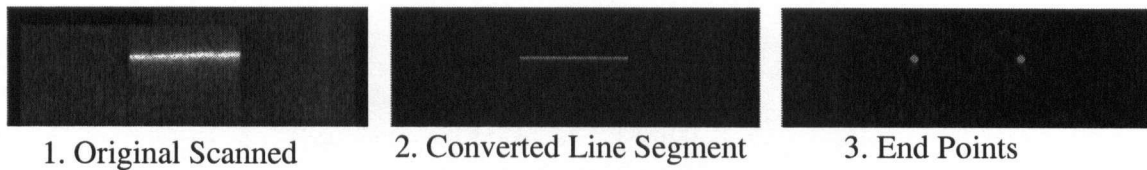


**Figure 42. Example of image converted into line segments and end points.**

Having all pixel locations processed through the calibration equations is very time consuming; therefore, reducing the number of pixel locations reduces the complexity of the image analysis algorithms, which in turn, reduces computing time. The routine was also given the actual thickness of the calibration block in millimeters. For each image, the routine calculates a calibration ratio [Eq.1] between the actual lengths of the calibration block over the pixel length obtained from the captured images. Table 1 is an example of eight images that were used to calculate the calibration ratio. X-Image data is the length of the laser line from the captured image of the flat calibration block. X-Actual data is the actual length of the flat calibration block measured with a laser profilometer. The Y data is the shift of the laser line caused by the movement of the flat calibration block away from the fence.

$$\text{Calibration Ratio (mm/pixel)} = [\text{Actual Length (mm)}] / [\text{Image Length (pixels)}] \quad [\text{Eq.1}]$$

Actual Length (mm) = Actual length of the calibration block in millimeters

Image Length (pixels) = Length of the calibration block in the captured image in pixels

Table 1. Example of calibration ratio.

Image Sequence	X – Image (pixels)	X – Actual (mm)	Y Centroid (pixels)	Calibration Ratio (mm/pixel)
Image 1*	347	31.1	239	0.090
Image 2	345	31.1	253	0.090
Image 3	344	31.1	282	0.090
Image 4	342	31.1	298	0.091
Image 5	338	31.1	333	0.092
Image 6	337	31.1	350	0.092
Image 7	334	31.1	378	0.093
Image 8	330	31.1	425	0.094

\* first image taken of flat calibration block against the fence

After the calibration ratios are calculated, a 1<sup>st</sup> order polynomial fit between the calibration ratios (dependent) and the Y centroid (independent) for each image is created.

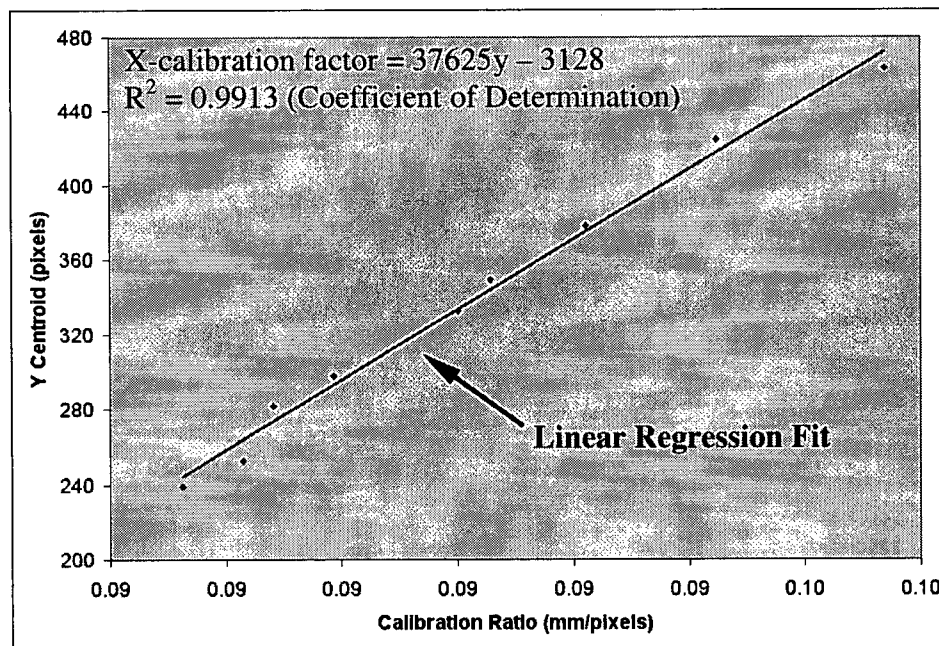


Figure 43. 1<sup>st</sup> order simple linear regression fit.

The equation generated from the linear fit is the X-calibration factor [Eq.2]. The X-calibration factor is used to correct magnification distortion by repositioning the pixels in the scanned images to their corrected locations.

### **X-calibration factor defined**

$$\text{X-Calibration Factor (mm/pixels)} = [B_o \text{ (mm/pixel)}] \times [Y \text{ (pixels)}] + [\text{Intercept}] \quad [\text{Eq. 2}]$$

$$\text{X-Calibration Factor (mm/pixels)} = \text{Dependent Calibration Factor}$$

$$B_o = \text{Coefficient (from regression)}$$

$$Y = \text{Independent Factor (Y Centroid)}$$

For example, in Figure 44, the line segment "A" in the scanned image of the groove is too short. The y-coordinates from  $P_1$  and  $P_2$  are evaluated through the x-calibration factor equation [Eq.2]. The X-calibration factor is then multiplied by the x-coordinates of  $P_1$  and  $P_2$ , which corrects the distortion and shifts the points from  $P_1$  and  $P_2$  to  $P_3$  and  $P_4$ .

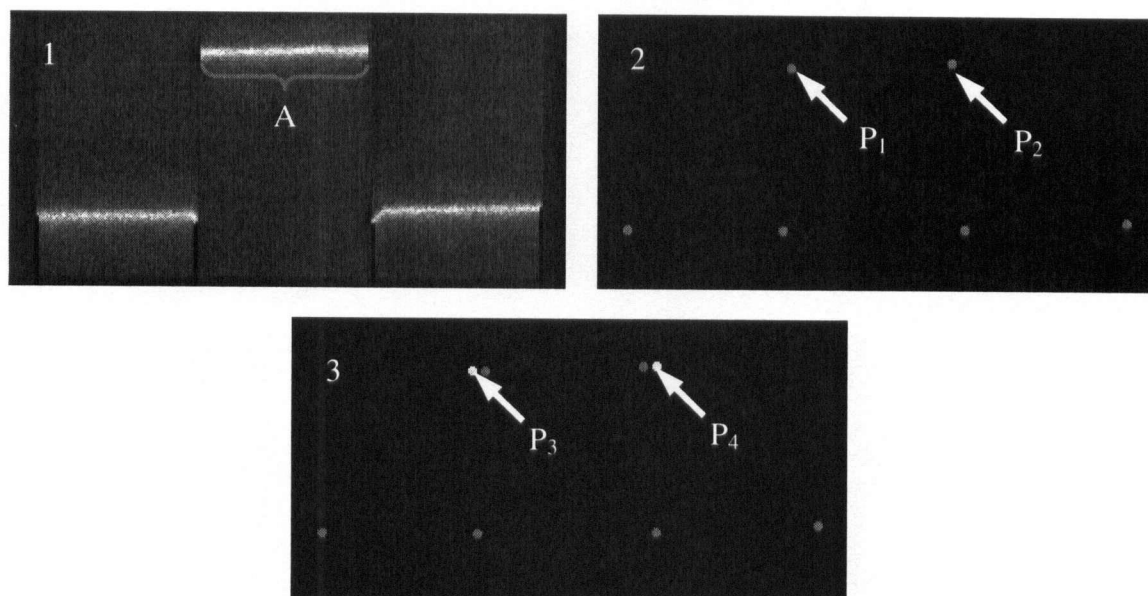


**Figure 44. Groove image converted into defining points and calibrated (1. original image, 2. un-calibrated end points, 3. calibrated end points overlaying un-calibrated end points).**

A 1<sup>st</sup> order simple linear polynomial fit was chosen because of its simplicity and sufficient accuracy. Higher order polynomial fits were studied, but the accuracy gained was small. The same set of data was fitted with 1<sup>st</sup> to 6<sup>th</sup> order polynomials. The coefficient of determination increased from 0.9913 to 0.9970 which was considered negligible (Table 2).

**Table 2. Varying degrees of polynomial tested.**

Degree of Polynomial	R <sup>2</sup> (Coefficient of determination)
1 <sup>st</sup> order linear regression fit	0.9913
2 <sup>nd</sup> order linear regression fit	0.9949
3 <sup>rd</sup> order linear regression fit	0.9950
4 <sup>th</sup> order linear regression fit	0.9959
5 <sup>th</sup> order linear regression fit	0.9962
6 <sup>th</sup> order linear regression fit	0.9970



### 4.3.2.2 Depth Distortion Calibration

The depth distortion calibration routine creates a correction factor to correct the y-positions of all scanned objects. The image from the stepped calibration block is used to create the correction factor. Similar to the magnification calibration routing, the bounding box function finds the y-centroid for each step (Figure 45).

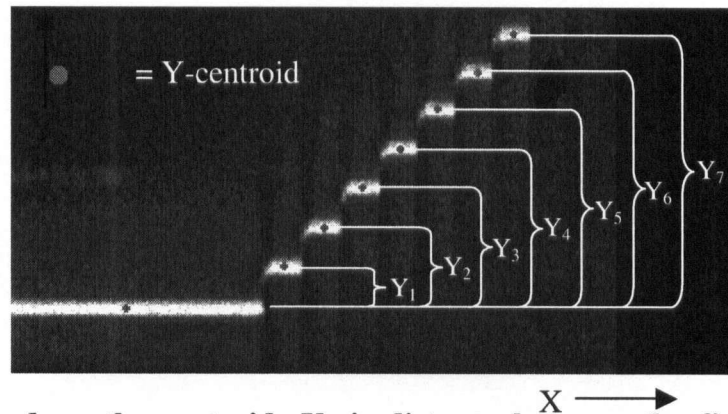


**Figure 45.** Based on the centroid;  $Y_1$  is distance between the first step and the second step.  $Y_i$ 's are found for every object in the image.

The displacement between each centroid was calculated from  $Y_1$  to  $Y_7$ . The calibration routine was also given the actual distances between each step. A linear polynomial fit was generated between the real world (dependent) and image (independent) distance between each step. Equation 3 is the function generated from the polynomial fit, Table 3 is the data that was used to generate the polynomial fit, and Figure 46 is the graphical representation of a polynomial fit. Similar to the magnification distortion calibration routine, higher order polynomial fits were studied; however, the increase in accuracy was negligible.



### Depth distortion calibration equation defined

$$\text{Calibrated Y (mm)} = [B_o(\text{mm/pixel})] \times [Y(\text{pixels})] + [\text{Intercept}] \quad [\text{Eq. 3}]$$

Calibrated Y (mm) = Dependent Calibration Factor

$B_o(\text{mm/pixel})$  = Coefficient (from regression)

Y (pixels) = Independent factor (Y centroid)

**Table 3. Example data used in 1<sup>st</sup> order simple linear polynomial fit.**

Step	Independent Factor (Pixels)	Step Distance (mm)
Y <sub>1</sub>	240	0.0
Y <sub>2</sub>	269	2.5
Y <sub>3</sub>	297	5.0
Y <sub>4</sub>	324	7.5
Y <sub>5</sub>	351	10.0
Y <sub>6</sub>	378	12.5
Y <sub>7</sub>	404	15.0
Y <sub>8</sub>	430	17.5

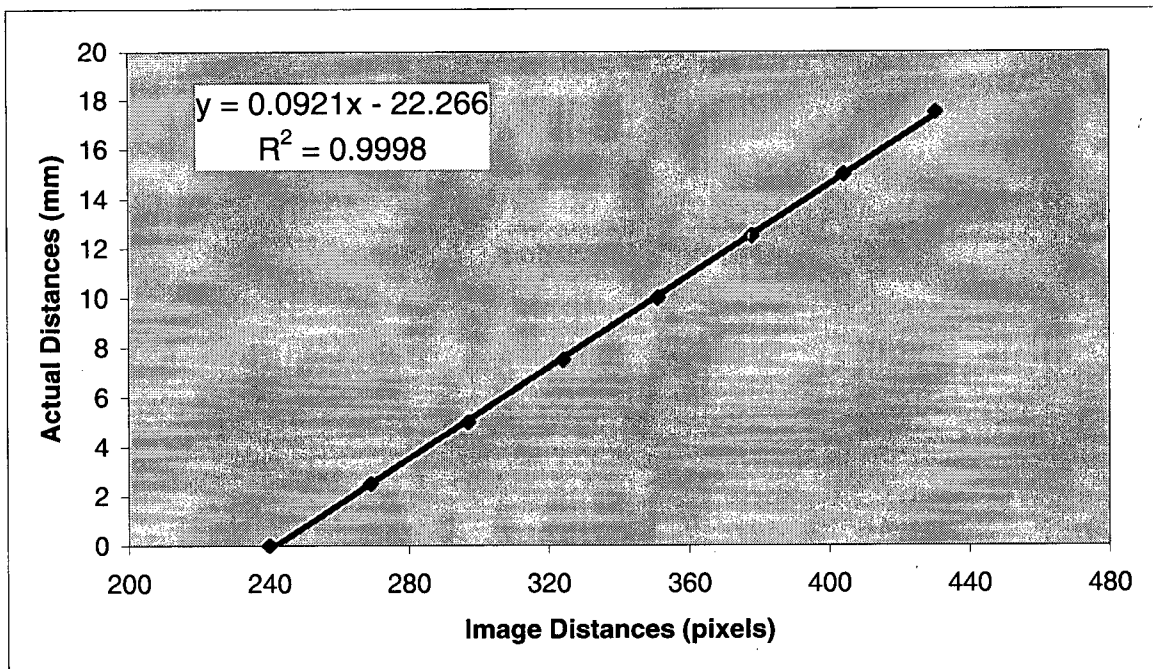


**Figure 46. Depth distortion calibration polynomial fit.**

To calibrate an image, the routine takes in and evaluates the y-coordinate of an end point. The resultant value is the corrected y-position for that end point. For example, the defining points labeled, “Original Point,” in Figure 47 are not calibrated. After the y-coordinates of these points are evaluated, the points are repositioned to the “Calibrated Point” position.

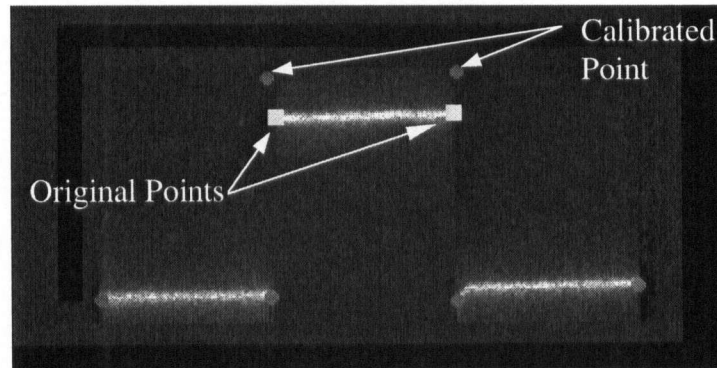


**Figure 47. Distortion calibration routing repositioning groove to correct position.**

### **4.3.3 Image Analysis**

After performing the calibration procedures, the AQCS is ready to collect and analyze part images. Since the system was developed as a proof of concept, the laboratory system processes the raw image data files after they have been collected and not in real-time<sup>4</sup>. As previously mentioned, the pixel map data is converted into a black and white image and the objects within the image are then converted into line segments where the start point, end point and centroid define an object. These points are used to measure the part.

---

<sup>4</sup> Real-time image analysis consists of capturing and analyzing the image simultaneously.

#### 4.3.3.1 Tongue and Groove Image Analysis

The tongue and groove use very similar image analysis techniques to determine the critical dimensions. After the data is converted into line segments and calibrated through both calibration routines, the output data represents an estimate of the true dimensions of the tongue and groove. Therefore, the widths of the tongue, groove and shoulders (B, C and D in Figure 48) are identified by the calibration routine. The depth of the shoulders (or the height of the tongue) is the difference between the centroid of the laser-line lying over the tongue and the shoulder ( $A = \text{Centroid 2} - \text{Centroid 1}$  and  $E = \text{Centroid 2} - \text{Centroid 3}$ ).

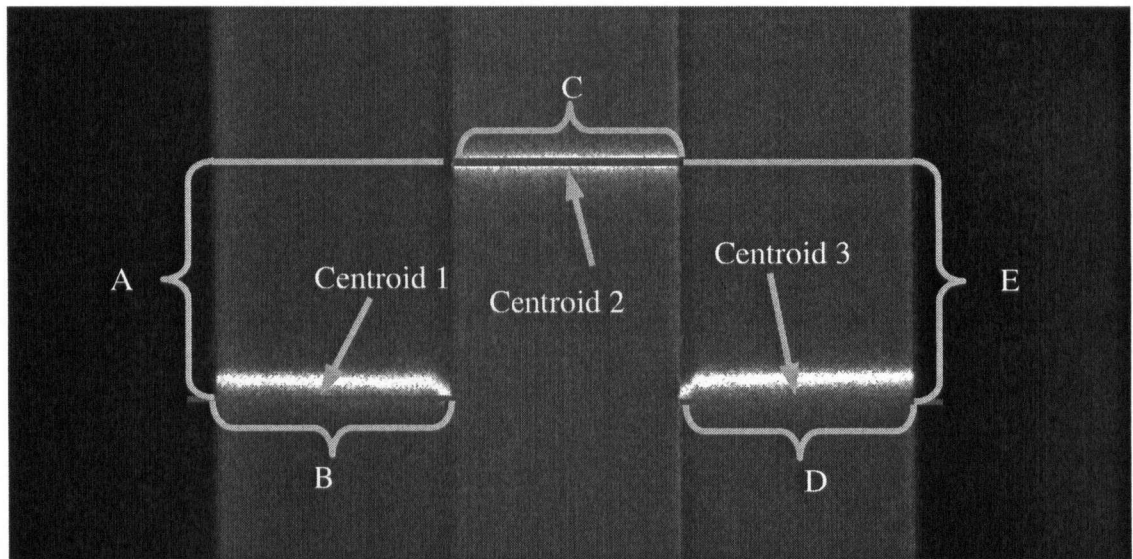


**Figure 48. Calibrated critical dimensions on the tongue (A. Left shoulder depth, B. Left shoulder width, C. Tongue width, D. Right shoulder width, E. Right shoulder depth).**

#### 4.3.3.2 Chamfer Image Analysis

The chamfer required an additional procedure prior to calibration. It was necessary to determine the transition point where the board surface meets the chamfer face (Figure 49).

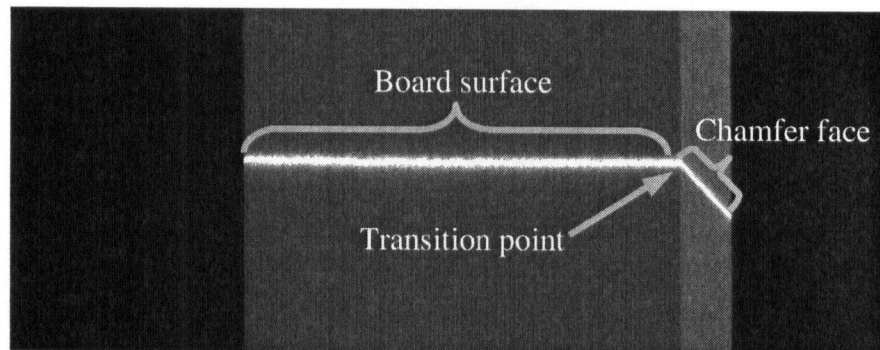


**Figure 49. Transition point used to separate board surface and chamfer face.**

The thickness of laser-line in the raw image data is several pixels wide, making it difficult to determine the exact transition point between the board surface and chamfer face. It was necessary to reduce the number of data points to find the transition point. For each row of pixels in the y-coordinate, the median pixel was kept and the rest were discarded (Figure 50). This created a single line that represents the profile (Figure 50).

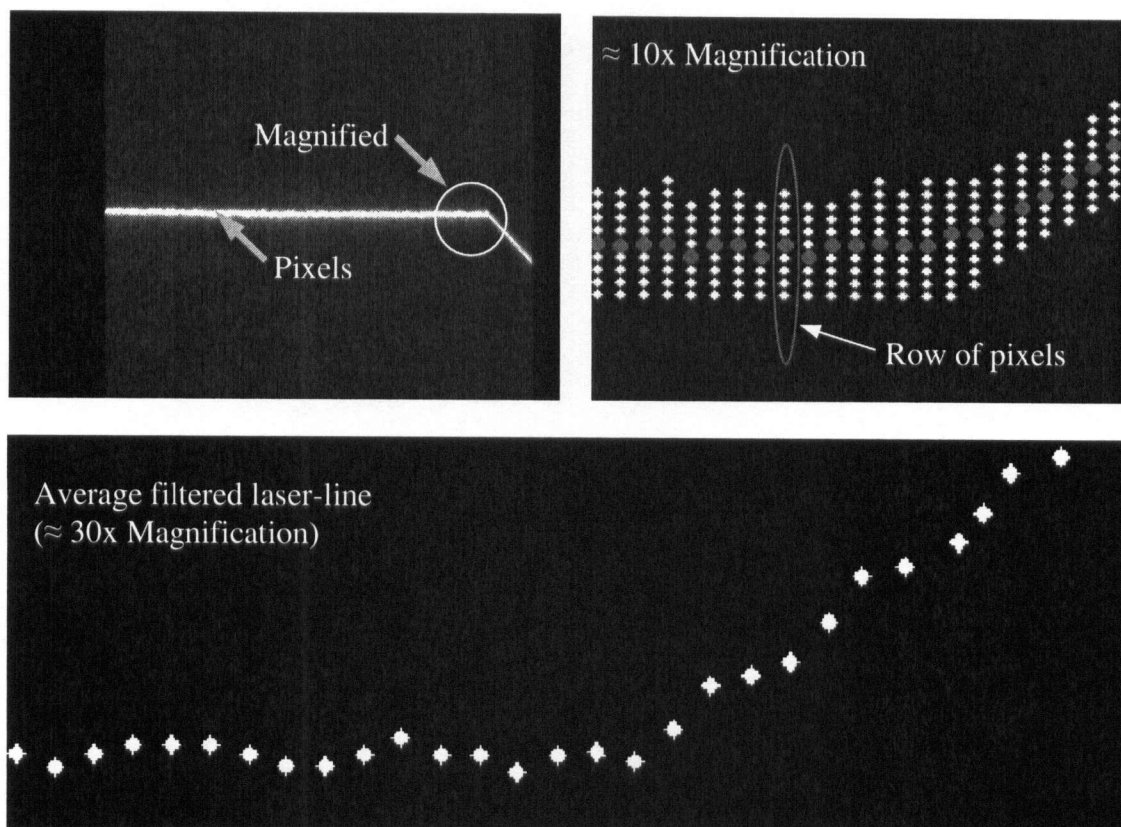


**Figure 50. Chamfer laser-line is filtered to generate a single line.**

The line is then broken into the board surface and chamfered face with a geometric-fit based algorithm. The algorithm starts by finding the minimum and maximum points in the data (Figure 51).

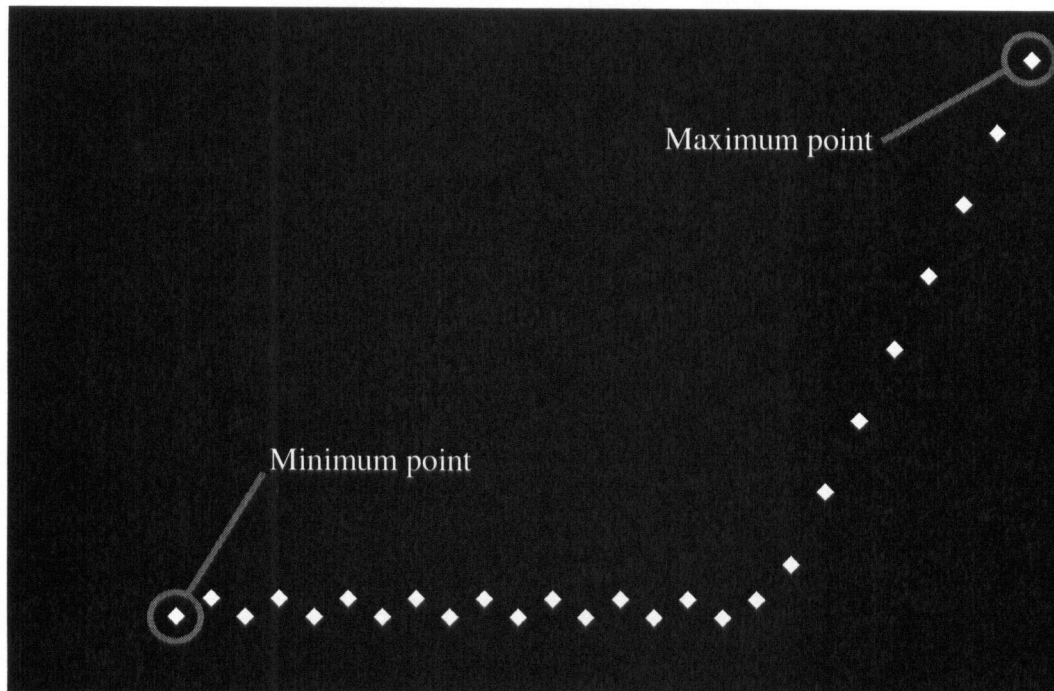


**Figure 51. Hypothetical chamfer with minimum and maximum data point highlighted.**

The algorithm attempts to find the point to break the data into the board surface and face by using a three-point circle fit equation (Wilson, J.W., 1986). The equation returns the radius of a circle that touches three-points (APPENDIX C). The algorithm fits a circle that touches the minimum, maximum points and a test point in between these two points (Figure 52). A circle is test-fitted through every point in the data set. This method was found to be the most effective in finding the transition point. A change in slope method was also tested, but it was found to be less effective. One end of a line segment was anchored at the “Minimum point” while the other end was attached to each proceeding point and the slope was determined. In an ideal scan of the chamfer, the transition point would have been the point at which the slope increases. However, the slope was overly sensitive to the minute changes along the laser line making it difficult to detect the transition point.



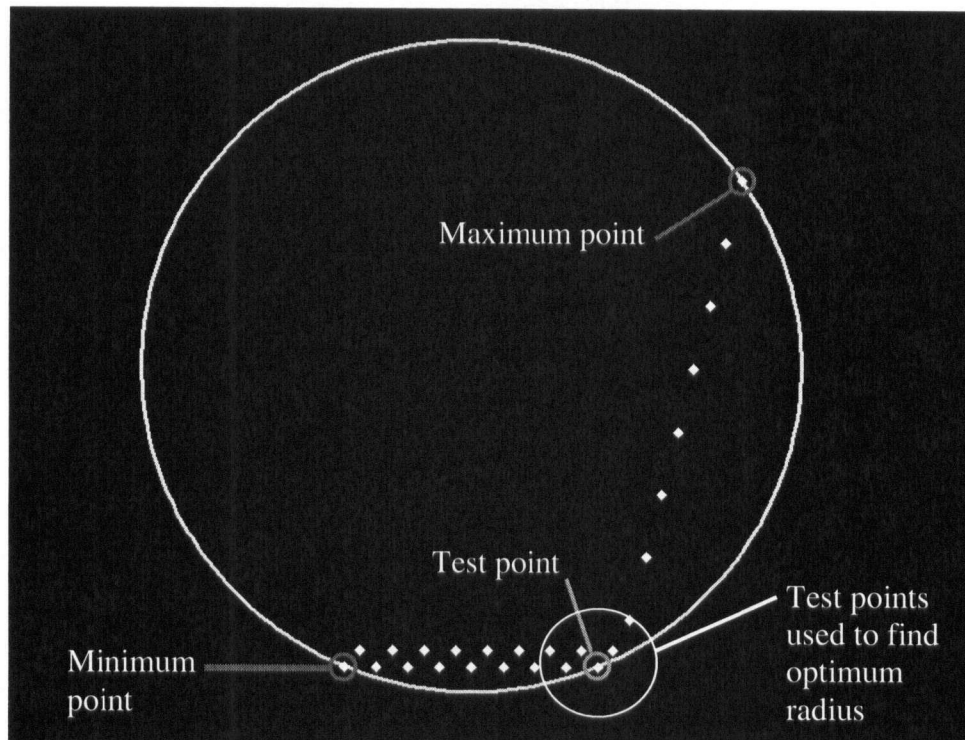


**Figure 52. Three-point circle fit equation fitting a circle between the minimum, maximum points and a test point.**

The radius changes for each test point along the chamfer. The transition point is the point that minimizes the radius of the fitted circle and estimated to be where the board surface and chamfer intercept. To verify the equation, a hypothetical chamfer was created and multiple test-points were used to calculate the radius.

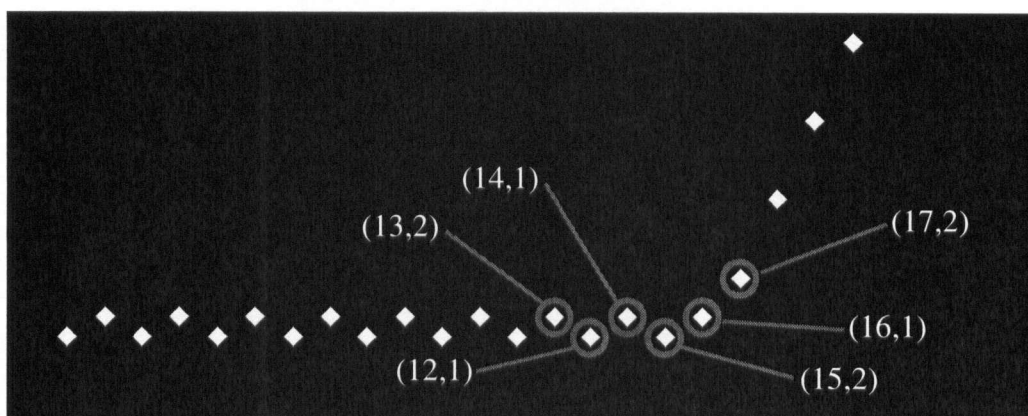


**Figure 53. Multiple test-points chosen to verify three-point circle fit equation.**

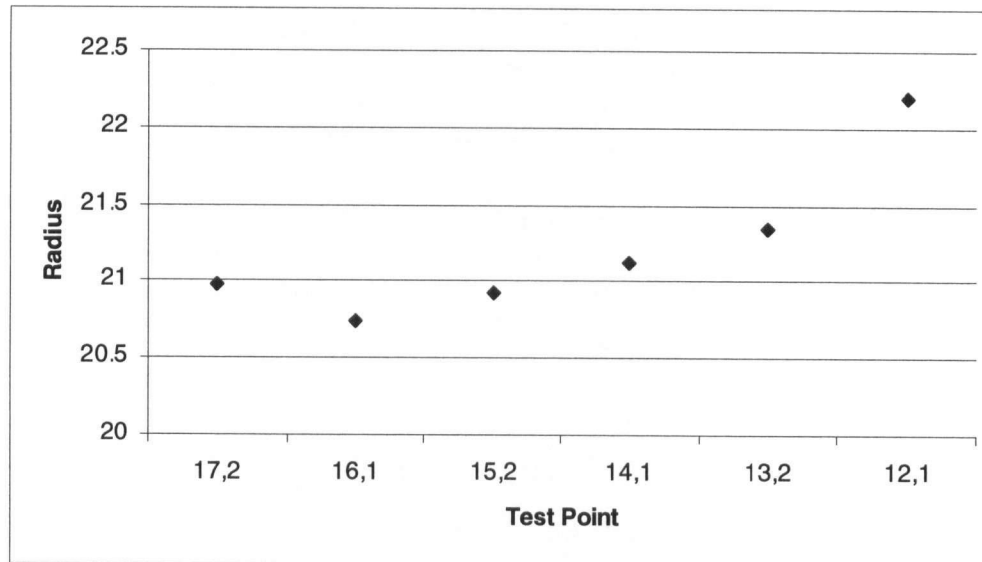


**Figure 54. Radius calculated for each test-point. The smallest radius, (16,1) is the break point.**

Once the smallest circle is found, the minimum, maximum and transition point were kept are used to measure length and the angle between the board surface and chamfered face (Figure 55).

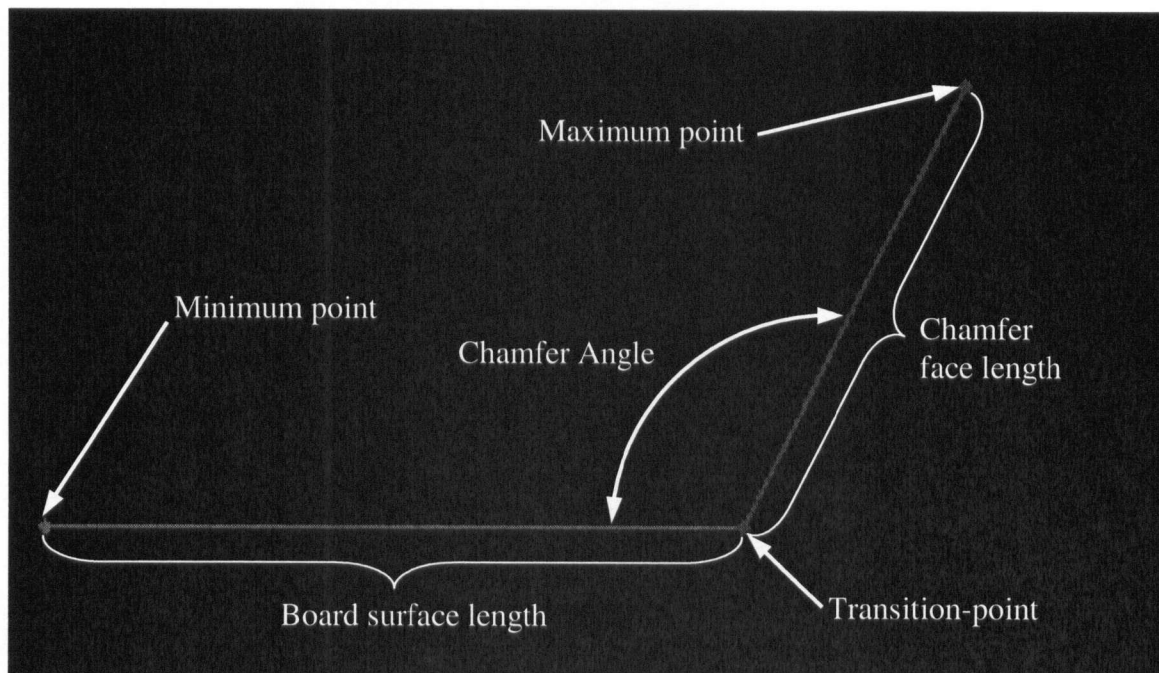


**Figure 55. Board surface length, chamfer face length and chamfer angle are used in control charts.**



#### **4.3.4 Control charts**

After the data was analyzed, the part dimension data was saved and used to produce X-bar and S charts to track the performance of the machine (APPENDIX D: Control Charts from Collected Data). S charts were used in the AQCS because there were enough samples taken (greater than 10 samples). However, the industrial system could include additional control charts and other statistical process control information. To produce the control charts, multiple scans were taken of each part and key dimensions were provided from each scan (Figure 56, Step 2). For example, a single tongue scan contains the width from each shoulder and tongue and the depth of each shoulder (Figure 56, Step 3). The multiple scans are averaged so that each component is represented by a single measurement for each critical dimension (Figure 56 step 4). These dimensions are then plotted in separate control charts for each critical dimension of interest. The control limits are based on historical data, but the user can also set additional customized control limits as early warning limits where machine operators are alerted that a potential out of control situation is imminent.

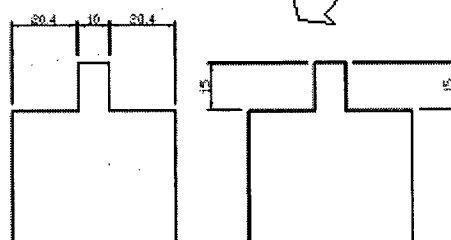
1. Multiple boards  
are scanned



2. Multiple scans  
are taken of each board



3. Each scan contains  
critical dimensions of  
each part.



4. For each critical  
dimension, the  
measurements  
obtained are  
averaged.

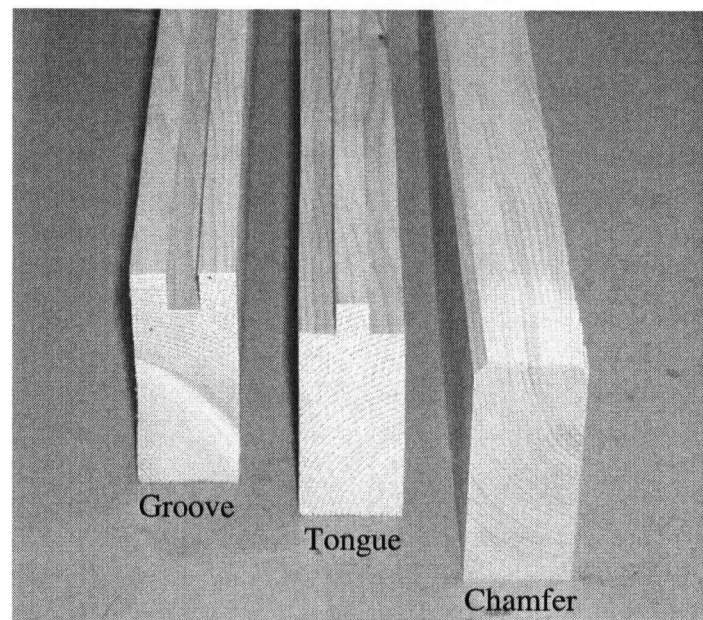
BOARD 1 Dimension Data				
	Sample 1	to	Sample n	Averaged Measurement
Shoulder 1 Width	20.4		$X_{n1}$	$X_{n1} = (20.4 + \dots + X_{n1})/n$
Shoulder 2 Width	20.4		$X_{n2}$	$X_{n2} = (20.4 + \dots + X_{n2})/n$
Tongue Width	10		$X_{n3}$	$X_{n3} = (10 + \dots + X_{n3})/n$
Shoulder 1 Depth	15		$Y_{n1}$	$Y_{n1} = (15 + \dots + Y_{n1})/n$
Shoulder 2 Depth	15		$Y_{n2}$	$Y_{n1} = (15 + \dots + X_{n2})/n$

Figure 56. Steps required in preparing data for control charts.

#### 4.3.5 Laboratory Testing

To evaluate the AQCS, several parts of each profile (tongue, groove and chamfer) were scanned and analyzed (Figure 57). Subalpine fir\* (*Abies lasiocarpa*) boards were used for the all profiles. However, changing humidity levels caused the tongue and groove parts to warp and twist. The chamfered parts did not experience this problem because less material was removed to create the profile. The removal of material can release locked-in stress causing the components to distort. The tongue and groove parts

were then replaced with bigleaf maple and MDF, which are both more dimensionally stable when compared to subalpine fir (APPENDIX E: Part Drawings).



**Figure 57. Subalpine fir test parts.**

The boards were planed, sawn and profiled using standard woodworking machines. The prepared parts were manually pushed through the scanning bed and images were captured at one-inch intervals with an average total number of twelve scans per part. The scan intensity level was set to 128 bits. The data was then processed through the image analysis software. The measurements were verified against measurements taken with a pair of calipers and a Solarius Development LaserScan profilometer.

Because of potential measurement errors, it was felt that the calipers alone were not sufficient to measure the accuracy of the AQCS. To verify both measurement methods, the components were also measured with the profilometer (Figure 58).

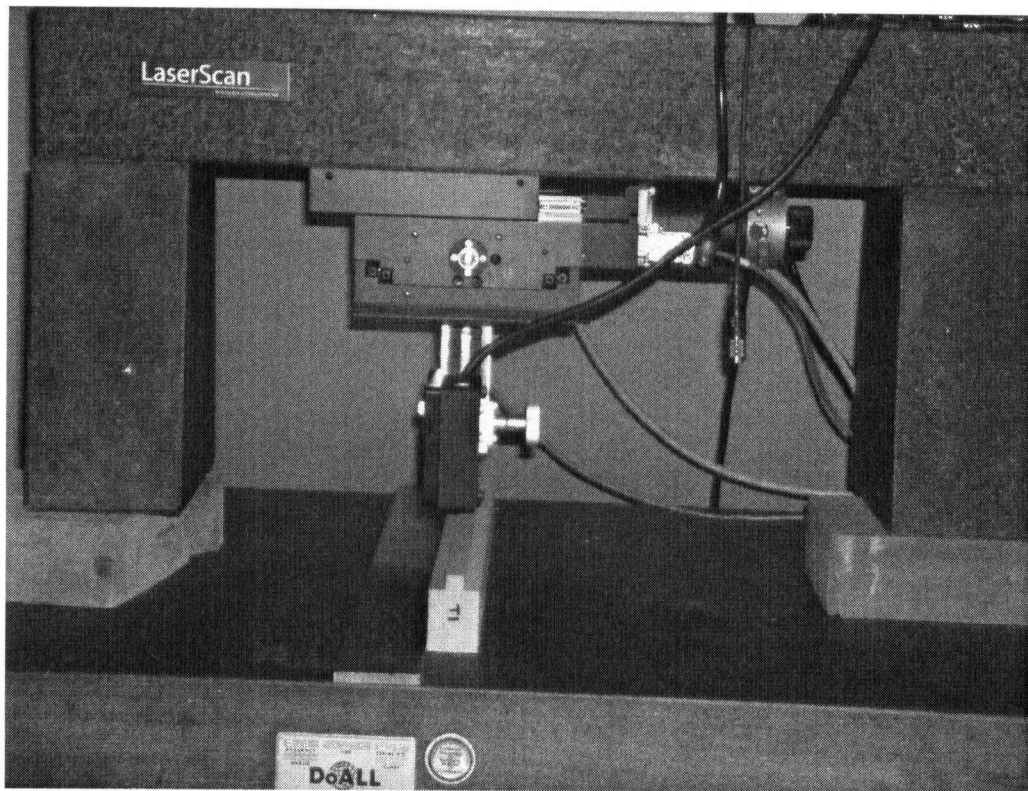


**Figure 58. Solarius Development LaserScan profilometer.**

The profilometer is a laser-based scanning tool used to measure surface roughness. Although not specifically designed to measure distances, the profilometer does track the distance of the scanned surface. The profilometer uses a Keyence laser triangulation sensor mounted on an X and Y stage. The profilometer has a measurement resolution of 1  $\mu\text{m}$  and the stage has a movement accuracy of  $\pm 1 \mu\text{m}$ . The resolution of the profilometer is one hundred times greater than the required resolution of the AQCS. Because of its higher resolution, the profilometer can provide definitive measurements of the components to verify the measurements collected with the calipers and AQCS. Two tongue (T1 and TM3) and two groove (G9 and GM5) parts were measured using the profilometer. Defects were purposely machined into these parts. TM3 and GM5 were used to verify width measurements and T1 and G9 was used to verify depth

measurements. Dimension "A" in parts TM3 and GM5 was decreased approximately 1-mm (Figure 59) and dimension "B" in parts T1 and G9 was decreased approximately by 1-mm (Figure 60).

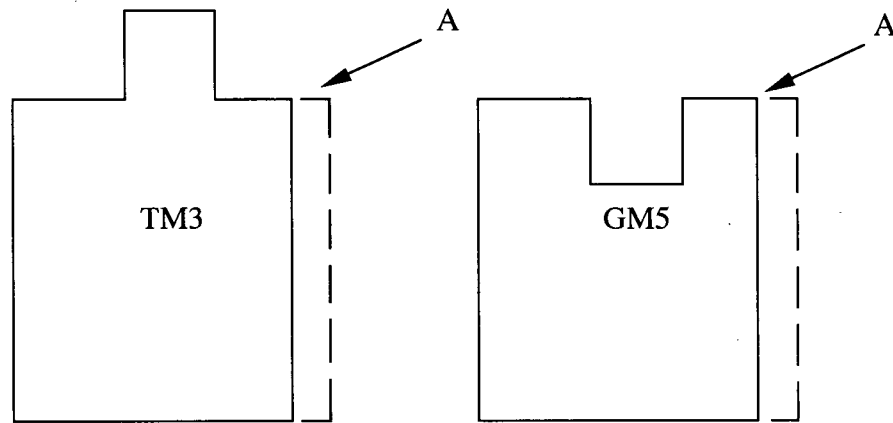


**Figure 59. Defective components TM3 and GM5.**

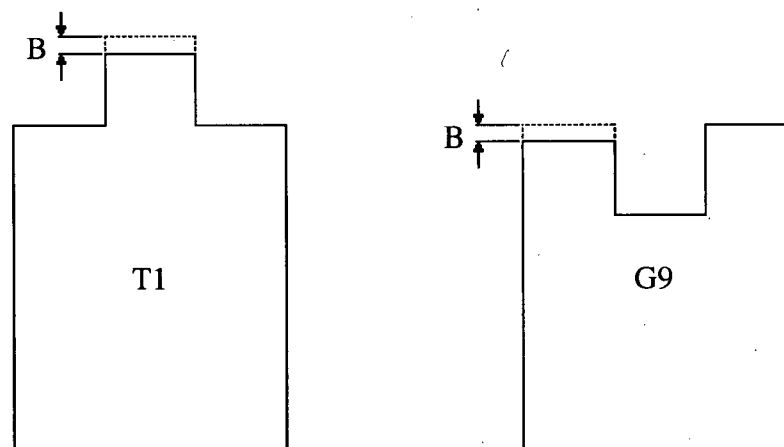


**Figure 60. Defective components T1 and G9.**

The width of TM3's tongue could not be measured because the depth change between the tongue and the shoulders was beyond the profilometer's measurement range of  $\pm 5$  mm (Figure 61).

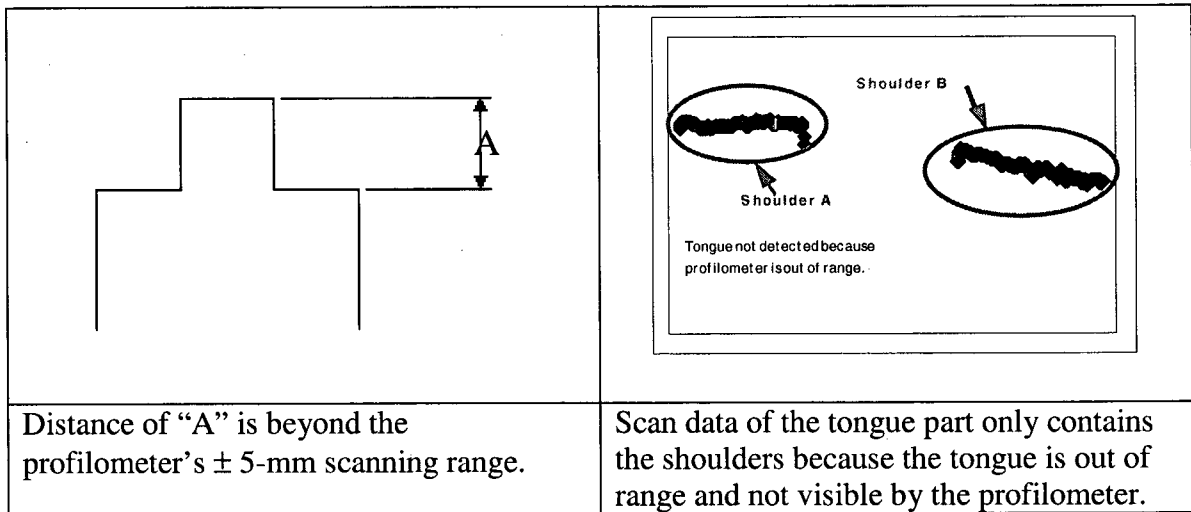


**Figure 61. Distance "A" is beyond the profilometer's scanning range.**

Fortunately, only the shoulders were altered so the profilometer was setup to measure the shoulders and ignore the tongue. Groove GM5 also faced similar limitations where the width of the groove was not measured. This problem did not affect the measurements of T1 and G9.

To assist in the development of the system, Canwood Furniture Inc. was chosen as a test facility for the system. The AQCS was designed around the DET because it was most susceptible to tolerance problems. A laboratory system was built to test the concept. The laboratory system encountered a perspective distortion problem, which was remedied with a calibration routine. Image analysis software was developed to measure the dimensions of the tongue, groove and chamfer parts. To verify the accuracy of the AQCS, the AQCS results were tested against a traditional pair of calipers and a highly accurate laser scanning profilometer.

## **5 Results and Discussion**

### **5.1 Laboratory test results**

Upon collecting data using the three measurement methods, the measurements were compared to determine the accuracy of the AQCS. The AQCS automatically analyzes and compiles the scanned data into X-bar and S control charts (APPENDIX D: Control Charts from Collected Data), the procedures of which are outlined in Section 3.3.1 and Section 4.3.4. To ensure that the data is normal, the data was tested using normal probability plots (APPENDIX H: Normal Probability Plot). The control limits on the control charts were set to three standard deviations. Each control chart tracks a specific critical dimension. Upon visual inspection of the X-bar charts, the data points fell near the targeted dimensions. However, analysis between the targeted and scanned data was performed with consideration of machining variation and the (lack of) dimensional stability of wood.

Machining variation can potentially cause dimensional variation. This type of variation can come from worn cutters, fences, bearings, shafts, operator's judgment and the accuracy limitations of the equipment. Since the test parts were machined on a table saw, fence alignment and adjustment, saw tooth wear and manual feeding can also all potentially contribute to machining variation.

Wood is also prone to shrinkage and dimensional changes when dried. Even though the parts were machined from seasoned maple, subalpine fir and MDF, varying humidity could have potentially caused the parts to change. The subalpine fir tongue and groove parts changed so excessively that they were discarded and replaced with seasoned

maple and MDF. After machining, most of the subalpine fir tongues twisted and the grooves collapsed (Figure 62).

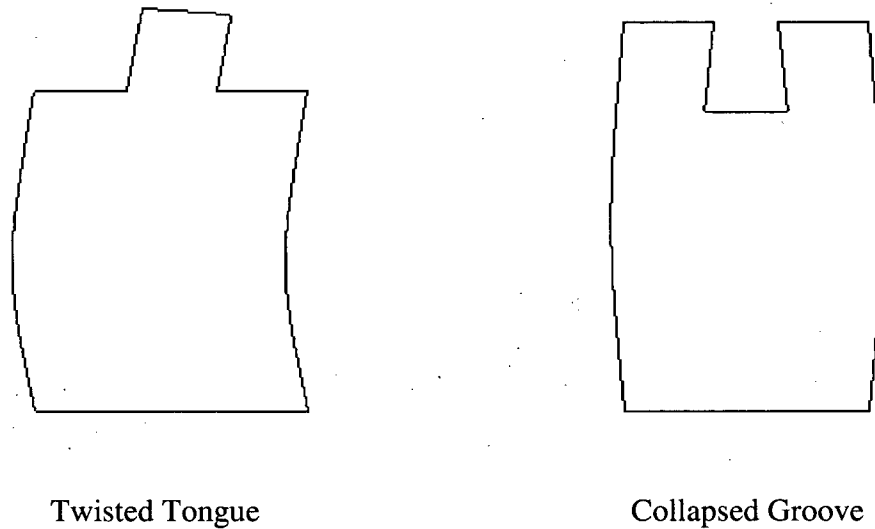


**Figure 62. Subalpine fir parts affected by drying stresses.**

The internal drying stresses caused the parts to change, and the problem was exacerbated when material was removed to create the tongue and groove. This made it impossible to take repeated measurements using the three methods because the dimensions changed between each measurement. Upon visual inspection, the chamfered parts appeared to be less affected by drying stresses and were acceptable for testing.

To verify the accuracy of the AQCS, four parts (tongue: TM3 and T1 / groove: GM5 and G9) were measured using all three-measurement methods and the results from each method were compared. Parts TM3 and GM5 were used to test the width measurement accuracy of the AQCS. The results from the three independent methods showed that the widths of the parts were undersized by approximately 1 to 1.5 millimeters during machining (Figure 63 and Figure 64).



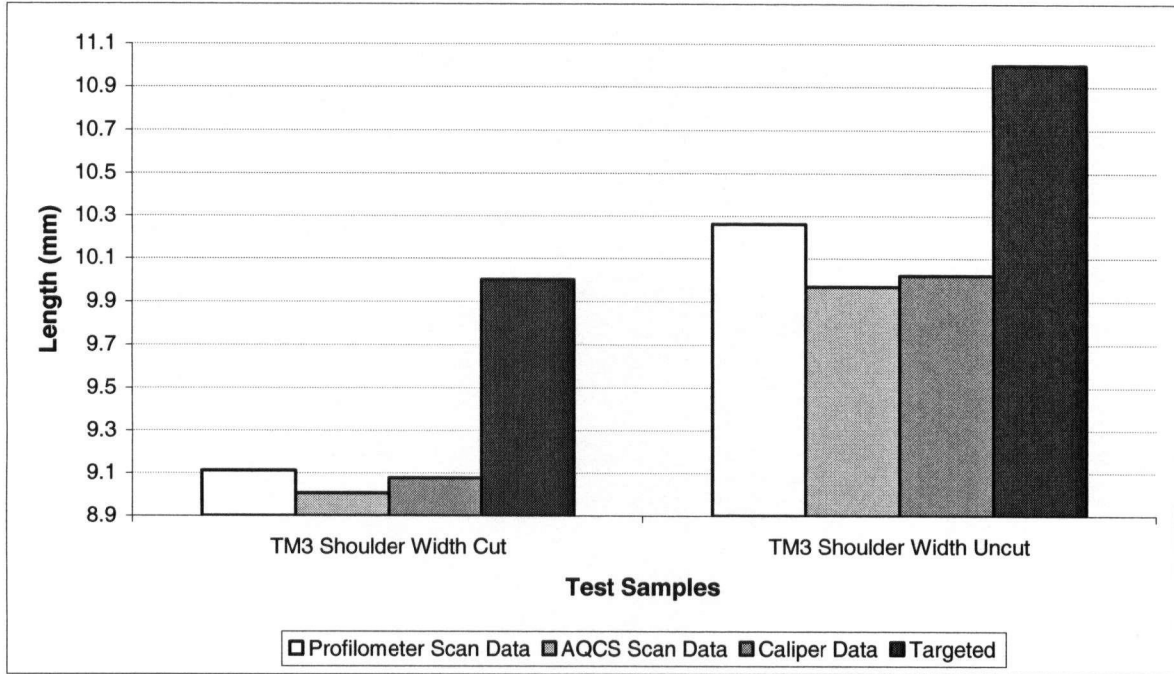


**Figure 63. Average measurements of both shoulders of part TM3 from the three measurement methods.**

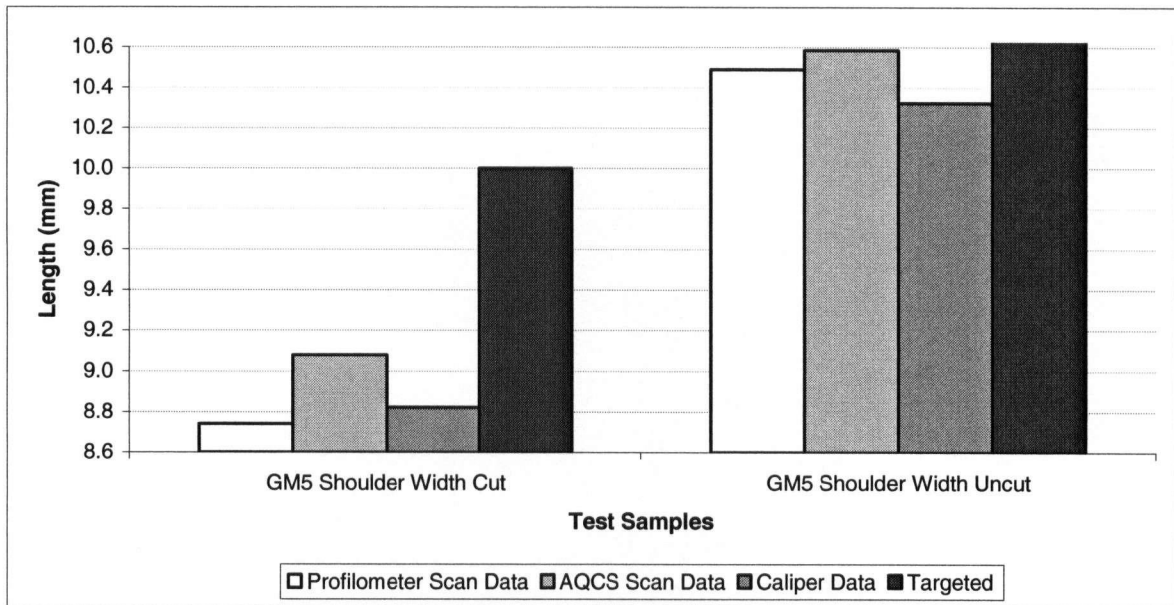


**Figure 64. Average measurements of both shoulders of part GM5 from the three measurement methods.**

Parts T1 and G9 were used to test the depth measurement accuracy of the AQCS. The AQCS measured the distance between the tongue and the shoulders of T1 and the change in length of the shortened shoulder of G9 (Figure 60). The results from the profilometer and AQCS appear to be similar (Figure 65).

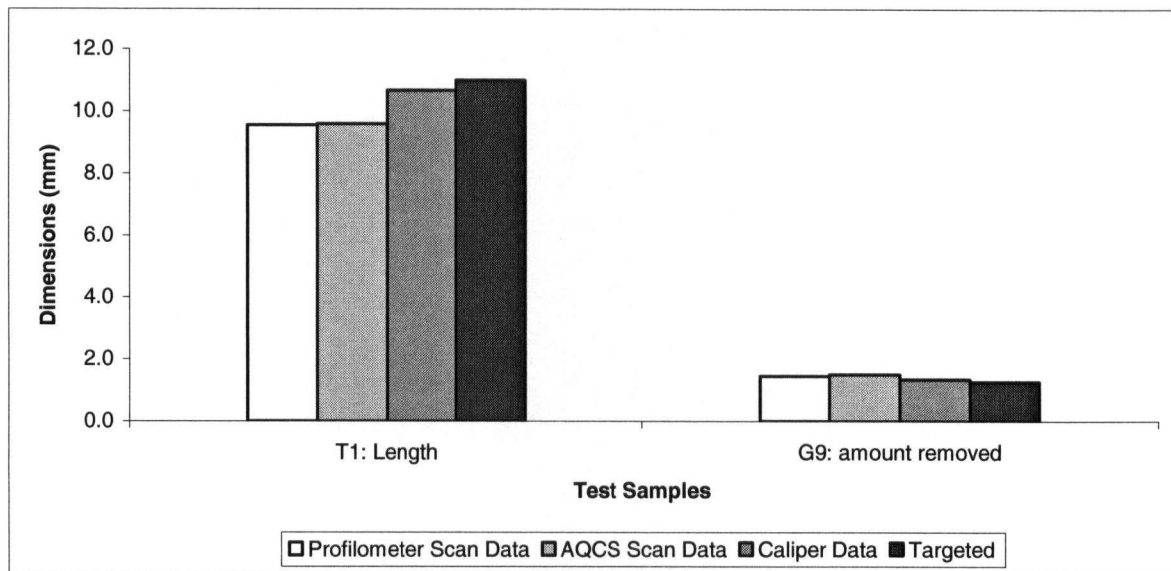


**Figure 65. Average measurements of both tongue depth of T1 and G9 from the three measurement methods.**

The width results, however, fluctuated between  $\pm 0.1$  to  $0.15$  mm and the depth results fluctuated  $+ 0.05$  mm from the profilometer's results. The variation found within these results exceeded the system requirements as stated by industry contributors. Many different factors may have contributed to the variation in these results, such as calibration errors, movement of the part during scanning and machining variation.

A one-way analysis of variance (ANOVA) test ( $\alpha = 0.05$ ) was performed to determine whether the AQCS results were statistically significant from those results obtained from the calipers and profilometer. The ANOVA test (APPENDIX F: ANOVA

Test Data) was performed because the variation in results for all three methods exceeded the targeted accuracy (Figure 66), which may indicate that the results may have been affected by thickness variations along the length of the test parts.

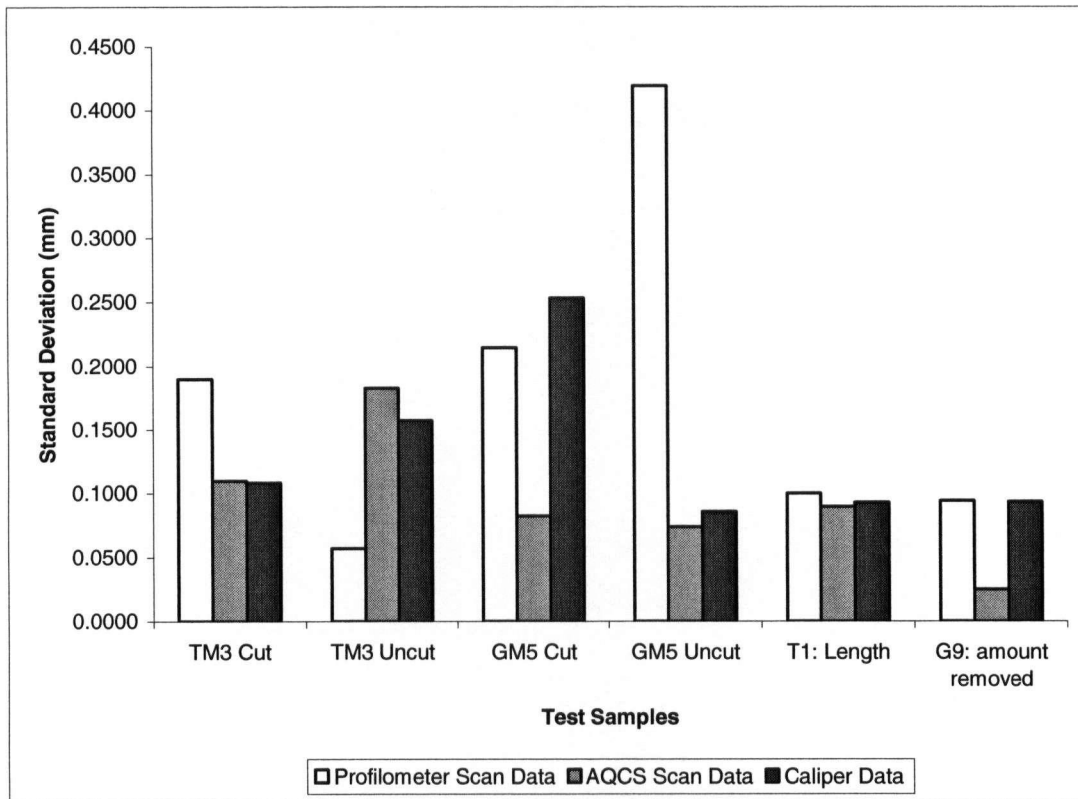


**Figure 66. Measurement variation results from each measurement method.**

Attempts were made to have the measurements taken in approximately the same locations for all three methods; however, specific setups were required for each method and pinpointing the exact sampling locations for all three methods was nearly impossible. The ANOVA test results revealed that some of the critical sample dimensions were significantly different (Table 4). For the samples that were significantly different, the Bonferroni test ( $\alpha = 0.05$ ) was performed to determine which of the measurement methods were significantly different (Table 5 and APPENDIX G: Bonferroni Test).

**Table 4. ANOVA test results.**

Sample	F	F crit	Test	ANOVA Test Results
G9 Shoulder Length	2.89	5.53	$F > F_{crit}$	No Significant Difference
GM5 Cut Shoulder	3.64	5.49	$F > F_{crit}$	No Significant Difference
GM5 Uncut	6.70	5.49	$F < F_{crit}$	Significant Difference
T9 Tongue Length	61.94	5.49	$F < F_{crit}$	Significant Difference
TM3 Cut Shoulder	1.02	5.57	$F > F_{crit}$	No Significant Difference
TM3 Uncut	37.00	5.53	$F < F_{crit}$	Significant Difference

GM5 and T9's Bonferroni test results indicate no significant difference between the AQCS and profilometer. TM3's results, however, do indicate some significant difference. For the most part, the caliper's results indicated some significant differences.

**Table 5. Bonferroni test results.**

GM5 Uncut Shoulder	CD		$ \bar{Y} \cdot \ell - \bar{Y} \cdot q $	Bonferroni Test Results
AQCS vs. Profilometer	0.1658	>	0.0945	Not Significantly Different
Caliper vs. Profilometer	0.1768	>	0.1669	Not Significantly Different
Caliper vs. AQCS	0.1837	<	0.2613	Significantly Different
T9 Tongue Length	CD		$ \bar{Y} \cdot \ell - \bar{Y} \cdot q $	Bonferroni Test Results
AQCS vs. Caliper	0.1246	<	0.4332	Significantly Different
AQCS vs. Profilometer	0.1246	>	0.0834	Not Significantly Different
Profilometer vs. Caliper	0.1246	<	0.5166	Significantly Different
TM3 Uncut Shoulder	CD		$ \bar{Y} \cdot \ell - \bar{Y} \cdot q $	Bonferroni Test Results
AQCS vs. Caliper	0.0999	>	0.0509	Not Significantly Different
AQCS vs. Profilometer	0.0952	<	0.2943	Significantly Different
Profilometer vs. Caliper	0.0952	<	0.2435	Significantly Different

## **5.2 System Improvements**

During laboratory testing, several limitations were uncovered. To meet industry's requirements, additional hardware and software modifications are required. Specifically, four hardware improvements were needed so that the system could consistently achieve the targeted 0.1 mm accuracy.

### **5.2.1 Camera resolution**

The current resolution of the Tamron lens and Basler camera is 0.1 mm/pixel. Under certain lighting conditions, the image acquisition software had greater difficulty in determining which pixel fell within the user-defined threshold. In some instances, the pixel intensity bordered the threshold value and may have been accepted. This created error in the image and the extent of the error was proportionate to the resolution of the hardware. The current system has an accuracy of  $\pm 0.1$  mm (a range of 0.2 mm), making it inadequate to accurately measure to within 0.1 mm. It is necessary to have a resolution that is at the least double the required accuracy of the system.

### **5.2.2 Depth of Field**

The current lens has a limited depth of field. Depth of field is the range where two objects that are placed at different distances away from the lens remain in focus. For this lens, objects must be within 10 mm of each other to remain in focus. This limits the dimensions of the parts being scanned. For example, the groove depth could not exceed 10 mm because the camera was not able to focus on the laser line inside the groove. Depth of field also affects the calibration routine because the focus is lost between the steps on the stepped calibration block (Figure 67).

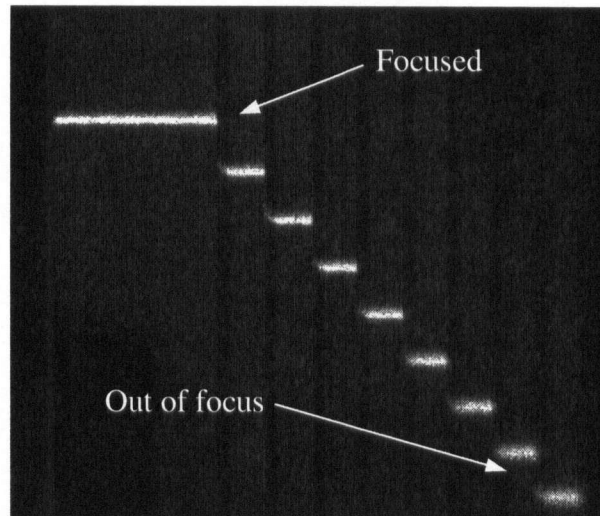


**Figure 67. Calibration block focusing problem.**

### **5.2.3 Calibration Equipment**

It was assumed that the stepped and flat calibration blocks were both precision-machined; however, when the precision of the blocks was verified, a higher precision micrometer showed otherwise. The steps of the stepped calibration block were found to vary by 0.1 mm and the flat calibration block varied by 0.05 mm. A commercial system will require precision-machined inert calibration blocks with a tolerance that does not significantly affect the precision of the AQCS.

### **5.2.4 Mounting base**

The melamine-coated particleboard base did not have the rigidity required for a mounting base for the laser and camera. Once the system was calibrated, any movement between the camera and laser caused problems. The calibration routine is based on the initial setup. If the relationship between the camera and laser changes after the initial calibration, the incoming data will not be accurately calibrated. The scanning bed was also found to be a problem because the bed was not level. This lack of flatness caused

parts to sit differently and affect the captured image. The solution to this issue is to mount the camera and laser in a rigid precision-machined steel or aluminum case with a sturdy mounting frame and to transport the parts across a precision-machined bed.

### 5.2.5 Laser-line shadowing

Laser-line shadowing occurs when the center of the laser is offset from the centre of the part. The laser-line is projected in a fanned pattern where a protruding section of a part will block the laser-line from reaching the section that is behind the protrusion. For example, the protruding tongue shadows the shoulders from the laser-line (Figure 68).

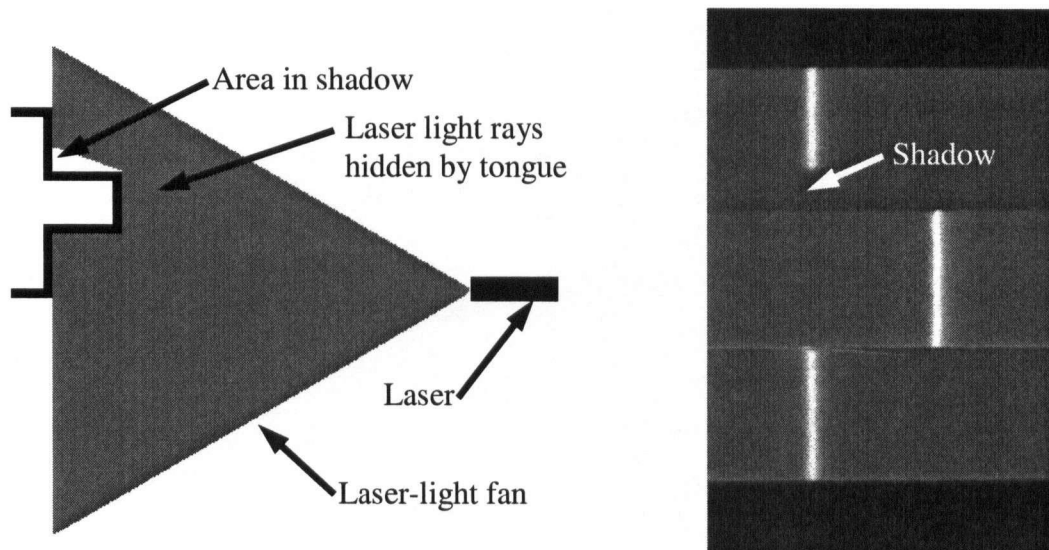


**Figure 68. Shadowing due to offset laser-line.**

The laboratory system was setup so that the centre of the laser was always in the centre of the part. Unfortunately, it would be highly inefficient to have machine operators adjusting the laser-line for each batch and too costly to automate the laser-line adjustment process. A potential solution is to use two overlapping laser-lines (Figure 69). The second laser-line would overlap the first laser-line and illuminate the areas that are shadowed from the first laser-line (Figure 70).

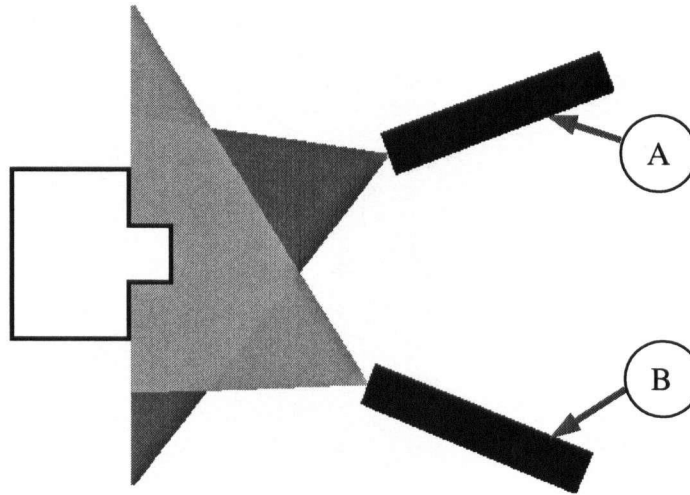


**Figure 69. Overlapping laser-lines to eliminate shadowing.**

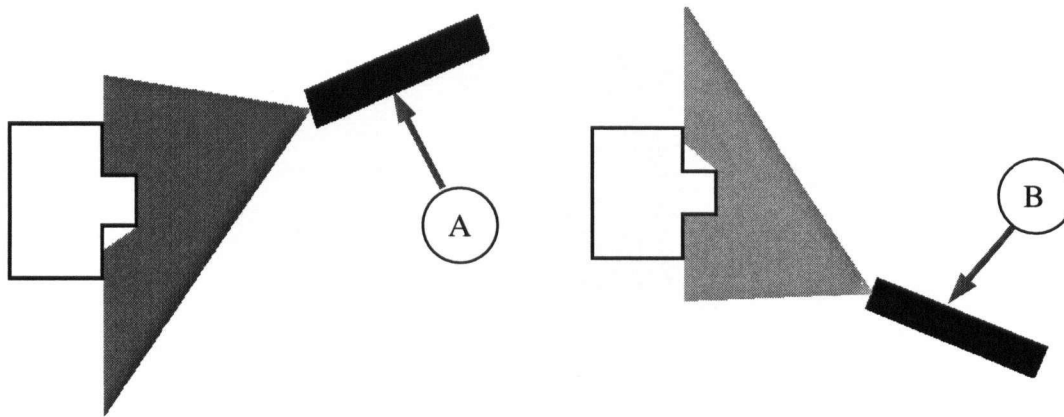


**Figure 70. Laser A illuminates Laser B's shadowed areas and vice versa.**

### **5.2.6 Laser-line intensity**

The output of the 0.9-mW laser used in the laboratory system did not have enough intensity to illuminate dark spots such as knots and discoloured grain. In the laboratory system, the aperture on the camera was opened fully and the image acquisition software threshold intensity was lowered to detect dimly lit pixels. These settings required the system to operate in complete darkness because external light affected the



image. An industrial system would need a costly and less flexible enclosure to block out external light. A 35-mW laser would provide a much higher intensity laser-line (Stocker Yale, 2004). With a brighter laser-line, an enclosure is not needed since the aperture can be closed down, minimizing the external light that enters the camera.

### **5.2.7 Software improvements**

The analysis software is currently hard coded to deal with specific profiles: tongues, grooves and chamfers. The software does not have the ability to monitor other profiles without additional programming. An industrial system should be able to deal with any part that is being produced from the machine. This requires an additional piece of software that converts part drawings into data that the system can interpret and look for in the scanned images.

## **5.3 Wood Machining Tolerances**

The specified measurement resolution of the AQCS was 0.1-mm, which may have been an overly optimistic target. Based upon visual inspection and the opinions of the machine operators, the dimensional defects can be measured with a measurement resolution greater than 0.1-mm. Therefore, the resolution of the proof-of-concept system is perhaps sufficient, but it would necessary to conduct a separate study on machining tolerances to determine the required measurement resolution.

## **5.4 System Applications**

Based on the laboratory trials, the AQCS is potentially well suited for a variety of automated processes that are found in the value-added wood industry. Although its intended design was for a double-end tenoner, the system was also designed with other

machine centres in mind. The moulder has the most in common with the double-end tenoner because it produces profiled shapes such as mouldings, window and door frames, flooring and a variety of other profiled parts; therefore, the system could easily be adapted to a moulder.

Industry feedback on the demonstration of the system has been positive and additional applications were suggested. One common suggestion was a panel scanning system that checked for defects and hole locations. An edged-glued panel manufacturer suggested a system that checked for defects such as cracks, splits and knotholes on panels leaving the gluing press. This system would warn operators of a defective panel and allow them to pull the panel out and fix the defects. Another manufacturer suggested a system that measured the locations of drilled holes on panels leaving an automated drilling machine. This system would check for proper initial setup and misalignment due to wear on the machine. Since cracks, splits, knotholes and drilled holes show changes in depth, the system could be used as a panel inspection system. The system will require new hardware because the current system has a limited field of view that is inadequate to inspect across a four-foot wide panel.

## 6 Conclusion

In order to maintain competitiveness, optimization is becoming increasingly required within the Canadian secondary manufacturing sector. For many years, value-added companies have relied on proven traditional woodworking techniques; highly skilled craftsmen who meticulously fabricated high quality products. However, traditional techniques are ineffective in the modern high-volume manufacturing plants that are needed to compete globally.

Highly advanced machines and their machine operators have replaced highly skilled craftsman. These machines have revolutionized the industry by introducing automation to a labour-intensive industry. Unfortunately, quality control is one area in production that has been overlooked. Many secondary wood products companies see benefits in quality control programs, but their current techniques are dated and not adequate for a modern plant. This problem stems from a workforce with limited education and the lack of affordable quality control technologies. To rectify this problem, organizations such as the Wood Products Quality Council of Canada have been formed to help educate the workforce. However, there are currently no suppliers of affordable quality control technologies. Quality control equipment suppliers have concentrated on other industries, such as plastics, steel and a variety of other high-tech industries. The technologies developed for these industries are expensive and unobtainable by most value-added manufacturers. Therefore, it was conceived that the development of a dedicated and affordable quality control system would benefit the industry.

Based on suggestions from industry, a proof of concept of an optically-based automated quality control system was developed. The system took existing technologies found in other industries and adapted them to a system designed specifically with the needs of the value-added industry in mind. The system was based on a basic optical metrology technique known as pattern projection, where a digital camera and laser-line were used to map the surface profile of parts leaving a machine centre. The proof of concept system was developed to test potential applications and limitations of the system. To meet the industry's tolerance requirements of  $\pm 0.3\text{mm}$ , the system's target accuracy was set to  $\pm 0.1\text{mm}$ .

To test the accuracy of the system, the system scanned three different profiles common to furniture manufacturing (tongues, grooves and chamfers). The accuracy of the system was verified with traditional quality control tools – digital calipers and digital micrometers. The system was able to identify the critical dimensions of each component and to create control charts for each simulated production run. Unfortunately, the system did not attain the required accuracy. Through further investigation, it was determined that variability throughout the hardware made it impossible to achieve the accuracy required. Several hardware factors that affected the accuracy of the system included the lack of camera resolution, lack of precision in the mounting and calibration hardware, and several optics problems. Fortunately, many of these problems can be remedied through a change of hardware and modifications to the software. However, this would most likely increase the cost of the system, making it much more difficult to implement in smaller Canadian plants. The current proof of concept system is not ready for commercialization;

however, the knowledge gained from the development of this system can be applied to the further development of a commercial system.

Further research is required to complete the development of a commercial automated quality control system. To increase the accuracy of the system, it would be necessary to use a more expensive higher resolution camera. However, as technology advances, the cost of high-resolution cameras will come down, making it possible to maintain a low cost system. It is also necessary to reduce the system's sensitivity to the movement of the parts passing through the system. Firstly, the components require a much more rigid hold system to prevent the parts from moving. Secondly, since movement is inevitable in a wood products plant, a tracking algorithm must be developed to track the movement of the part. This tracking algorithm would be used in conjunction with the calibration routine to accurately track and calibrate the images.

## Reference

“Aberration” Nikon (n.d.). August 23, 2004 <[www.ave.nikon.co.jp/bi\\_e/encyclo/ad.htm](http://www.ave.nikon.co.jp/bi_e/encyclo/ad.htm)>

“Aberrations and Distortion.” Nikon (n.d.). April 12, 2004  
<[http://nikon.topica.ne.jp/bi\\_e/encyclo/ad.htm](http://nikon.topica.ne.jp/bi_e/encyclo/ad.htm)>

Ali, A., Saccoccio, S., and Thompson, J. “Softwood Lumber Dispute.” CBC Online News. (March 2001). September 20, 2003  
<[http://www.cbc.ca/news/indepth/background/softwood\\_lumber.html](http://www.cbc.ca/news/indepth/background/softwood_lumber.html)>

Anderson, R. B., Patterson, D. W. “Use of Statistical Process Control in the Furniture and Cabinet Industries.” Forest Prod. J. 46(1) (1996): 36-38

Bhote, K.R. World Class Quality, AMA Membership Publications Division, New York, 1988 pp.67

Bluman, A.G. Elementary Statistics: a step-by-step approach 3<sup>rd</sup> Edition. WCB McGraw-Hill, United States, 1997 pp.664

British Columbia Ministry of Forests. “The Forestry Revitalization Plan.” British Columbia Government. (March 2003). August 15, 2003  
<http://www.for.gov.bc.ca/mof/plan/frp>

Burke, M. W. Image Acquisition. Chapman and Hall, London, England, 1996

“Cant Recovery” LMI 3D Machine Vision September 6, 2002  
<http://www.lmint.com/cfm/index.cfm?It=901&Id=1&Se=85&Sv=0>

CBC News Online staff. “U.S. lobbies to tax Canadian lumber.” CBC News. (March 31, 2001). August 18, 2003 <<http://www.cbc.ca/cgi-bin/templates/view.cgi?news/2001/03/31/softwood10331>>

Cielo, P. Optical Techniques for Industrial Inspection. Academic Press, Inc., New York, 1988, pp.10

Chiu, J. Wood Product Quality Council. (Personal communication). Vancouver, BC. November 2003

“Circle Touching 3 Points” Intellitech Inc., September 28, 2001  
<[http://www.delphiforfun.org/Programs/Math\\_Topics/circle\\_from\\_3\\_points.htm](http://www.delphiforfun.org/Programs/Math_Topics/circle_from_3_points.htm)>

“Competitive Situation Domestic Production.” Industry Canada. (April 5, 1999). September 3, 2003 <<http://strategis.ic.gc.ca/SSG/dd73189e.html>>

"Components of Machine Vision System" Farlex Inc. 2004  
<<http://encyclopedia.thefreedictionary.com/Machine%20vision>>

Edgar, T.F. "A Batch Processing Module" Enterprise. (2003). February 10, 2004  
<[http://web.mit.edu/che-curriculum/2003/cape\\_cod/presentation\\_by\\_Edgar.pdf](http://web.mit.edu/che-curriculum/2003/cape_cod/presentation_by_Edgar.pdf)>

Europa, "Forest Based Industries." (January 7, 2004). August 25, 2004  
[http://europa.eu.int/comm/enterprise/forest\\_based/woodworking\\_en.html#7](http://europa.eu.int/comm/enterprise/forest_based/woodworking_en.html#7)

Gara, M. Image Acquisition Software 2003

Gurevich, G.J and Nice, K. "How Digital Cameras Work" How Stuff Works. 2004 <<http://www.howstuffworks.com/digital-camera.htm/printable>>

Harding, K. "3D Machine Vision as a Shop Floor Metrology Tool." Machine Vision Online. (n.d.) November 22, 2003  
<[http://www.machinevisiononline.org/public/articles/General\\_Electric.pdf](http://www.machinevisiononline.org/public/articles/General_Electric.pdf)>

Hardin, R.W. "Dual cameras evaluate ceramic circuit boards." Vision System Design. June 2003 25-29 < <http://vsd.pennnet.com/>>

"How does the Qbase System Work?" Qbase. March 26, 2004  
<<http://www.qbase.com>>

Industry Canada Manufacturing Branch. "The Residential Furniture Industry of Canada." Industry Canada. (n.d.). August 9, 2003  
<[http://strategis.gc.ca/epic/internet/infurniture-meuble.nsf/vwapj/snapshotResidentialEng.pdf/\\$FILE/snapshotResidentialEng.pdf](http://strategis.gc.ca/epic/internet/infurniture-meuble.nsf/vwapj/snapshotResidentialEng.pdf/$FILE/snapshotResidentialEng.pdf)>

John, G. "Triangle, Inscribed and Circumscribed" North Carolina School of Science and Mathematics. 2004  
<<http://192.154.43.167/goebel/statecon/Topics/triangl/TRIANGL.htm>>

Lawrence, P.D., Mauch, Konrad. Real-Time Microcomputer System Design: An Introduction. McGraw-hill Inc., 1987, pp. 3

Lévesque, Yves. "Technology Roadmap: Lumber and Value-Added Wood Products." Industry Canada. (September 25, 2003). October 11, 2003.  
<<http://www.strategis.ic.gc.ca/epic/internet/infif.nsf/vwGeneratedInterE/fb01370e.html>>

Lucero, A. G. and de Queiroz, A.A. "A Method to Optimize Scheduling in Small Batch Manufacturing" (2002). February 10, 2004  
<<http://culiacan.udo.mx/~gortega/Basys2002-55.pdf>>

Kidger, M.J. Fundamental Optical Design. The International Society for Optical Engineer. Bellingham, Washington, 2002, pp. 63

- Kotelnikov, V. "Glossary" Ten<sup>3</sup>. March 4, 2004  
<[http://www.1000ventures.com/business\\_guide/glossary\\_lean\\_kaizen.html](http://www.1000ventures.com/business_guide/glossary_lean_kaizen.html)>
- Kozak, R. A., Maness, T.C. "Quality Assurance for Value-added Wood Producers in British Columbia." Forest Prod. J. 51(6) (2001): 47-55
- Kozak, R. A., Maness, T.C. "A system for continuous process improvement in wood products manufacturing." Holz als Roh-und Werkstoff. 61(2003): 95-102
- Kundrot, R.A. 2000. "Optimizing Plant Operations. Forest Product Society 54<sup>th</sup> Annual Meeting – Session 12, Quality and Process Control: State-of-the-Art in the Forest Products Industry", Lake Tahoe, NV, June 21, 2000. RAK Consulting, Springfield, OR.
- Masi, C.G. "Vision system rolls mixed wheel rims." Vision Systems Design. April 2003, 23-26
- Merriam Online Dictionary 2004 <<http://www.merriam-webster.com/cgi-bin/dictionary?book=Dictionary&va=mass+production&x=19&y=16>>
- Montgomery, D.C. Introduction to Statistical Quality Control 3<sup>rd</sup> Edition. John Wiley & Sons Inc. New York, 1997, pp. 4
- "A Glimpse into the Future of Canada's Forests and Forest Sector." Nature Resources Canada. (2003). August 25, 2004 <[http://www.nrcan-rncan.gc.ca/cfs-scf/national/what-quoi/sof/sof03/feature01a\\_e.html](http://www.nrcan-rncan.gc.ca/cfs-scf/national/what-quoi/sof/sof03/feature01a_e.html)>
- "ODAC Measuring Head" Zumbach Electronics AG 2004  
<<http://www.zumbach.com/e/product/odac.asp>>
- "Profile." WPQC. February 19, 2004 <<http://www.wpqc.com>>
- "Profilemaster Specifications" Zumbach Electronics AG 2004  
<<http://www.zumbach.com/e/product/tdprofilemaster.asp>>
- "Quality Systems Terminology." American Society for Quality Control. 1978 ANSI/ASQC A3-1978. Milwaukee, WI.
- Kozak, R.A., Maness, T.C. and Staudhammer, C.L. "Real-time Size Control Systems in Wood Products Manufacturing." UBC Faculty of Forestry Research Poster Presentations, Vancouver, January 22, 2002
- "Rear Axle Inspection" LMI 3D Machine Vision September 6, 2002  
<http://www.lmint.com/cfm/index.cfm?It=901&Id=64&Se=83&Sv=0>
- "Retail Sales by Commodity" Statistics Canada. (May 28, 2003). September 24, 2003 <<http://www.statcan.ca/english/Pgdb/trade39.html>>



Sandak, J., Tanaka, C., "Evaluation of surface smoothness using a light-section shadow scanner." Journal of Wood Science. 51(3) (2005). 270-273

Saint-Pierre, Etienne "Expansion, Free Trade and Size of Establishment" Statistics Canada Manufacturing, Construction and Energy Division (August 1999). September 21, 2003 <<http://www.statcan.ca/english/freepub/35-251-XIE/1999/35-251.htm>>

"Solve for Radius" The Math Forum, 2003  
<http://forum.swarthmore.edu/dr.math/problems/culpepper9.9.97.html>

Statistics Canada Manufacturing, Construction and Energy Division. "Expansion, Free Trade and Size of Establishment" Statistics Canada. (August 1999). September 21, 2003 <<http://www.statcan.ca/english/freepub/35-251-XIE/1999/35-251.htm>>

Stocker Yale Sales Representative. (Personal communication). Stocker Yale Canada Inc. May 2004

"Technology Roadmap Lumber and Value-Added Wood Products" Industry Canada September 25, 2003 <<http://strategis.ic.gc.ca/epic/internet/infif.nsf/vwGeneratedInterE/fb01447e.html>>

"The Canadian Furniture Industry - An Overview" Industry Canada. (June 18, 2003). September 3, 2003 <<http://strategis.ic.gc.ca/epic/internet/infurniture-meubles.nsf/vwGeneratedInterE/rf03598e.html>>

"The Residential Furniture Industry of Canada." Industry Canada Manufacturing Branch. (June 15, 2003). October 12, 2003  
<[http://strategis.gc.ca/epic/internet/infurniture-meuble.nsf/vwapj/snapshotResidentialEng.pdf/\\$FILE/snapshotResidentialEng.pdf](http://strategis.gc.ca/epic/internet/infurniture-meuble.nsf/vwapj/snapshotResidentialEng.pdf/$FILE/snapshotResidentialEng.pdf)>

"Timber Joints" diyidata.com 2004  
<[http://www.diyidata.com/techniques/timber\\_joints/box\\_joints/box\\_joints.htm](http://www.diyidata.com/techniques/timber_joints/box_joints/box_joints.htm)>

"The World Furniture Industry: Production – Trade – Market" Union Europeenne de L'ameublement. (September 2005). August 11, 2006. <<http://www.ueanet.com>>

"Vision/Mission" Kaizen Institute Inc. 2003 <<http://www.kaizen-us.com/vision.php>>

Wilson, A. "Telecentric Lenses Focus on Machine Vision." Vision system. Jan 2004. pp. 37

"Why Standards Matter" International Organization for Standards. (n.d) Feb 16, 2004 <<http://www.iso.ch/iso/en/aboutiso/introduction/index.html>>

Wilson, A. "Telecentric Lenses Focus on Machine Vision." Vision system. Jan 2004. pp. 37

Wilson, J.W. "Problem Solving with Heron's Formula" University of Georgia.  
October 10, 1986 <<http://jwilson.coe.uga.edu/emt725/Heron/Heron.html>>

Wong, D.C. (Personal communication). Vancouver, BC. October 2003

Young, T.M., Winistorfer, P.M. "SPC: Statistical Process Control and the Forest  
Products Industry." Forest Prod. J. 49(3) (1999): 10-16

## APPENDIX A: Hardware Specifications

Hardware specifications used to develop the automated quality control system

Camera	
Camera Manufacturer/Model	Basler Vision Technology A301f
Resolution	658x494 pixels
Sensor type	Sony ICX414AL Interline transfer progressive scan CCD
Max. Frame Rate	80 frames/s
Video Output Type	IEEE 1394
Approx. Retail Value	\$3300 (Canadian Dollar)
Video Card	
Manufacture/Model	Matrox Meteor-II / 1934
Approx. Retail Value	\$400 (Canadian Dollar)
Lens	
Lens Manufacture/Model	Tamron 2/3" 35MM F/2.1
Focal Length	35mm
Iris Range	F/2.1-22
Mount	C
½" Angle of View	10.4° x 7.8°
Approx. Retail Value	\$275 (Canadian Dollar)
Laser-line	
Laser Manufacturer	Lacey-Harmer
Model	Laser Blazer
Output	0.9 mW
Wavelength	530 - 680 nm
Standoff range	2'-0"
Working range	0'-2"
Approx. Retail Value	\$400 (Canadian Dollar)

## APPENDIX B: Lens Aberration Test Data

Data used to analyze for lens aberration problems. The data contains the X and Y position, angle and width for each of the horizontal and vertical grid line.

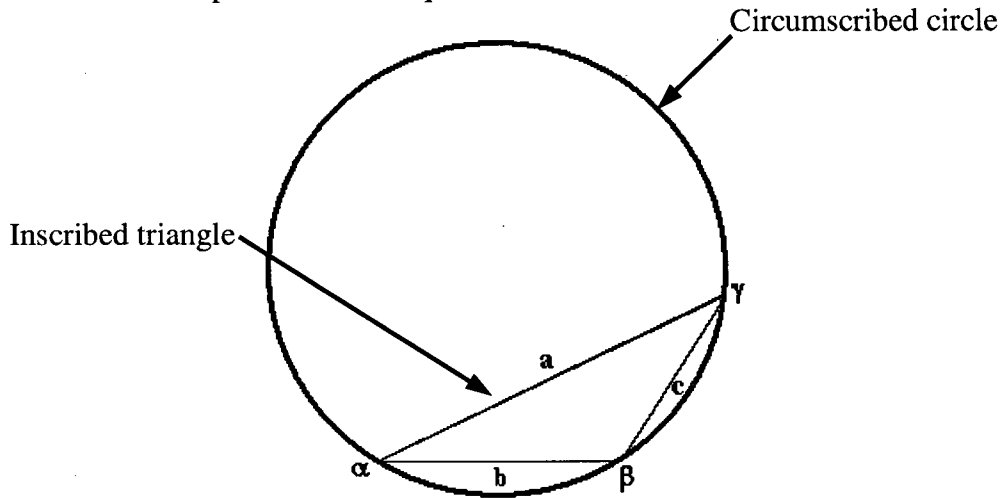
Horizontal Grid Lines (Pixels)					
	Markers	Position X	Position Y	Angle	Width
H-Line 1	H1	335.59	27.98	0.30	3
	H2	335.59	31.45	0.29	3
H-Line 2	H3	335.59	85.48	0.29	4
	H4	335.59	88.97	0.28	3
H-Line 3	H5	335.59	141.99	0.29	3
	H6	335.59	145.53	0.28	2
H-Line 4	H7	335.59	198.58	0.24	3
	H8	335.59	202.17	0.22	3
H-Line 5	H9	335.59	255.11	0.28	2
	H10	335.59	258.79	0.27	2
H-Line 6	H11	335.59	311.52	0.2	3
	H12	335.59	315.16	0.19	3
H-Line 7	H13	335.59	367.95	0.27	2
	H14	335.59	371.81	0.24	2
H-Line 8	H15	335.59	424.44	0.18	3
	H16	335.59	428.17	0.17	3
Statistics					
Minimum		335.59	27.98	0.17	2.00
Mean		335.59	228.44	0.25	2.75
Maximum		335.59	428.17	0.30	4.00
Std. Dev.		0.00	133.96	0.04	0.58

Vertical Grid Lines (Pixels)					
	Markers	Position X	Position Y	Angle	Width
V-Line 1	V1	46.77	241.11	90.19	3
	V2	50.73	241.11	90.19	2
V-Line 2	V3	103.45	241.11	90.19	2
	V4	107.35	241.11	90.19	2
V-Line 3	V5	159.9	241.11	90.2	3
	V6	163.76	241.11	90.2	2
V-Line 4	V7	216.62	241.11	90.26	3
	V8	220.57	241.11	90.24	2
V-Line 5	V9	274.06	241.11	90.2	3
	V10	277.93	241.11	90.21	3
V-Line 6	V11	330.86	241.11	90.22	3
	V12	334.74	241.11	90.21	3
V-Line 7	V13	387.6	241.11	90.29	2
	V14	391.55	241.11	90.28	2
V-Line 8	V15	444.46	241.11	90.29	2
	V16	448.43	241.11	90.32	2
V-Line 9	V17	501.23	241.11	90.23	3
	V18	505.08	241.11	90.27	3
V-Line 10	V19	557.67	241.11	90.29	2
	V20	561.62	241.11	90.25	3
V-Line 11	V21	614.31	241.11	90.29	3
	V22	618.41	241.11	90.33	4
Statistics					
Minimum		46.77	241.11	90.19	2.00
Mean		332.60	241.11	90.24	2.59
Maximum		618.41	241.11	90.33	4.00
Std. Dev.		183.86	0.00	0.05	0.59

Horizontal	Mean	Standard Deviation
Angle	0.25°	0.04°
Compensated Angle	≈ 0.00°	
Width	2.75 pixels	0.58 pixels
Vertical		
Angle	≈ 90.24°	0.05°
Compensated Angle	90.00°	
Width	2.59 pixels	0.59 pixels

## APPENDIX C: 3-point Circle Fit

Explanation of three-point circle fit equation:



$\alpha$ = minimum point
$\beta$ = test point
$\gamma$ = maximum point
a, b, and c are the lengths of the line segments

Based on the  $\alpha$ ,  $\beta$ , and  $\gamma$  points, the three-point circle fit equation calculates the radius of the circumscribed circle, (equation 1). “K” is the area of the inscribed triangle created by the three points. Heron’s formula is used to calculate the area of the inscribed triangle (equation 2) (Wilson, J.W., 1986). The “s” is the semi-perimeter of the inscribed triangle (equation 3). Heron’s formula requires the length of the line segments (a, b, and c) that make up the inscribed triangle (equation 4, 5, and 6).

(Equation 1 (Intellitech, 2004))

$$Radius = \frac{abc}{4K}$$

(Equation 2)

$$K = \sqrt{s(s-a)(s-b)(s-c)}$$

(Equation 3 (North Carolina School of Science and Mathematics, 2004))

$$s = \frac{(a + b + c)}{2}$$

(Equation 4 (The Math Forum, 2003))

$$a = \sqrt{(\gamma_x - \alpha_x)^2 + (\gamma_y - \alpha_y)^2}$$

(Equation 5 (The Math Forum, 2003))

$$b = \sqrt{(\beta_x - \alpha_x)^2 + (\beta_y - \alpha_y)^2}$$

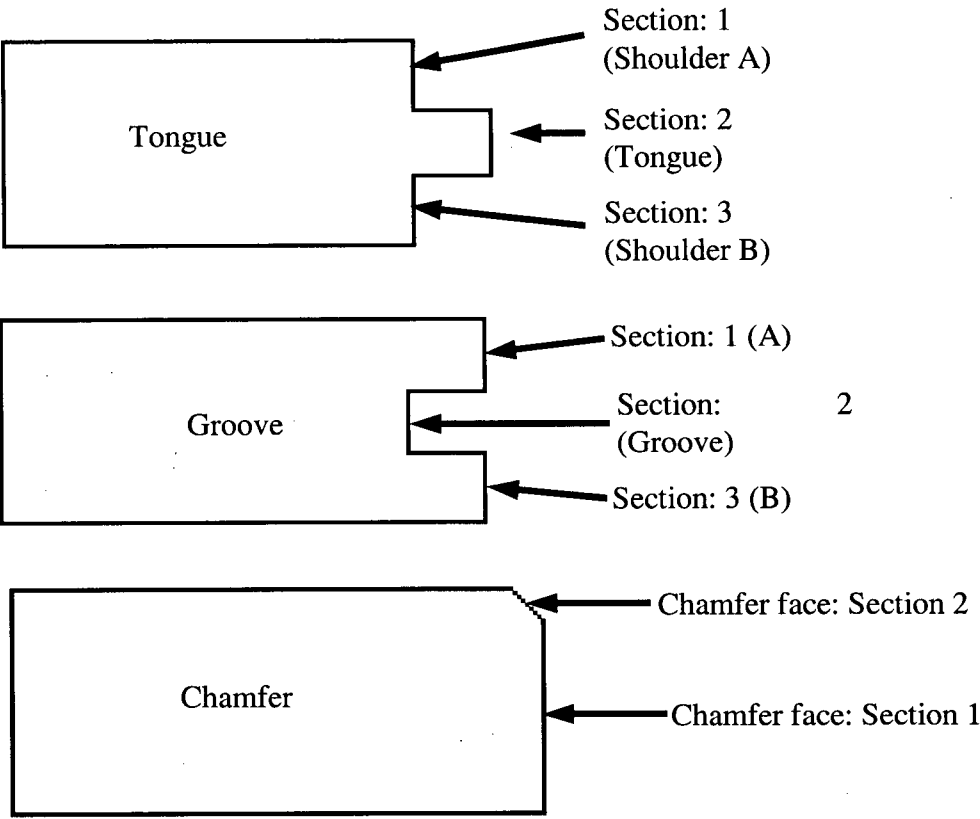
(Equation 6 (The Math Forum, 2003))

$$c = \sqrt{(\gamma_x - \beta_x)^2 + (\gamma_y - \beta_y)^2}$$

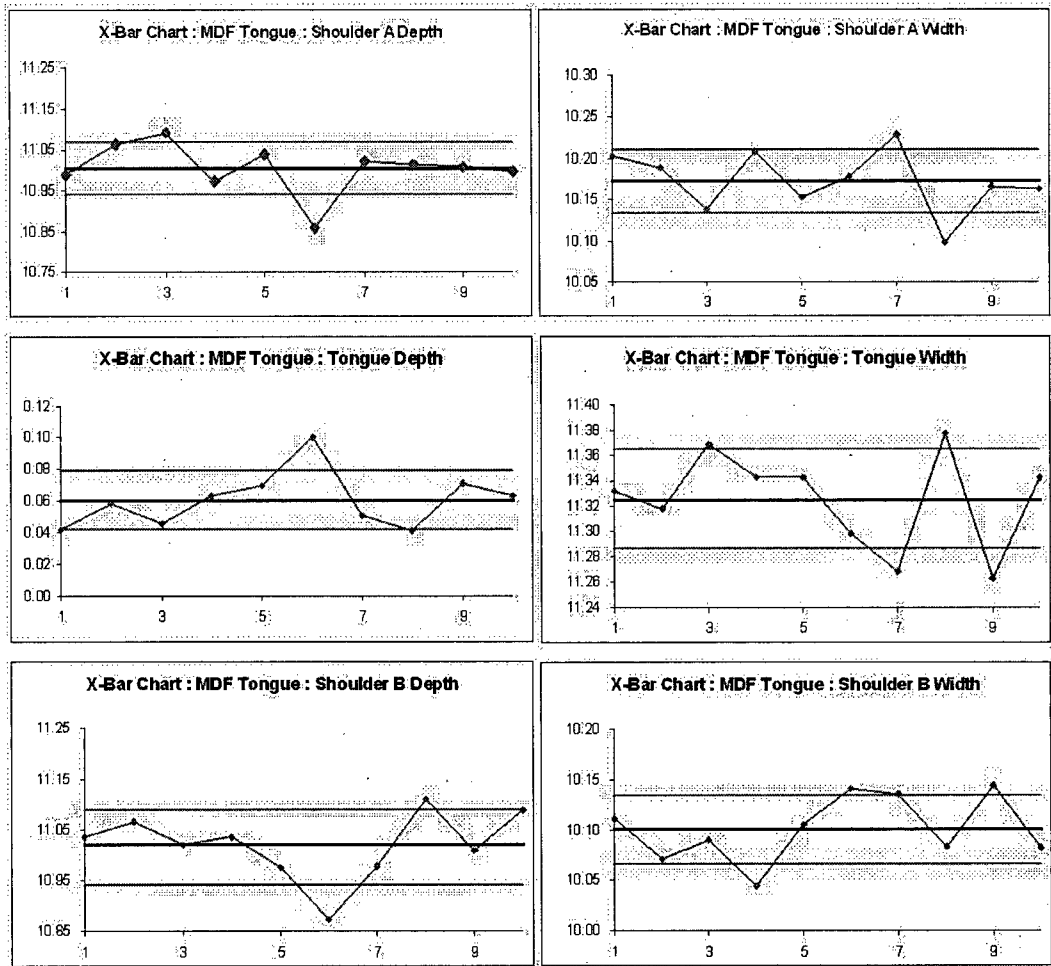


# APPENDIX D: Control Charts from Collected Data

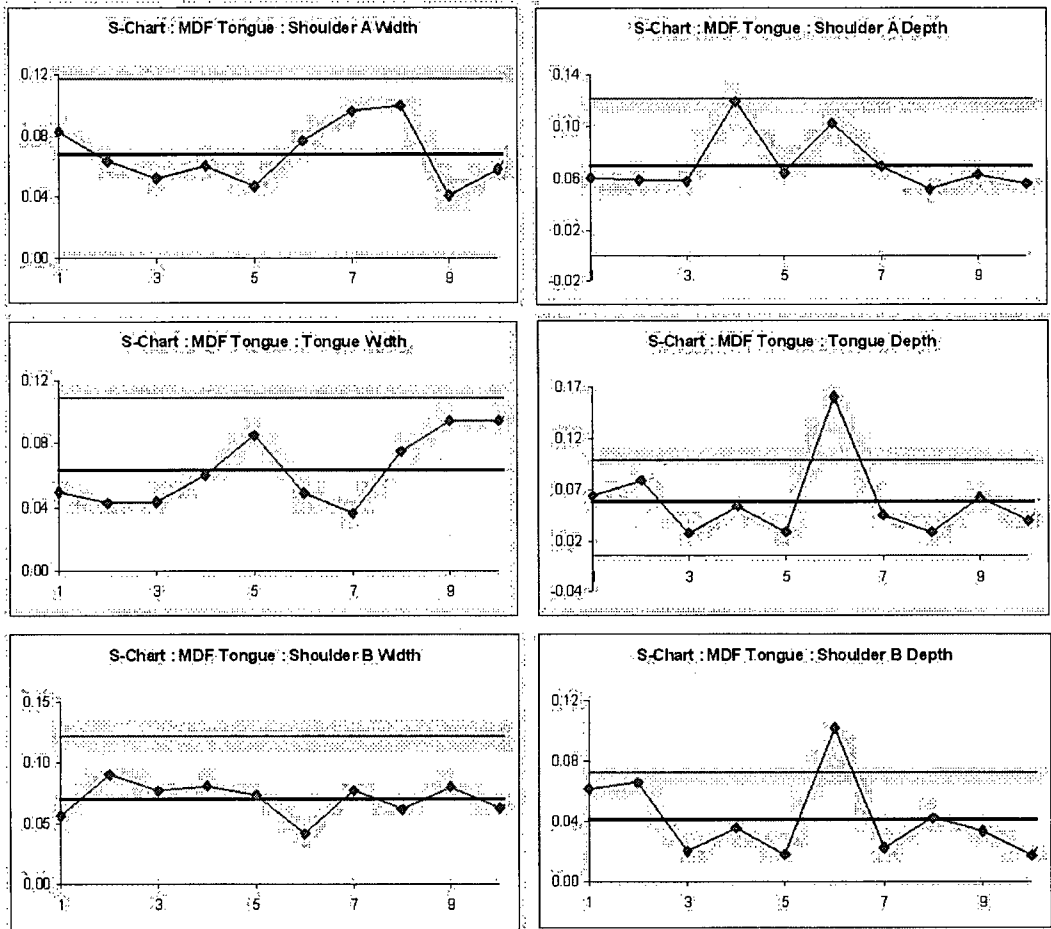
Control charts generated from the AQCS. The titles for control charts refer to the labeled part drawings.



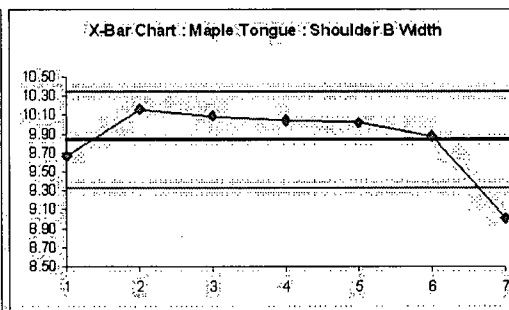
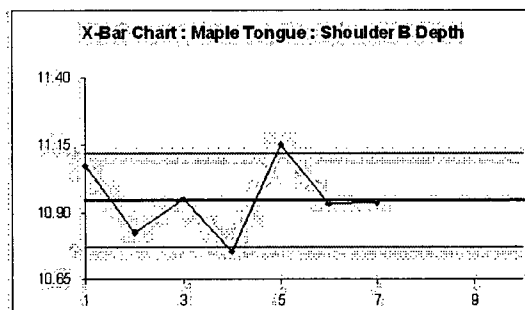
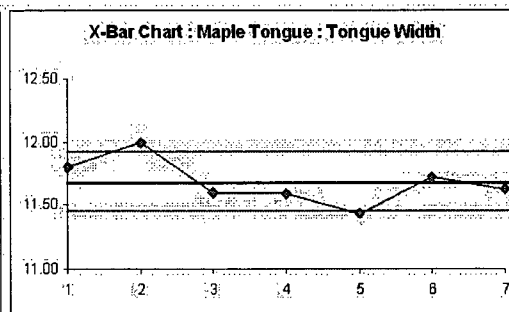
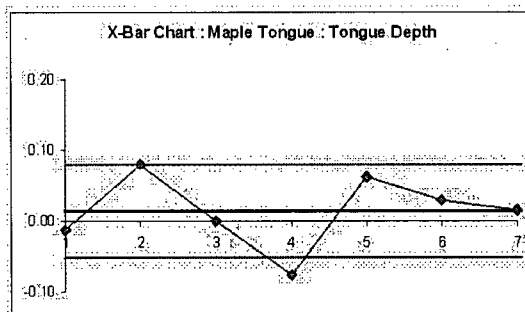
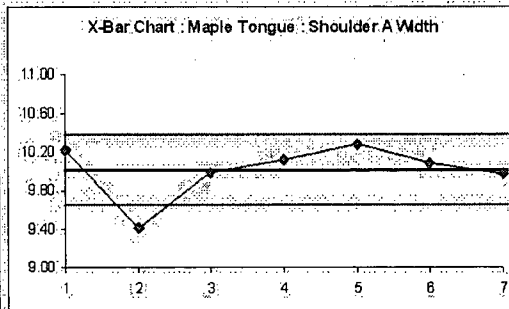
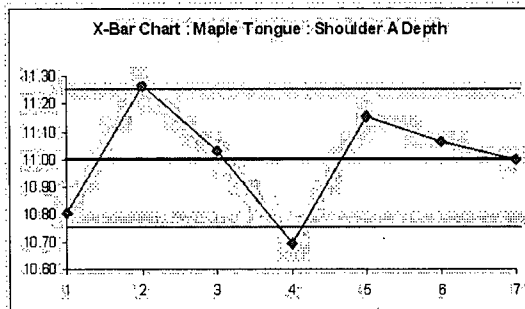
X-Bar chart for MDF tongue component:



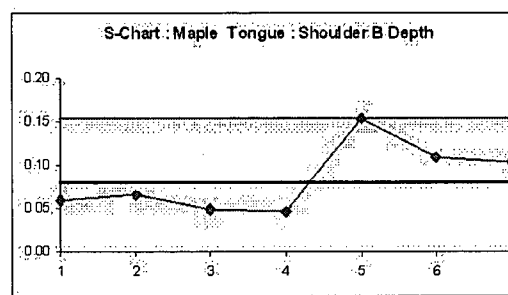
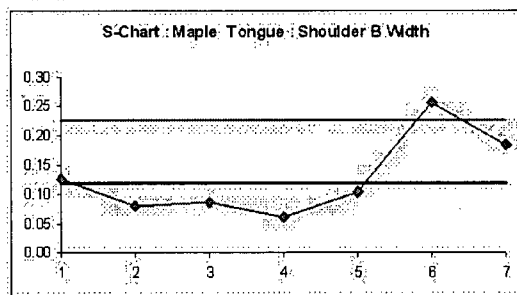
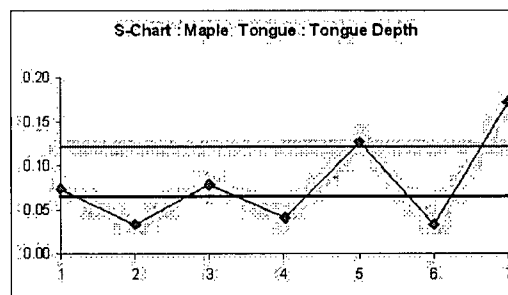
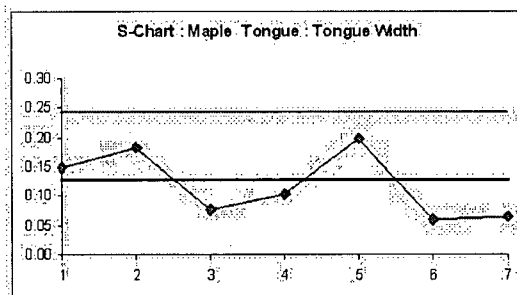
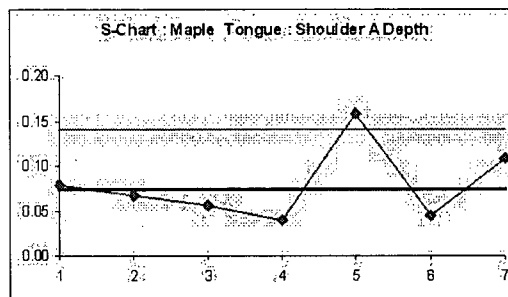
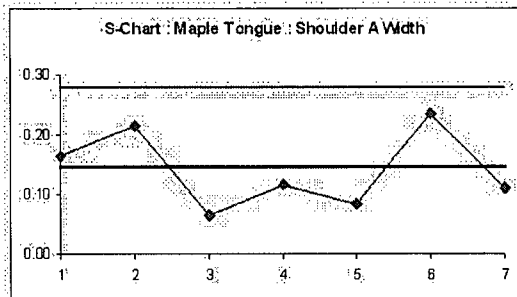
S-chart for MDF tongue component:



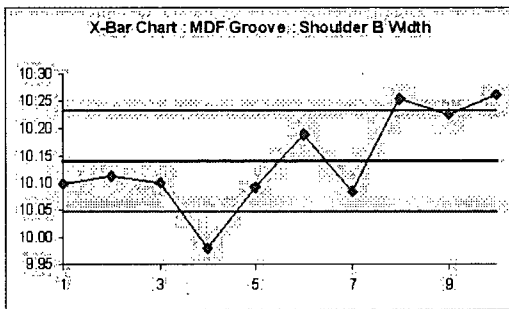
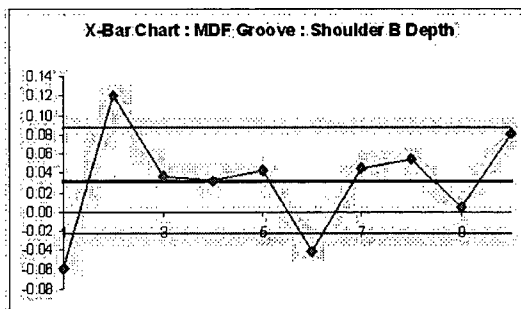
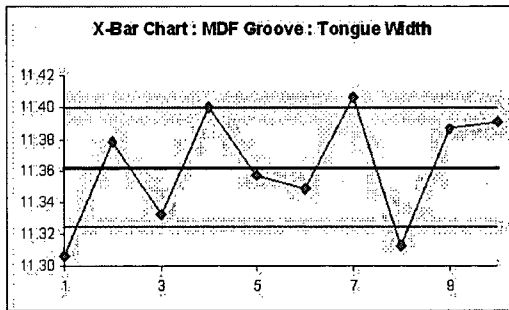
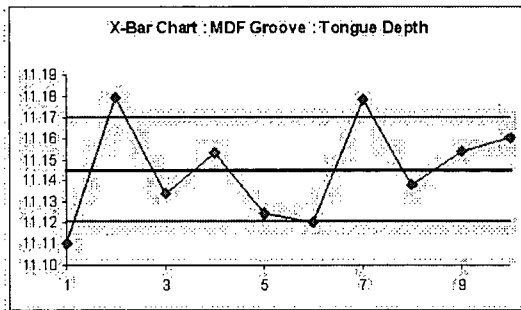
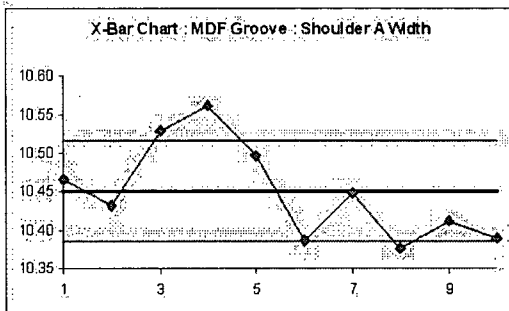
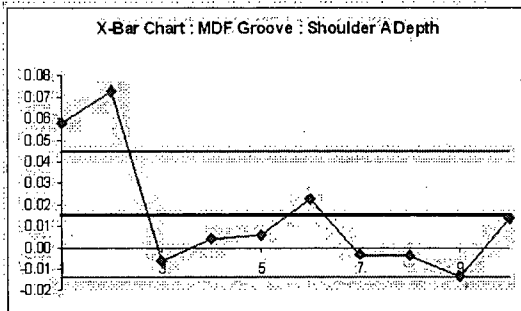
# X-Bar chart for maple tongue component:



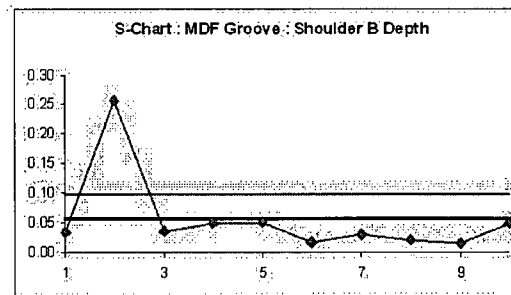
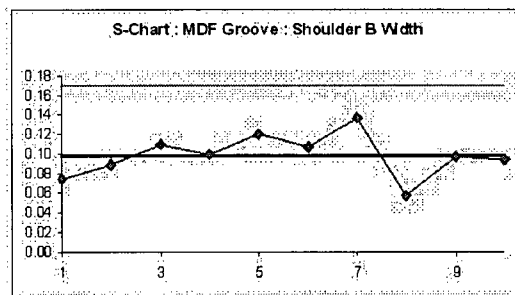
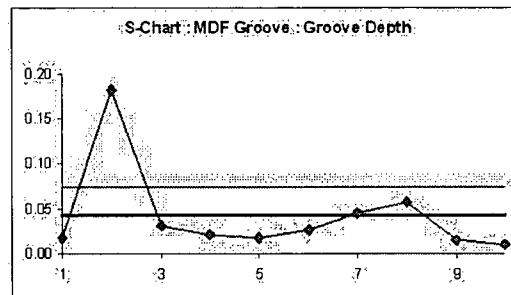
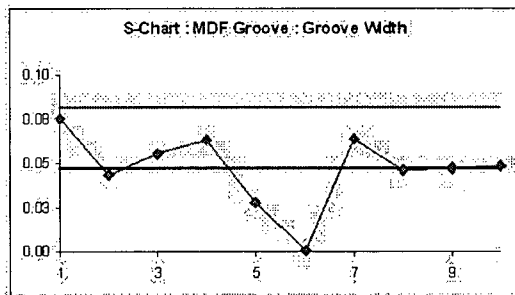
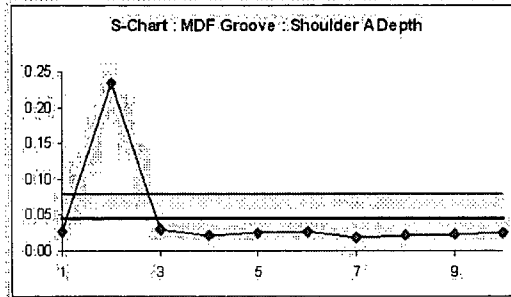
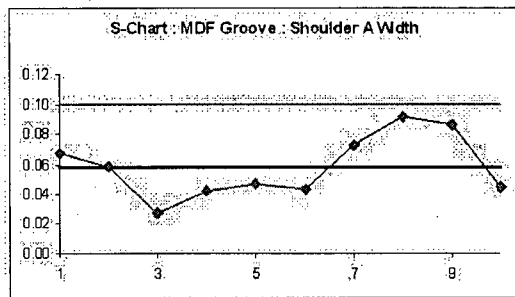
# S- chart for maple tongue component:



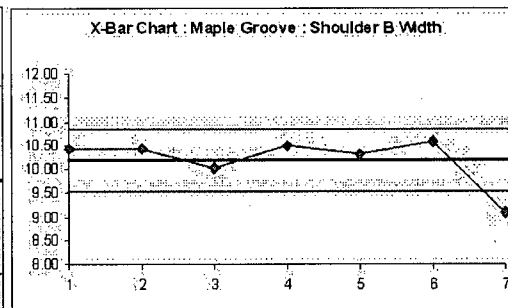
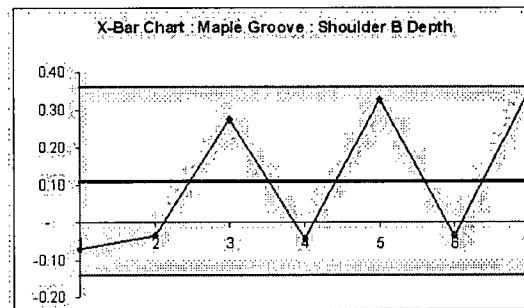
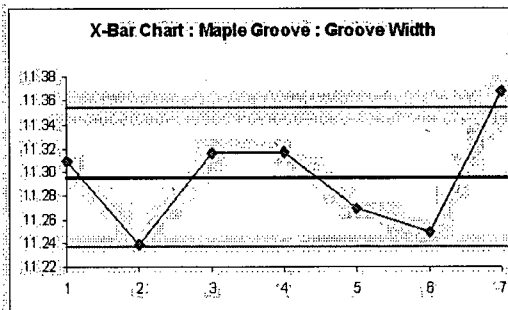
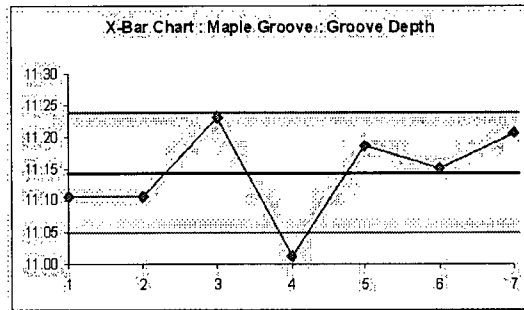
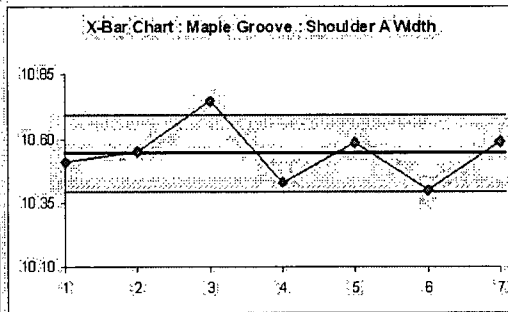
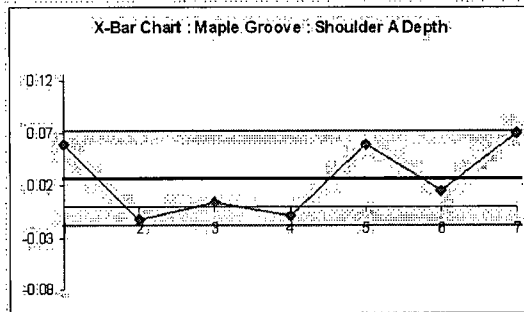
# X-Bar chart for MDF groove component:



# S-chart for MDF groove component:

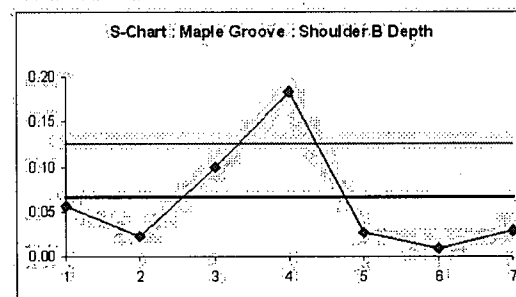
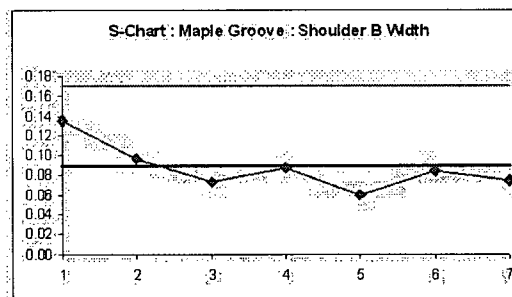
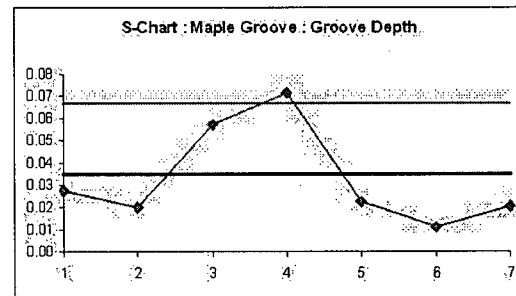
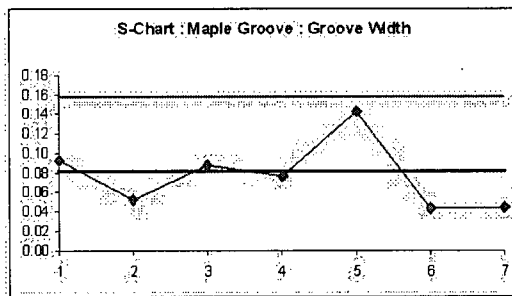
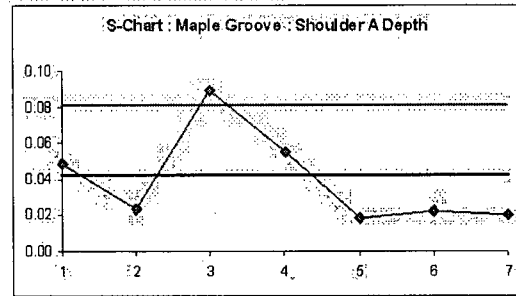
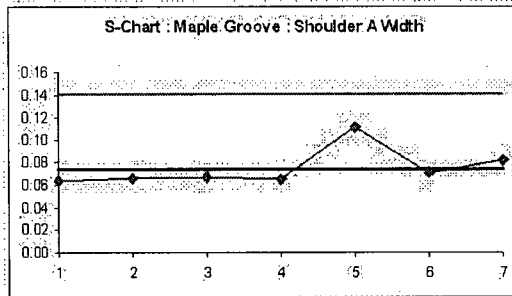


# X-Bar chart for maple groove component:

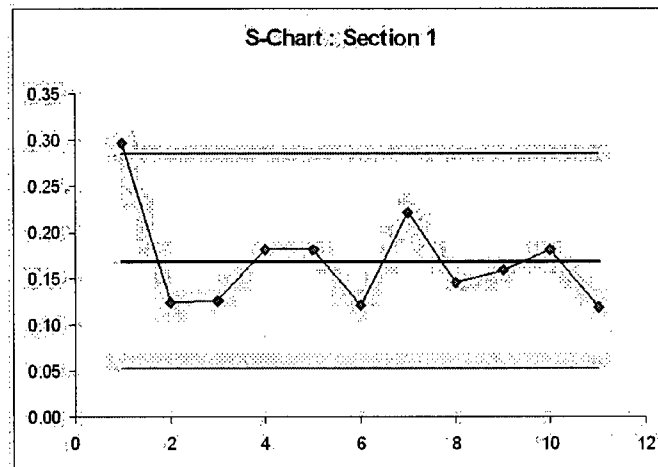
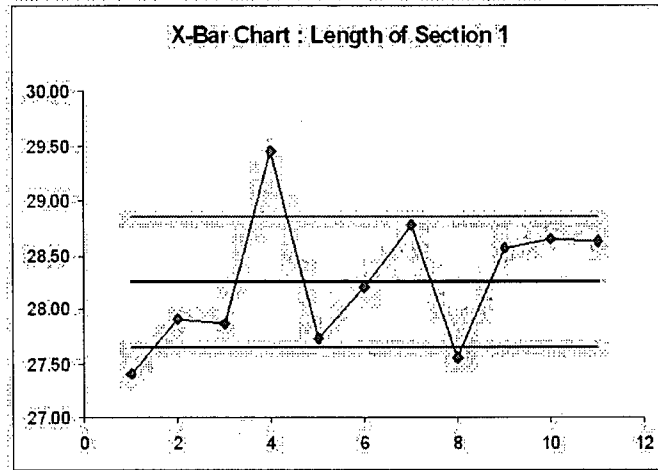




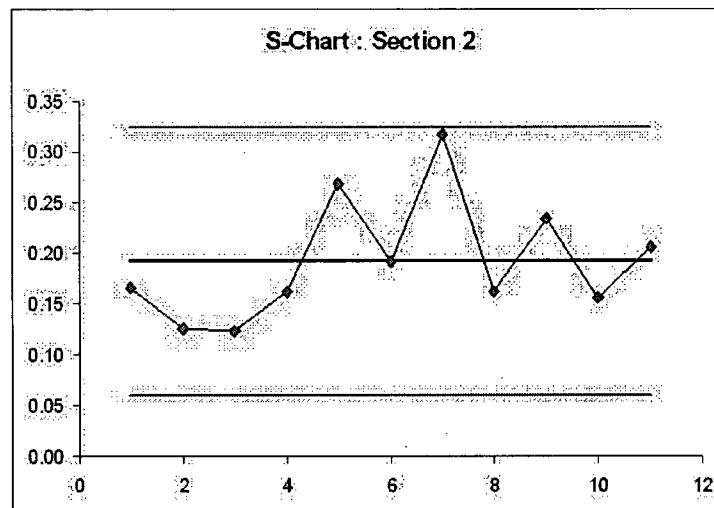
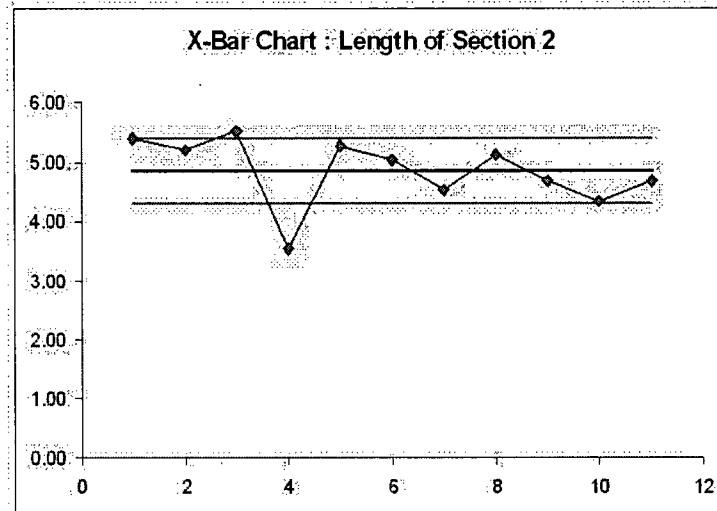
# S-chart for maple groove component:



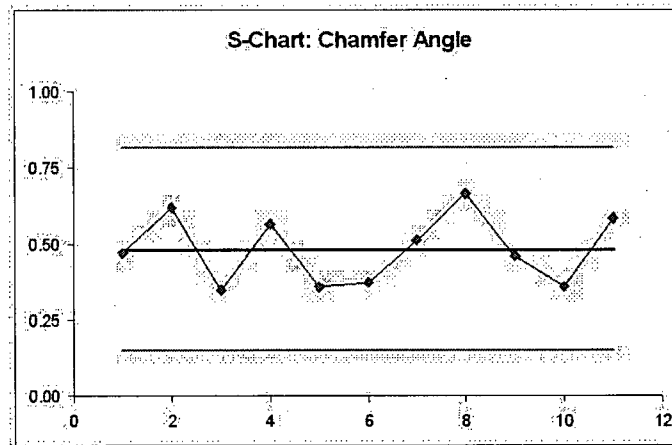
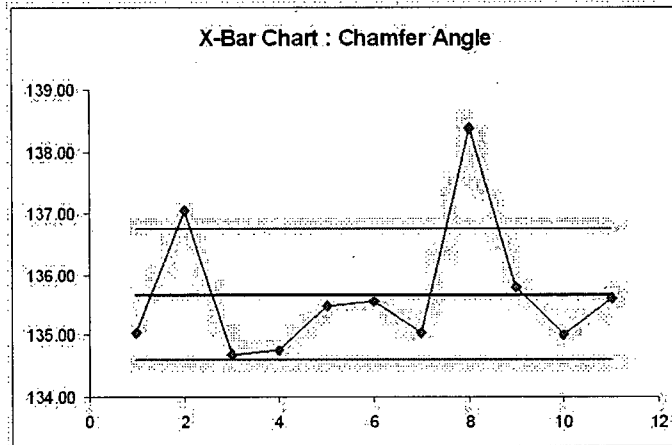
### X-bar and S-chart for chamfer Section 1



### X-bar and S-chart for chamfer Section 2

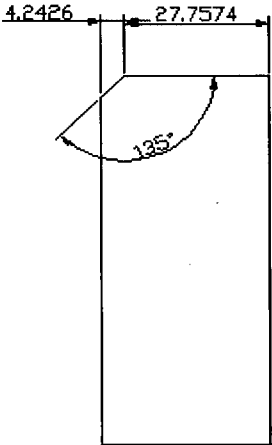
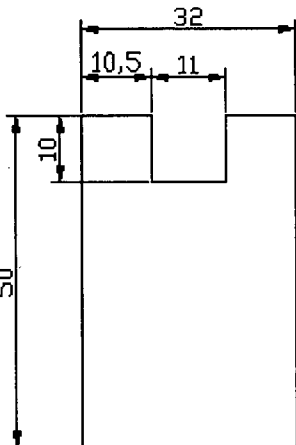
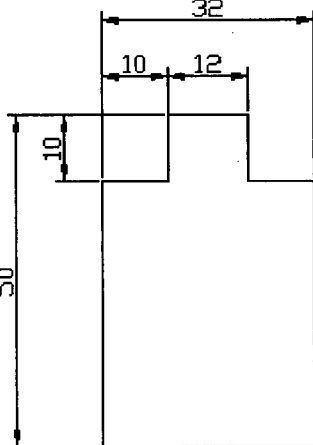


### X-bar and S-chart for chamfer angles



## APPENDIX E: Part Drawings

Dimensioned drawings for each of the test parts.

		
Chamfer	Groove	Tongue

## APPENDIX F: ANOVA Test Data

ANOVA test data used to compare between the AQCS, caliper and profilometer.

One-way ANOVA: G9 Shoulder Length Change						
Groups	Count	Sum	Average	Variance		
AQCS	10	14.5701	1.4570	0.0099		
Caliper	7	9.4200	1.3457	0.0102		
Profilometer	12	16.6497	1.3875	0.0088		
Source of Variation	SS	df	MS	F	P-value	F crit
Between Groups	0.0550	2	0.0275	2.8913	0.0735	5.5263
Within Groups	0.2471	26	0.0095			
Total	0.3021	28				

One-way ANOVA: GM5 Cut Shoulder Width						
Groups	Count	Sum	Average	Variance		
AQCS	10	90.7942	9.1	0.0055		
Profilometer	12	104.8886	8.7	0.1758		
Caliper	8	70.5800	8.8	0.0641		
Source of Variation	SS	df	MS	F	P-value	F crit
Between Groups	0.6563	2	0.3282	3.6443	0.0397	5.4881
Within Groups	2.4313	27	0.0900			
Total	3.0876	29				

One-way ANOVA: GM5 Uncut Shoulder Width						
Groups	Count	Sum	Average	Variance		
AQCS	10	105.8635	10.5863	0.0068		
Profilometer	12	125.9023	10.4919	0.0460		
Caliper	8	82.6000	10.3250	0.0073		
Source of Variation	SS	df	MS	F	P-value	F crit
Between Groups	0.3070	2	0.1535	6.6962	0.0043	5.4881
Within Groups	0.6188	27	0.0229			
Total	0.9258	29				

One-way ANOVA: T9 Tongue Length Change						
Groups	Count	Sum	Average	Variance		
AQCS	11	104.1774	9.4707	0.0038		
Caliper	8	72.3000	9.0375	0.0227		
Profilometer	11	105.0946	9.5541	0.0100		
Source of Variation	SS	df	MS	F	P-value	F crit
Between Groups	1.3611	2	0.6806	61.9437	0.0000	5.4881
Within Groups	0.2966	27	0.0110			
Total	1.6578	29				

## APPENDIX G: Bonferroni Test

Bonferroni Critical Difference Equations:

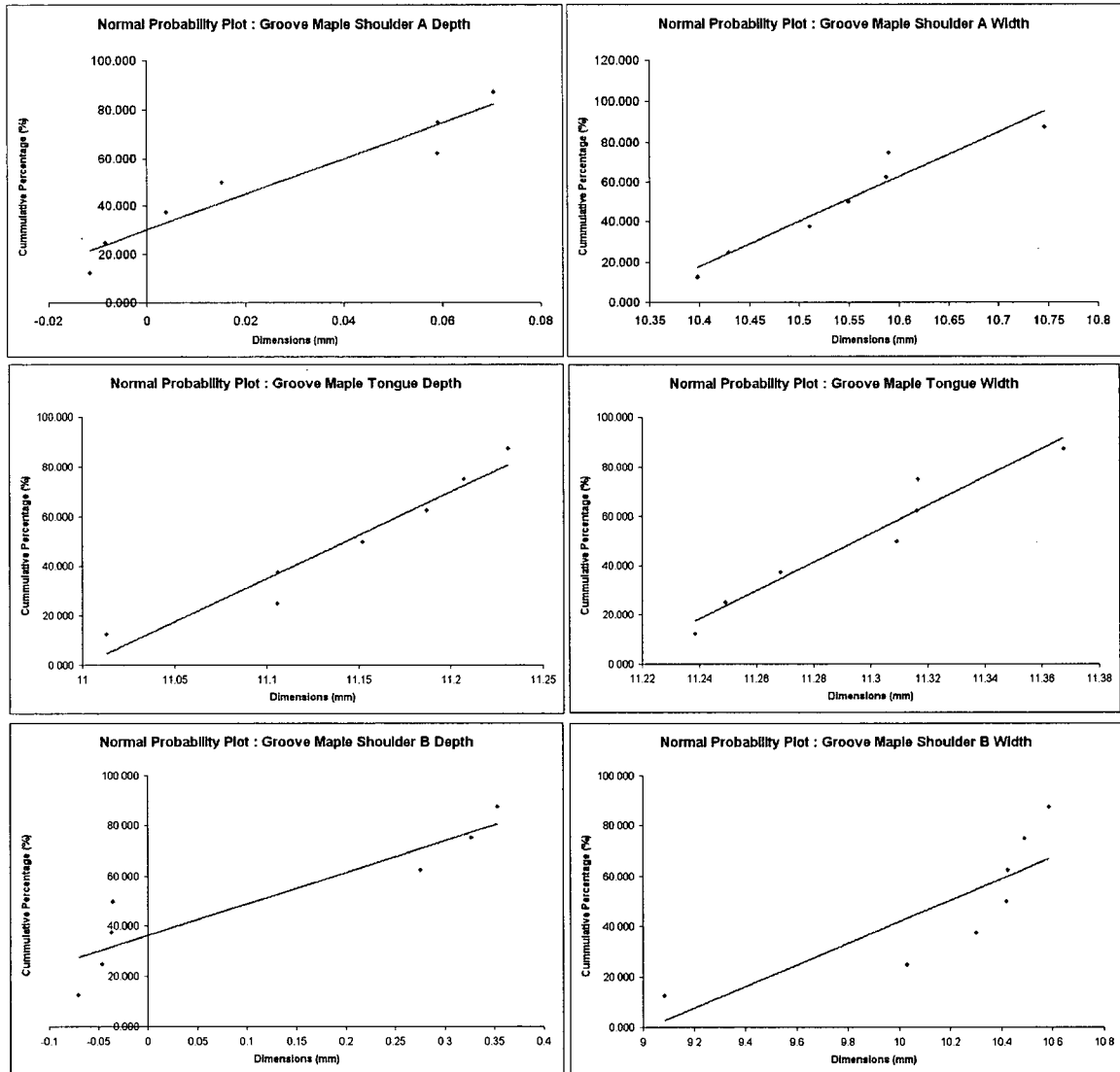
$CD = \left( t_{\frac{\alpha}{2m}} \right) (v) \left( \sqrt{MSe \left( \frac{1}{n_\ell} + \frac{1}{n_q} \right)} \right)$	
<b>CD</b>	Critical Difference
$\left( t_{\frac{\alpha}{2m}} \right)$	Bonferroni Statistic
<b>MSe</b>	Mean Square Error
$n_\ell$	Sample Size for one of the compared samples
$n_q$	Sample Size for the other compared samples

$CD < \left  \bar{Y} \cdot \ell - \bar{Y} \cdot q \right $	Significantly Different
$\bar{Y} \cdot \ell$	Sample Mean for one of the compared samples
$\bar{Y} \cdot q$	Sample Mean for the other compared samples

$CD > \left  \bar{Y} \cdot \ell - \bar{Y} \cdot q \right $	Not Significantly Different
$\bar{Y} \cdot \ell$	Sample Mean for one of the compared samples
$\bar{Y} \cdot q$	Sample Mean for the other compared samples

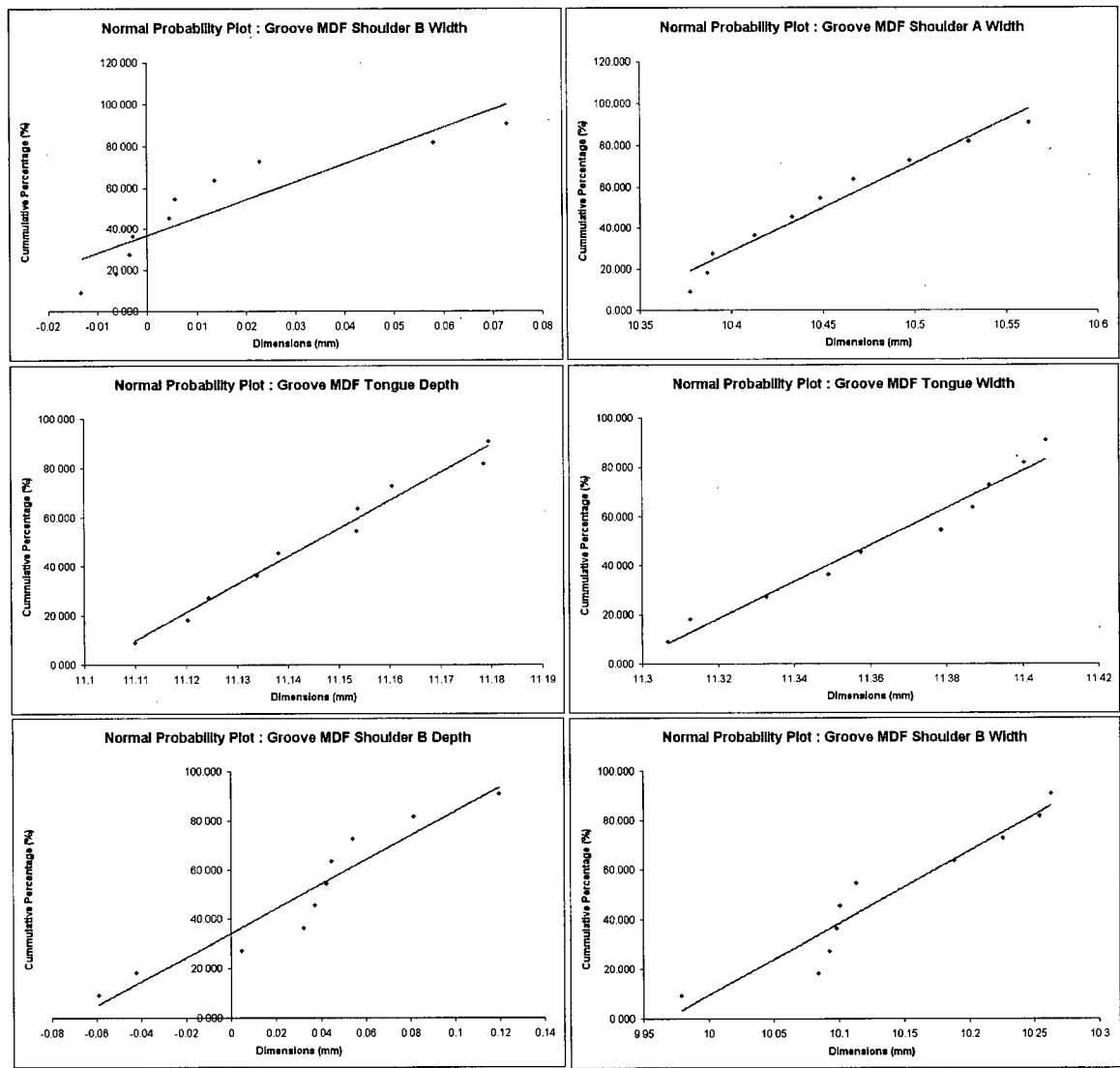
# APPENDIX H: Normal Probability Plot

## Normal Probability Plots for Groove Maple Parts

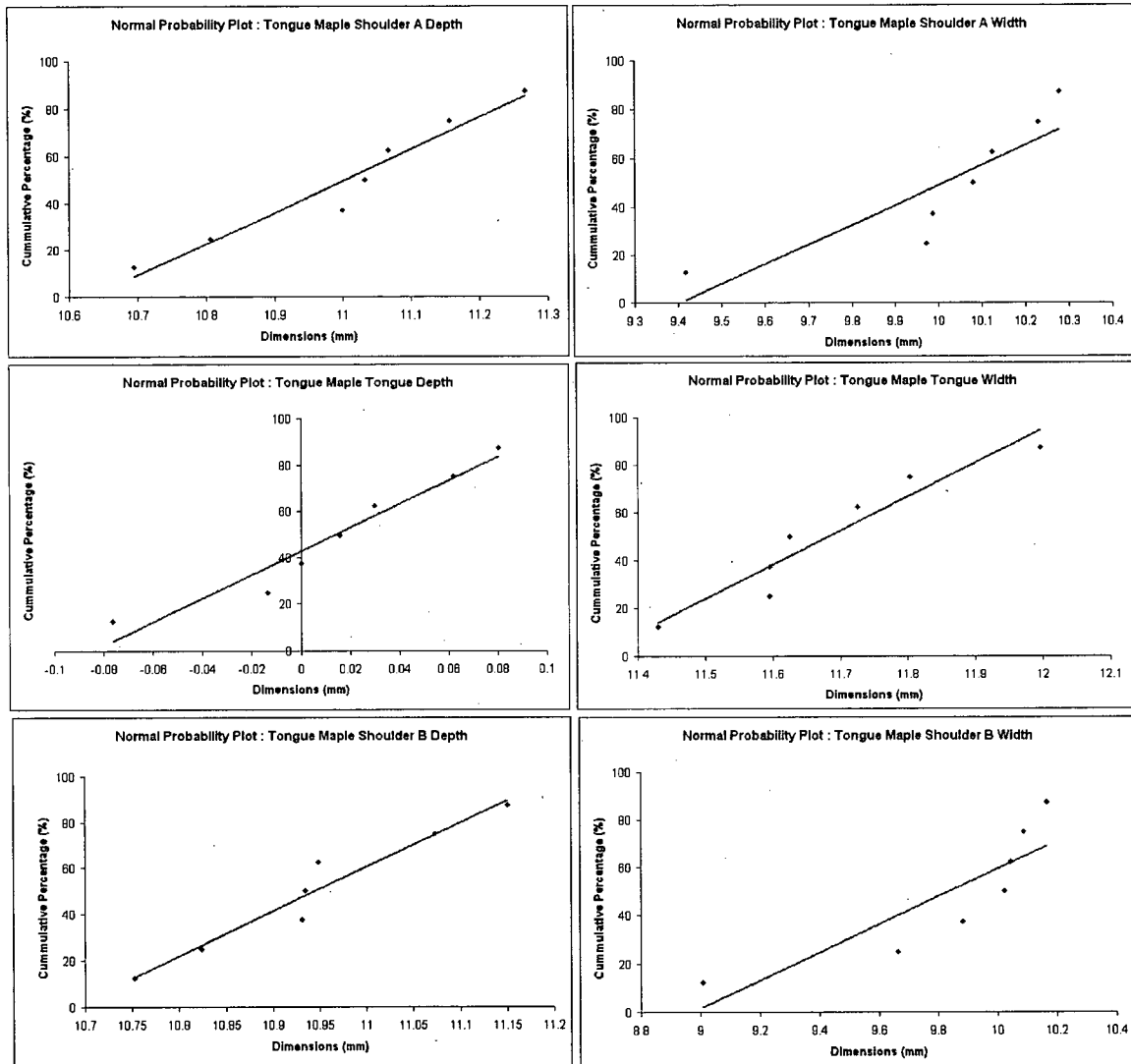




Normal Probability Plots for Groove MDF Parts



## Normal Probability Plots for Tongue Maple Parts



## Normal Probability Plots for Tongue MDF Parts

